# Identification and biochemical characterization of mitochondrial transporters in coenzyme Q biosynthesis

By

Jonathan Tai

A dissertation submitted in partial fulfillment of

the requirements for the degree of

Doctor of Philosophy

(Biochemistry)

at the

UNIVERSITY OF WISCONSIN-MADISON

2023

Date of final oral examination:  3/23/2023

This dissertation is approved by the following members of the Final Oral Committee:
    David J. Pagliarini, Honorary Fellow, Biochemistry, University of Wisconsin-Madison,
        and Professor, Cell Biology & Physiology, Washington University
    Katherine Henzler-Wildman, Professor, Biochemistry
    Alan D. Attie, Professor, Biochemistry
    Joshua J. Coon, Professor, Chemistry and Biomolecular Chemistry
    Mark E. Burkard, Professor, Medicine

# Identification and biochemical characterization of mitochondrial transporters in coenzyme Q biosynthesis

Jonathan Tai

Under the supervision of Professors David J. Pagliarini and Katherine Henzler-Wildman

At the University of Wisconsin-Madison

## Abstract

Coenzyme Q (CoQ) is a redox-active lipid that plays a critical role in many cellular processes, including the mitochondrial respiratory chain. CoQ is synthesized on the matrix side of the mitochondrial inner membrane using the precursors 4-hydroxybenzoate (4-HB) and isoprenoid pyrophosphates. These precursor molecules are first synthesized in the cytosol before being imported into the mitochondrial matrix. The import of 4-HB and isoprenoid pyrophosphates is believed to require protein transporters, as their negative charge prevents them from passively crossing the mitochondrial inner membrane. However, the molecule identities of these transporters are unknown. In this dissertation, I investigate the mechanisms of mitochondrial 4-HB and isoprenoid pyrophosphate transport. In Chapter 1, I provide an early history and brief review of CoQ biosynthesis and mitochondrial transporters. In Chapter 2, I discuss our work identifying Hem25p—a mitochondrial glycine transporter in heme biosynthesis—as an isopentenyl pyrophosphate (IPP) transporter in *Saccharomyces cerevisiae*. Using metabolic tracing and targeted uptake assays, we establish Hem25p as the major fungal IPP transporter and define the kinetics of IPP import. In Chapter 3, we explore 4-HB transport via a combination of *in silico* homology modeling and uptake assays. Our preliminary results implicate Coq2p—an integral membrane prenyltransferase—in 4-HB uptake. In the final chapter, I provide concluding remarks

and discuss future directions for this work. Taken together, the work described in this dissertation advances our understanding of CoQ biosynthesis and mitochondrial biology.

**Acknowledgements**

I would first like to thank my advisor Dave for all of his support throughout my time in this program. Graduate school was full of challenging moments, and I'm extremely fortunate to have you as an advisor to help me navigate it all. You took a bet on me when I was a lab-less third year medical student, and doubled-down on that bet when you gave me this project. Thank you believing in me and for bringing me closer to Stacy by moving the lab to St. Louis (I assume this was the reason).

I also thank my co-advisor Katie Henzler-Wildman for taking me on as step-graduate student. You certainly did not have to agree to be my advisor when we moved, let alone meet with me on a monthly basis. You've been a major source of support throughout graduate school and the move to St. Louis, and I am grateful for all of your transporter wisdom.

To Alan, Prof. Coon, and Mark, thank you for all of the suggestions, guidance, and patience as I toiled on this project. Mark, you have been there even before I officially joined the program, and I look forward to seeing this program grow under your leadership.

To everyone in the Pagliarini lab (past and present), thank you for all of the insightful discussions, assistance, and snacks. There are too many of you to name here, but I truly enjoyed getting to know each and every one of you. Special shout out to my first cubemate Molly McDevitt–cat cube 4eva.

To Rachel and Sean, founding members of Team25, thank you for helping me get this project to where it is now. I am excited to see what you will discover next.

To mom, dad, Michelle, Mickey, and Nico, thank you for believing in me and pushing me to be a better person. Somehow you all looked past my C in AP Chemistry.

To Stacy, thank you for being there for me though it all. Thank you for at least pretending to listen when I would ramble on about science. I do think that you are the second-most knowledgeable person on Hem25p in the world, even though you didn't ask to be. I'm excited to see where our future takes us.

And finally, to our cats Beau and Fiona: meow (thank you).

# Table of Contents

# Chapter 1: Introduction

Jonathan Tai

## Abstract

When Eugene Kennedy and Albert Lehninger discovered that the enzymes for oxidative phosphorylation (OxPhos) are in mitochondria, it launched an era of biochemical investigation into mitochondrial bioenergetics. Indeed, in the decades since, numerous details about OxPhos have been worked out, including the discovery of coenzyme Q (CoQ, ubiquinone) and the development of chemiosmotic theory. Yet, many aspects of mitochondrial biology remain remarkably obscure–a fact highlighted by our near complete inability to address mitochondrial dysfunction in the clinic. Contributing to this gap in knowledge is the finding that nearly a quarter of the mitochondrial proteome has no defined function or is, at best, partially characterized. At the same time, many established biochemical processes in mitochondria are incompletely annotated. Two examples of such processes are the biosynthesis of CoQ and the mitochondrial carrier system (MCS). In this chapter, I introduce both processes, providing a brief historical overview and highlighting our current knowledge. This chapter will serve as the foundation for my work in later chapters.

**Coenzyme Q**

*Coenzyme Q function*

      CoQ is a redox-active lipid composed of a quinone head group attached to a long, hydrophobic polyisoprenoid side chain[1,2] (Figure 1A). The quinone head group can receive and donate electrons, forming ubiqinol (CoQH$_2$) when fully reduced with 2 electrons ($e^-$), ubisemiquinone when singly reduced with $1e^-$, or ubiquinone (CoQ) when fully oxidized (Figure 1B). The side chain of CoQ, also called the tail, is made of repeating 5-carbon isoprene units. The number of repeats varies by species and is denoted by a subscripted number following 'CoQ.' For example, humans have 10 isoprene units (CoQ$_{10}$), while yeast have 6 (CoQ$_6$), and *Escherichia coli* have 8 (CoQ$_8$). Because of this long tail, CoQ is highly hydrophobic and is therefore anchored in the lipid membrane. The combination of being small, redox-active, and hydrophobic allows CoQ to freely diffuse along membranes, shuttling electrons for redox reactions.
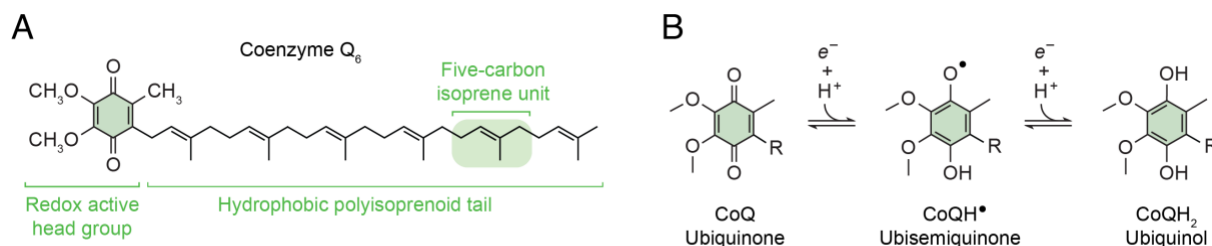


**Figure 1. Structure and redox activity of CoQ. (A)** Structure of the oxidized form of CoQ$_6$, the variant found in *S. cerevisiae*. (**B**) Redox activity of CoQ, showing the oxidized, semi-reduced, and fully reduced forms. Figure adapted from Guerra et al[2].

      CoQ's canonical role is that of a cofactor in the mitochondrial electron transport chain (ETC)[1,2]. CoQ accepts electrons from Complexes I and II and transfers them to Complex III (Figure 2). The reduction of CoQ at Complex I is coupled to the translocation of protons across

the mitochondrial inner membrane. At Complex III, CoQ participates in the 'Q cycle,' where it not only donates electrons to cytochrome *c*, but also assists in the movement of protons across the membrane[3]. Thus, as a redox cofactor, CoQ plays an essential role in the generation of the proton motive force that drives OxPhos.

Outside of this canonical role, CoQ is increasingly recognized for its functions in other cellular processes (Figure 2). CoQ is a cofactor in pyrimidine biosynthesis[4,5], fatty acid beta-oxidation[6], proline catabolism[7], and sulfide detoxification[8]. In brown adipose tissue, CoQ plays critical role in thermogenesis by regulating the expression of the uncoupling protein UCP1[9]. CoQ also regulates the mitochondrial permeability transition pore, whose opening results in the initiation of apoptosis[10]. Although primarily known for its functions in mitochondria, CoQ also plays important roles in extramitochondrial membranes. At the plasma membrane, CoQ acts as a lipophilic antioxidant, thereby maintaining membrane integrity against oxidative stress and lipid peroxidation[11–13]. It is also here that CoQ was found to play a role against ferroptosis, a form of nonapoptotic cell death due to aberrant iron-dependent lipid peroxidation[14,15]. In bacteria, CoQ is necessary to stabilize the cytoplasmic membrane against osmotic stress[16].
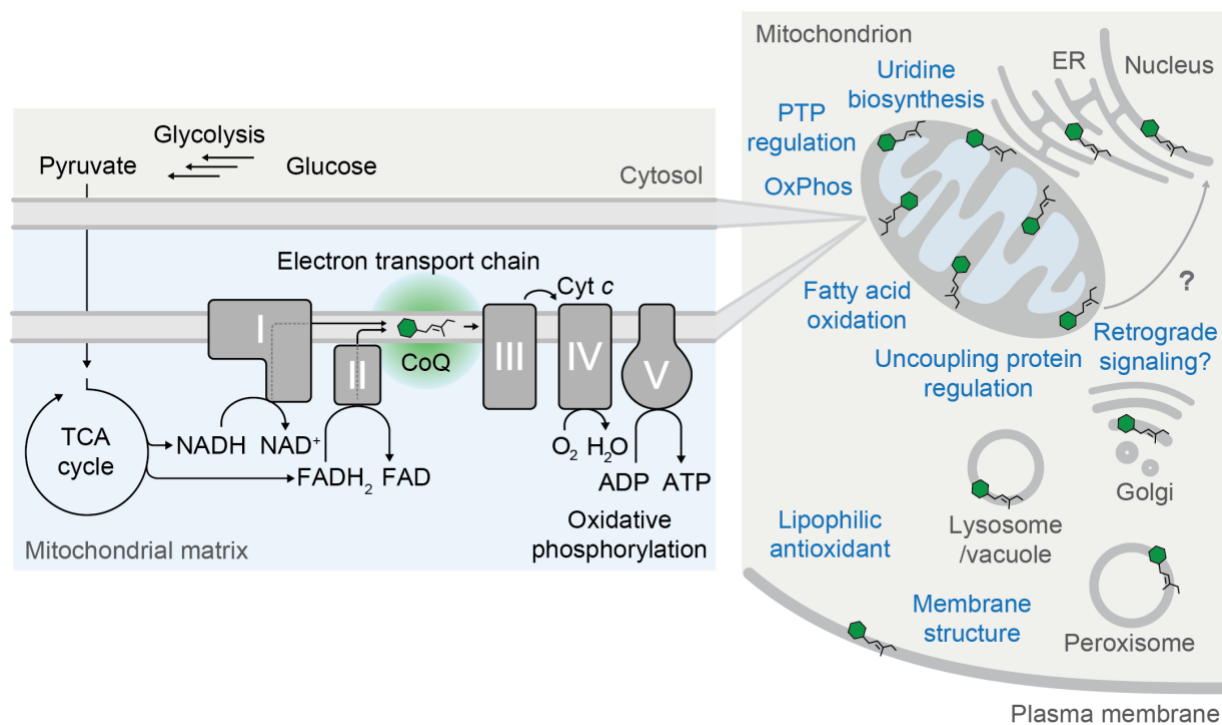
**Figure 2. Cellular functions of CoQ.** CoQ's canonical role is that of an electron carrier in the mitochondrial respiratory chain. However, CoQ is also located in other cellular membranes where it carries out various functions. Figure adapted from Stefely et al[1].

Given CoQ's importance in a wide array of cellular functions, deficiencies in CoQ can result in a number of human pathologies[17]. Like many other mitochondrial diseases, CoQ deficiencies are clinically heterogeneous with complex physiological sequelae[18]. The most affected organs are those with high energy demands, such as the brain, heart, kidneys, and skeletal muscle. As such, the major phenotypes of CoQ deficiency include encephalopathy, cerebellar ataxia, infantile multisystemic disease, nephropathy, and isolated myopathy[19]. Primary CoQ deficiencies are a result of mutations in CoQ biosynthetic genes, all of which are nuclear encoded. However, CoQ deficiency can also result from mutations in genes not directly linked to CoQ biosynthesis[20]. In these cases of secondary CoQ deficiency, the underlying mechanisms can vary

and are poorly understood. One example is the myopathic form of CoQ deficiency in patients carrying *ETFDH* mutations[21]. In one study, fewer than half of diagnosed CoQ deficiency cases had a molecular diagnosis, suggesting that additional pathogenic mutations exist[19]. Further work is needed to fully elucidate the causes and pathogenic mechanisms of secondary CoQ deficiencies.

The role of CoQ on the aging process and longevity is more obscure. While mitochondrial dysfunction is hallmark of aging, whether age-related mitochondrial defects such as decreased respiratory capacity and increased oxidative stress are causative of, or secondary to the aging process remains uncertain[22,23]. Changes in CoQ biosynthesis and abundance can affect the mitochondrial function and the aging process; however, the mechanisms are poorly understood. Although CoQ abundance decreases with age[24], studies in mice and *Caenorhabditis elegans* suggest that mild CoQ deficiencies can increase lifespan[25–27]. One possible explanation is that decreases in CoQ, along with other mitochondrial defects, generates mitochondrial reaction oxygen species which act as signaling molecules to activate pro-longevity responses[22]. While this still requires further validation, it underscores the crucial role of CoQ in mitochondrial function and physiology.

*Discovery and early biosynthesis research*

CoQ was first identified in the late-1950s by two independent labs at UW-Madison and the University of Liverpool[28,29]. At Wisconsin, Frederick Crane, working in David E. Green's lab, was attempting to dissect the organization of enzymes in the TCA cycle and OxPhos[30]. During the fraction steps, Crane noticed that the isolated cytochromes were bound with lipids, suggesting that lipids may have functional roles in electron transport. Crane then attempted to identify this new lipid vitamin, first in cauliflower mitochondria and then in beef heart mitochondria. When the

extracted mitochondrial lipids were chromatographed, he noticed three carotenoid peaks as well as a broad yellow band. Isolation of that yellow band yielded a similarly colored oil. The compound's absorption spectra was consistent with that of a quinone and the name 'Q275' was assigned, referring to its absorption peak at 275 nm[30]. Q275 was then found to have redox activity in mitochondria, suggesting a role for this redox-active lipid in mitochondrial electron transport.

At the same time, Richard Morton and colleagues at the University of Liverpool were investigating vitamin A biosynthesis. A lipid with an absorption peak at 272nm was isolated from the intestinal linings of horses[29]. However, the yield from this isolation was small, making any further study difficult. Later, using livers from rats deficient in vitamin A, a lipid with the same absorption peak was isolated in greater yield. This lipid, designated 'SA,' was later found to be have redox activity consistent with that of a quinone. In correspondence with the group at Wisconsin, SA was identified to be the same compound as Q275[30]. Given its widespread distribution in nature, Morton and colleagues re-named SA to 'ubiquinone[31].' Meanwhile, at Wisconsin, work was ongoing to elucidate the role of Q275 as a vitamin, of which people could be deficient in. As evidence for this 'vitamin Q' was still lacking at the time, Q275 was given the placeholder name 'coenzyme Q' until an essential vitamin function could be established[30].

The discovery of CoQ started an ongoing effort to elucidate its biosynthesis. The earliest studies, from the late-1950s to the mid-1960s, used [$^{14}$C]-labeled compounds to establish the biosynthetic precursors. Incubation of isolated tissues with labeled phenylamino acids resulted in the radiolabeling of CoQ's head group, thereby establishing phenylalanine as the ring precursor[32]. Subsequent studies then showed that phenylalanine is first converted to tyrosine, before being incorporated into CoQ[33]. However, conflicting reports were being published showing that radiolabeled tyrosine was not being incorporated. It was later shown that an impurity in the

commercial radiolabeled tyrosine preparation, 4-hydroxybenzaldehyde (4-HBz), was being incorporated and outcompeting tyrosine[34]. The discovery of 4-HBz as a precursor eventually led to the identification of 4-hydroxybenzoate (4-HB) as the universal head group precursor[35]. CoQ's polyisoprenoid tail, with its similarity to that of vitamin K, was believed to be derived from mevalonate, and therefore acetate[36]. Studies with $[^{14}C]$-mevalonate and $[^{14}C]$-acetate later confirmed their incorporation into CoQ's tail[33,37]. The methoxy groups on CoQ's head were thought to originate from 1C donors, and this was confirmed by $[^{14}C]$-formate labeling of the head group[33].

With the precursors now firmly established, work then proceeded to elucidate the biosynthetic pathway itself. By studying lipid extracts of the bacteria *Rhodospirillum rubrum*, biosynthetic intermediates were identified, and a near-complete pathway was proposed in 1966[38]. Additional work through the late 1960s and early 1970s identified mutants in *Escherichia coli* with specific defects in CoQ biosynthesis[39–42]. Isolation of accumulated lipids from these strains confirmed the proposed biosynthetic pathway in prokaryotes. Furthermore, biochemical activity assays provided the first evidence for enzymes in the pathway. The responsible genes were genetically mapped by conjugation. The results of these efforts are the first known CoQ biosynthetic proteins–the Ubi proteins.

Although accurate for prokaryotes, the pathway proposed in 1966 still needed refining for eukaryotic organisms. Nevertheless, the identification of biosynthetic intermediates enabled the first localization studies of CoQ biosynthesis. By the 1970s, studies were underway using radiolabeled precursors and isolated organelles to identify the site of CoQ biosynthesis. The ability of isolated mitochondria and mitochondrial membranes to incorporate radiolabeled precursors into

early biosynthetic intermediates suggested that the mitochondrial are the site of CoQ biosynthesis[43,44].

Despite these seminal studies, there were still outstanding questions about eukaryotic CoQ biosynthesis. The biosynthetic pathway, mostly worked out in bacteria, still needed experimental validation in eukaryotes. Complicating these efforts was the fact that the eukaryotic enzymes catalyzing the pathway were unknown. A key breakthrough came in 1975, when Alexander Tzagoloff developed a selection procedure to generate and isolate yeast mutants that were deficient in respiration[45]. These mutants had defects in certain mitochondrial proteins, such as cytochrome oxidase and ATP synthase. Included in this mutant library were strains with defects in CoQ biosynthesis. These strains were identified by their NADH-cytochrome *c* reductase activities, which were decreased in the mutants. These activities were restored upon the addition of exogenous CoQ, suggesting that the primary defect was a CoQ deficiency. The availability of these CoQ-deficient strains kickstarted a new wave of biochemical and genetic studies into CoQ biosynthesis. By isolating the biosynthetic intermediates that had accumulated in these mutants, new intermediates were identified that refined our understanding of the eukaryotic pathway to what it is today[46]. The development of genetic and molecular biology tools in the late 1980s and 1990s enabled the cloning and biochemical characterization of the first yeast *COQ* genes: *COQ1* and *COQ2*[47]. Seven additional complementation groups (*coq3-coq9*) were identified in this mutant library, laying the groundwork for mechanistic investigation into CoQ biosynthesis[48]. Indeed, spearheaded by Catherine Clarke and Alexander Tzagoloff, the 1990s and early 2000s saw the cloning of many of the responsible genes, in addition to the biochemical characterization of their protein products. Many of these proteins have been directly assigned to specific steps in eukaryotic pathway, yielding a fuller picture of CoQ biosynthesis[49–53]. However, it should be noted that the

pathway remains incompletely defined, and that there exists known Coq proteins with no assigned function[2]. Importantly, all the Coq proteins have been localized to the mitochondrial matrix, confirming mitochondrial CoQ biosynthesis[54]. Additional CoQ-related proteins, beyond those identified by Tzagoloff, continue to be discovered to this day, including Coq10p, Coq11p, and Coq21p[55–57]. The specific roles of these proteins are poorly understood, and more effort is needed to elucidate their functions.

While the Coq proteins were being characterized, it was becoming increasingly obvious that many of the Coq proteins were dependent on each other[58]. In other words, if one particular Coq protein was missing, then the levels of other Coq proteins would be decreased. Early hypotheses suggested that Coq proteins influenced the expression of each other. It was later found, using blue native polyacrylamide gel electrophoresis (BN-PAGE), that Coq3p-Coq9p organize into a metabolon, termed 'complex Q' or the 'CoQ-synthome[59]' (Figure 4). Subsequent studies with affinity enrichment mass spectrometry (AE-MS) in human cells showed that a similar metabolon exists in mammalians cells[60]. Because the enzymes that constitute complex Q are responsible for the later, head-group modifying steps, it has been suggested that the role for this complex is to increase the flux through these steps and/or sequester toxic intermediates[2,54]. However, the exact role, as well as the composition and stoichiometry of the constituent proteins, remains uncertain.

*Eukaryotic CoQ biosynthesis*

In eukaryotes, CoQ biosynthesis (Figure 3) begins in the cytosol with the generation of the precursors 4-HB and isoprenoid pyrophosphates. 4-HB, the canonical head group precursor, is derived from tyrosine and phenylalanine. The pathway from tyrosine to 4-HB is incompletely

defined, however the first and last steps are known[61,62]. Tyrosine is converted to 4-hydroxyphenylpyruvate (4-HPP) by the enzymes Aro8p and Aro9p in yeast. How 4-HPP is converted to 4-HBz is poorly understood. Thorough investigation using targeted LC-MS and *in vivo* rescue experiments yielded redundant pathways in yeast[63]. In mammalian cells, heavy $O_2$ tracing suggested 4-hydroxymandelate (4-HMA) as an intermediate in the pathway, consistent with yeast results[64]. The redundancies in the 4-HBz synthesis pathway suggest a robustness to single gene disruptions. The conversion of 4-HBz to 4-HB in yeast is catalyzed by Hfd1p, a broad-specificity aldehyde dehydrogenase[61,62]. The human ortholog of Hfd1p, ALDH3A1, can rescue respiratory growth in *hfd1Δ* yeast, suggesting that it may play a similar role in human CoQ biosynthesis[61]. However, this role for ALDH3A1 still needs to be validated. In bacteria and yeast, the shikimate pathway generates chorismate, which is further converted to 4-HPP for 4-HB synthesis[65]. Furthermore, yeast can convert chorismate into *para*-aminobenzoate (*p*ABA), an alternative head group precursor to 4-HB. Thus, yeast contain multiple redundant mechanisms to generate 4-HB and CoQ.

CoQ's tail is made of repeating 5-carbon isoprene units. The precursor subunits, isoprenoid pyrophosphates, are made by the mevalonate pathway in eukaryotes and the 2-*C*-methyl-D-erythritol 4-phosphate (MEP) pathway in prokaryotes[65]. Both pathways generate isopentenyl pyrophosphate (IPP), which then serves as a precursor for dolichol, sterols, and other terpenoids, in addition to CoQ[66]. Additionally, it is used for the prenylation of heme, proteins, and tRNAs. IPP can be isomerized by Idi1p to generate dimethylallyl pyrophosphate (DMAPP). DMAPP is critical for the head-to-tail polymerization reaction, serving as a 'seed' for the generation of geranyl, farnesyl, and other longer-chain pyrophosphates[67] (in this dissertation, these species will be collectively called 'isoprenoid pyrophosphates').

In the next stage of CoQ biosynthesis, the precursors are transported from the cytosol into the mitochondrial matrix. There, individual isoprenoid pyrophosphate units are stitched together to form the polyprenyl pyrophosphate containing the full length polyisoprenoid tail. This is catalyzed by a prenyltransferase Coq1p in yeast, and it is this protein that determines the different tail lengths among species[47,68]. The polyprenyl pyrophosphate is then attached to 4-HB by another prenyltransferase, Coq2p, thereby forming polyprenyl-hydroxybenzoate (PPHB)[69]. For these reactions, the only required cofactor is $Mg^{2+}$, which is needed for the prenyltransferase reactions.

In the final stage, PPHB undergoes a series of head group modifications to form mature CoQ (Figure 3). These chemical reactions in the stage include three hydroxylations, a decarboxylation, and three methylations (two *O*-methylations, one *C*-methylation). The genes encoding these biosynthetic proteins, *COQ3-COQ9*, were first described by Tzagaloff[48]. Subsequent biochemical characterization by Clarke and others, including the analysis of accumulated intermediates in mutant strains, resulted in the current proposed pathway in yeast[49–53]. There are minor differences between the pathway in yeast and bacteria, mainly between the order of the decarboxylation and hydroxylation/methylation reactions[65]. Auxiliary proteins include Yah1p and Arh1p, which transfer electrons for Coq6p function[70,71]. The head group modifications also require several cofactors that must either be transported into, or synthesized by, the mitochondria[1].
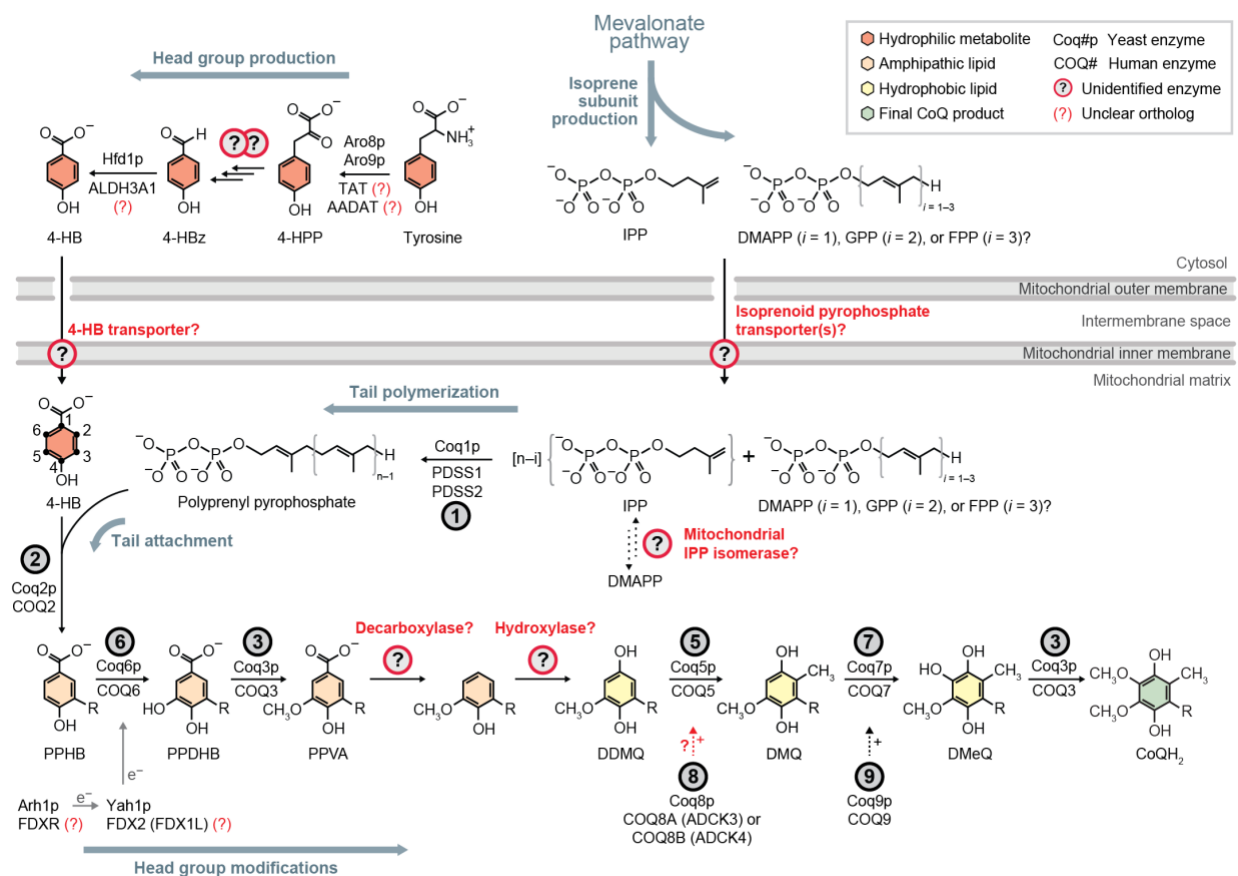
**Figure 3. Overview of eukaryotic CoQ biosynthesis.** For each step of the pathway, the responsible yeast biosynthetic enzymes and their human homologs are listed. Some steps lack biochemical evidence for the putative human homolog. In these cases, the enzymes are listed followed by a (?). Missing steps and unknowns are colored red. 4-HB, 4-hydroxybenzoate; 4-HBz, 4-hydroxybenzaldehyde; 4-HPP, 4-hydroxyphenylpyruvate; IPP, isopentenyl pyrophosphate; DMAPP, dumethylallyl pyrophosphate; GPP, geranyl pyrophosphate; FPP, farnesyl pyrophosphate; PPHB, polyprenyl-hydroxybenzoate; PPDHB, polyprenyl-dihydroxybenzoate; PPVA, polyprenyl-vanillate; DDMQ, demethoxy-demethyl-coenzyme Q; DMQ, demethoxy-coenzyme Q; DMeQ, demethyl-coeyzme Q. Figure adapted from Guerra et al[2].

As mentioned previously, the enzymes responsible for the head-group modifications (Coq3p-Coq9p) organize into a metabolon (complex Q, CoQ synthome) that is associated with the matrix side of the mitochondrial inner membrane[2,54] (Figure 4). The exact role for complex Q is uncertain, but is thought to enhance the efficiency of the reactions and/or sequester potentially toxic intermediates that inhibit the ETC. Complex Q assemble in a member- and substrate-dependent manner. Thus, disruption of one member of complex Q results in instability of the complex and decreased steady-state levels of the remaining members[59]. A key result of this co-dependency is the accumulation of a single intermediate, PPHB (the product of Coq2p), when each member of complex Q is disrupted independently[13,61]. While the levels of Coq1p and Coq2p remain the same in the absence of complex Q, cells lacking either of those proteins show decreased levels of complex Q proteins. Furthermore, LC-MS measurements of isolated complex Q components identified CoQ and biosynthetic intermediates[56]. This suggests that lipids are also a required component of complex Q, and that flux of lipid intermediates through the complex is needed for complex stability. The complex Q proteins were also shown to organize into the domains that were enriched at ER-mitochondria contact sites[72,73]. Whether these domains represent the global *in vivo* population of complex Q, or if it's just a subset, remains unknown. However, it strongly suggests a role for inter-organelle crosstalk in CoQ biosynthesis and distribution.
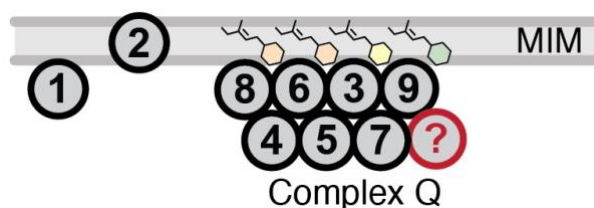


**Figure 4. General schematic of complex Q organization.** The CoQ biosynthetic proteins Coq3p-Coq9p organize into a metabolon (complex Q). CoQ and/or biosynthetic intermediates are a component of complex Q, and are believed to support complex integrity. The early biosynthetic

enzymes Coq1p and Coq2p, which provide the intermediate PPHB, do not interact with complex Q.

*Outstanding questions in CoQ biosynthesis*

Despite nearly 60 years of research into CoQ biosynthesis, many aspects of the pathway remain poorly characterized. In the biosynthesis of 4-HB, the pathway from 4-HPP to 4-HBz remains enigmatic, with investigations complicated by the presence of redundant pathways[63]. Though these redundant mechanisms are present *in vivo,* the complete elucidation of each individual pathway, its exact contribution, regulation, will greatly accelerate our understanding of CoQ biosynthesis. Additionally, the mechanism by which 4-HB and isoprenoid pyrophosphates reach the mitochondrial matrix is poorly understood. The biophysical characteristics of the mitochondrial inner membrane suggests that membrane transporter are needed for both precursors, however, no such proteins have been identified to date. As I will elaborate in the next section, efforts to identify transporters have been hampered by redundant mechanisms as well as difficult biochemical characterizations.

In the head-group modification stage, there are still steps in the eukaryotic pathway without an identified enzyme. The protein(s) responsible for the decaboxylation and hydroxylation of polyprenyl-vanillate (PPVA) to demethoxy-demethyl-coenzyme Q (DDMQ) remain(s) unknown. In bacteria, the decaboxylation and hydroxylation steps are catalyzed by UbiD and UbiH[40,74], respectively, with UbiD function supported by UbiX[75]. However, no eukaryotic homolog has been identified, suggesting an evolutionary split in CoQ biosynthesis between eukaryotes and prokaryotes. The different orders of the decarboxylation/hydroxylation and the hydroxylation/methylation steps between these two domains is evidence of this divergence[65].

Additional work is needed to identify the proteins responsible for these steps in eukaryotes, thereby closing the gaps in the pathway.

Many CoQ biosynthetic proteins have auxiliary functions that are poorly understood. These proteins (Coq4p, Coq8p, Coq9p, and Coq10p), have been shown to contribute to CoQ biosynthesis by genetic and biochemical studies, however their exact roles are unclear[2]. Furthermore, the number of other proteins that contribute to CoQ biosynthesis is unknown. These proteins likely evaded identification in previous genetic screens due to functional redundancies, making them nonessential under screening conditions. It is also possible that these proteins have roles in multiple cellular processes, thereby masking their role in CoQ biosynthesis. Thus, identifying and characterizing these additional proteins remains challenging. However, the development of novel genetic screening and '-omics' approaches should accelerate these efforts.

The exact composition of complex Q is also unknown, with efforts hindered by the difficulties of purifying reconstituting the complex *in vitro.* Thus, while it's known that Coq3p-Coq9p are constituents of complex Q, the presence of any additional proteins, their structural arrangement, and overall stoichiometry are unknown. Structural efforts using cryo-EM have elucidated some details about complex Q function. One recent study solved an octomeric complex of human COQ7 and COQ9[76], and proposed a mechanism whereby the complex deforms the lipid membrane, potentially enabling it to extract intermediates. Additional unknowns include the exact role of the ER-mitochondrial complex domains and the regulation of complex Q levels. Uncovering these details will greatly accelerate our efforts to understand CoQ deficiencies and develop new therapeutic approaches.

**The mitochondrial carrier system (MCS)**

*Bioenergetic justification and early history*

In 1949, Eugene Kennedy and Albert Lehninger demonstrated that fatty acid oxidation and the TCA cycle occur in mitochondria, and that these processes were responsible for the redox reactions that generated ATP[77]. In the decade that followed, work begun to fully understand these newly designated 'intracellular power plants.' Throughout the 1950s, the concepts of the respiratory chain, electron transport, and OxPhos were introduced and refined[78]. However, one aspect of this system remained elusive to researchers–the mechanism linking electron transport to ATP generation. At the time, the only known mechanism of ATP generation was that of substrate-level phosphorylation in glycolysis. Thus, using substrate-level phosphorylation as a model, a 'chemical' hypothesis was developed in which a common high-energy intermediate (denoted with '~') would supply the energy to generate ATP from ADP and $P_i$. However, such an intermediate was never found.

The problem of the missing intermediate was finally resolved in 1961, when Peter Mitchell introduced his theory of chemiosmosis[79]. Mitchell's theory, which was expanded and generalized in 1966, dismissed the idea of a chemical 'high-energy' intermediate[80]. Instead, the intermediate was a proton electrochemical potential across the mitochondrial membrane. The respiratory chain would not only transport electrons but would also pump protons across the membrane, generating a proton gradient. The electrochemical potential would then drive a proton-translocating ATP synthase, generating ATP from ADP and $P_i$. Thus, it was the energy of protons going down its electrochemical gradient and returning to the matrix that generated ATP. Mitchell's theory, developed without any experimental data, was not warmly received by the scientific community. It was not until the mid-1970s, following a series of confirmatory experiments with ATP

synthase[81–83], that chemiosmosis was finally accepted. For this development, Mitchell would win the Nobel Prize in Chemistry in 1978.

Mitchell's theory introduced four essential postulates[80], with which to further develop the theory or to test by experimentation. The postulates are summarized below:

(a) The membrane-located respiratory chain couples the transport of electrons to the translocation of protons across the membrane.

(b) A membrane-located ATP synthase reversibly couples the translocation of protons across the membrane to synthesis or hydrolysis of ATP.

(c) There exists a coupling membrane with low permeability to protons, other cations, and anions.

(d) The mitochondrial membrane contains a system of substrate-specific carriers that enable the reversible translocation of metabolites, including anionic species, without the collapse of the membrane potential.

Thus, in developing his theory of chemiosmosis, Mitchell implied the existence of mitochondrial transporters (also interchangeably called carriers, translocases, or translocators). The rest of the 1960s was dedicated to confirming the existence of these transporters to prove (or more likely, disprove) Mitchell's theory[84]. These studies were largely focused on the transport of ADP and ATP, but the transport of other substrates including malate, succinate, oxoglutarate, citrate, glutamate, and aspartate were also investigated[85]. These studies were accelerated by the discovery of actractyloside and bonkrekic acid as specific inhibitors of the ADP/ATP carriers[86,87], thus enabling accurate uptake measurements. By the end of the decade, enough evidence had accumulated such that mitochondrial metabolite transport was generally accepted.

The earliest studies relied on secondary measures of transport. In one such approach, ammonium salts of the anion under investigations are incubated with isolated mitochondria[85] (often from rat livers or bovine hearts). The ammonium is deprotonated, and the resulting free ammonia diffuses across the membrane. If the anion is transported ('penetrant'), it will be transported along with a proton or exchanged for hydroxide (the two are indistinguishable), and the mitochondrial ammonia will become protonated. This protonation traps the ammonium in the matrix increasing the osmolarity in the matrix. As water crosses membrane to due osmotic pressure, the mitochondria swell, decreasing its turbidity. Thus, by simply measuring the $A_{546}$, one can make a qualitative measurement of mitochondrial anion transport. This also provides a relatively easy approach to determine if a substrate is transported, especially if access to radiolabeled substrates is limited. This approach also provided the first proof that mitochondrial carriers function as a connected system[88]. Nevertheless, the qualitative and indirect nature of this assay limited the utility of this assay for kinetic measurements.

Direct assay systems were developed at the same time as the indirect approaches and provided a more quantitative measurement of transport[89]. These assays utilized radiolabeled substrates that allowed for accurate and sensitive uptake measurements. The biggest hurdle of the direct approach was development of rapid separation techniques to isolate mitochondria from the incubation media. This was crucial to ensure accurate kinetic, as opposed to equilibrium, measurements. In one approach, called centrifugal filtration, the uptake reaction is placed on top of a layer of silicone oil, which itself was atop a layer of perchloric acid. To stop the reaction, the tube is centrifuged, drawing the mitochondria in to the silicone oil layer and leaving the incubation media behind. Further centrifugation draws the mitochondria into the perchloric acid, quenching all metabolism and releasing any imported substrates into the acid for scintillation counting. A

different approach, sieve filtration, relies on microporous filters to separate mitochondria from the incubation media. While filtration is very quick, this approach also requires extensive washing of the filter, which may lead to matrix contents leaking out. The third approach, inhibitor-stop, uses inhibitors to rapidly halt all import, thereby trapping the substrates in the mitochondria. The mitochondria can then be isolated from the incubation media by simple centrifugation or by filtration. The rapid action of the inhibitor allows for more accurate kinetic measurements. This accuracy also benefits from the inability of imported substrates to leak out, as the carriers are inactive.

These mitochondrial uptake assays were used extensively to define the kinetics of many transported substrates. However, a major limitation of these assays was their inability to measure uptake in isolation. In other words, uptake was always measured in the presence of other carriers and proteins in the mitochondrial membrane. Since these carriers were linked together in a larger system, performing these assays in mitochondria could affect the measured kinetic parameters for a particular substrate or carrier. To address this Martin Klingenberg and colleagues developed a protocol for the solubilization, purification, and reconstitution of the ADP/ATP carrier from beef heart mitochondria[90–93]. Generally, these protocols involved solubilizing the isolated mitochondria with detergent, usually Triton X-100 or Triton X-114, to release the membrane proteins without aggregation. Purification is then accomplished on a hydroxyapatite column, which binds to soluble proteins, letting membrane proteins run off the column. The purified carriers are then reconstituted using egg-yolk phospholipids to form proteoliposomes. The reconstituted procedure initially involved multiple freeze-thaw cycles followed by sonication. This was later phased out as the cyclic detergent removal method, which involved slowly removing detergent by Amberlite resin, gained popularity[94]. The major benefit of the Amberlite resin was the complete removal of

detergent, yielding sealed liposomes. With the development of this purification and reconstitution approach, carriers could now be studied in isolation. Throughout the remainder of 1970s and the 1980s, additional carriers were studied by this method, resulting in the characterization of the oxoglutarate, dicarboxylate, and citrate carriers, among others[94]. These characterization efforts went on to confirm the existence of substrate-specific carriers, proving Mitchell's fourth postulate of chemiosmotic theory.

Biochemical analysis of these carriers showed that they each were made up of a single protein of approximately 30-32 kDa[95]. Sequencing and topology modeling of these carriers showed six transmembrane helices, consisting of three two-helix homologous domains. Each carrier also contained the conserved signature motif:

PX[D/E]XX[K/R]X[K/R]

The presence of these features in all the sequenced carriers suggested that they belong to the same protein family. As genomic sequences became available in the 1990s, this conserved motif was used to identify additional carriers. As a result, 35 and 53 carriers were identified in the yeast *Saccharomyces cerevisiae* and in humans[95], respectively. At the same time, the development of genetic tools was enabling the targeted disruption of yeast genes. This technique was used by Gottfried Schatz, who in 1995, identified Atm1p as a mitochondrial ATP binding cassette (ABC) transporter in yeast[96]. The discovery of a non-SLC25 mitochondrial transporter raised the possibility of additional non-SLC25 carriers. Indeed, since the identification of Atm1p, a number of ABC transporters and other non-SLC25 carriers have been identified in yeast and humans[97].

The identification of these carriers started an ongoing effort to identify their substrates and define their physiological roles. These studies were accelerated by the successful bacterial expression, purification, and reconstitution of recombinant carriers by Ferdinando Palmieri's lab[98].

Similar recombinant approaches were also used for expression in yeast[95]. Thus, it was no longer needed to purify carriers from large amounts of animal tissue (due to their low abundance in mitochondria[99]). This approach, consisting of expression, purification, reconstitution, and assay (EPRA), quickly became the gold standard for studies on mitochondrial carriers (Figure 5). However, it should be noted that this approach is not trivial. Overexpression of membrane proteins is often toxic to bacteria and yeast, lowering expression yield[95]. When overexpressed in bacteria, the carriers overwhelm the cell's ability to process and direct them to cytoplasmic membrane, resulting in the formation of inclusion bodies. These must be solubilized before being properly refolded and reconstituted into proteoliposomes–processes with very low efficiencies[100]. If expressed in yeast, the presence of native carriers with overlapping substrate specificities can hinder downstream applications. Thus, the EPRA methods comes with many challenges. Nevertheless, this technique has been instrumental to our understanding of mitochondrial carrier function. The past two decades have also seen the development of alternative expression strategies that enable the expression and functional insertion of carriers in the bacterial membrane[100,101]. These efforts, led by Edmund Kunji, have resulted in the regular use of *Lactococcus lactis* in mitochondrial transporter studies.
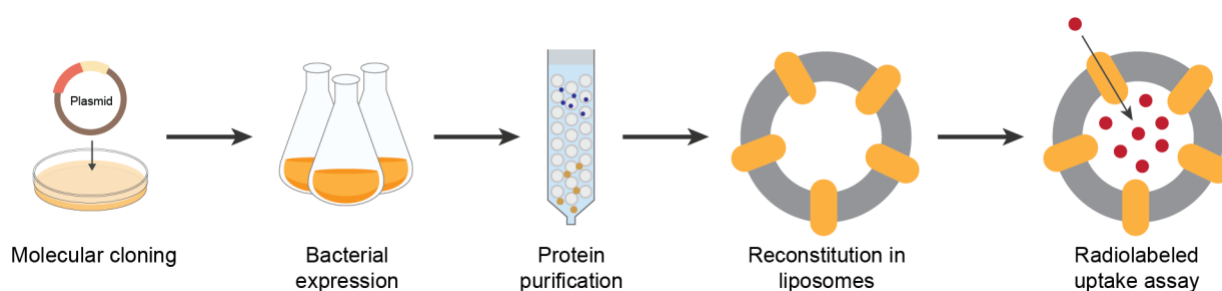


**Figure 5. Overview of the EPRA method.** This method is used to mitochondrial carriers in isolation. The approach involves cloning of the carrier of interest, expression in bacteria, purification, reconstitution into liposomes, followed by uptake assays with radiolabeled substrates.

With mitochondrial dysfunction being recognized in an increasing number of human diseases, mitochondrial carriers, with their roles as metabolite gatekeepers, have received renewed interest as of late. By harnessing the power of systems biology, recent studies have assigned novel functions to orphan transporters and identified secondary functions for previously established transporters. These studies have greatly helped our understanding of mitochondrial metabolism and may lead to the development of new therapeutics for mitochondrial diseases.

*SLC25 carriers*

The SLC25 (solute carrier family 25) family is a group of carriers located predominantly in the inner mitochondrial membrane. With 35 and 53 members in yeast and humans, respectively, it is the largest known family of SLCs[102]. The SLC25 carriers mediate the bulk of metabolite transport across the mitochondrial membrane, and as such, must accommodate a wide array potential substrates. Direct uptake assays, along with sequence alignments, have grouped these carriers into those that transport amino acids, di- and tri-carboxylates, fatty acids, inorganic ions, nucleotides, and coenzymes[95,103,104]. While the majority of these carriers mediate metabolite transport across the inner mitochondrial membrane, a handful are located in other cellular membranes where they carry out different functions. The human SLC25A17 (Ant1p in yeast) serves as peroxisomal transporter of nucleotides and other cofactors[105]. Additionally, the human SLC25A46 (Ugo1p in yeast) and SLC25A50 (also called MTCH2) are located in the outer mitochondrial membrane, where they are involved in lipid homeostasis[106] and membrane protein insertion[107], respectively.

The primary and secondary structures of most SLC25 carriers consist of approximately 300 residues organized into six transmembrane helices (Figure 6A). Further analysis, assisted by early crystal structures[108,109], identified three homologous 100-residue domains (repeats), each containing two transmembrane helices (one odd and one even numbered) and a short matrix α-helix connecting the two transmembrane helices. The N- and C-termini of the carriers are located in the intermembrane space and the conserved signature motif PX[D/E]XX[K/R]X[K/R] is in the odd numbered helix of each repeat[110]. The three repeats are organized around a central substrate translocation path, forming a threefold (tripartite) pseudosymmetry (Figure 6B). Within the substrate translocation path, at the center of the membrane, exists the common substrate binding site. This contains the contact points–individual or groups of residues that physically interact with the substrate. Carriers contain three contact points corresponding to each repeat. Homology modeling and bioinformatic analyses have identified the putative substrate binding sites in nearly every yeast and human carrier[111], thereby enabling targeted mutagenesis studies and prediction of substrates.
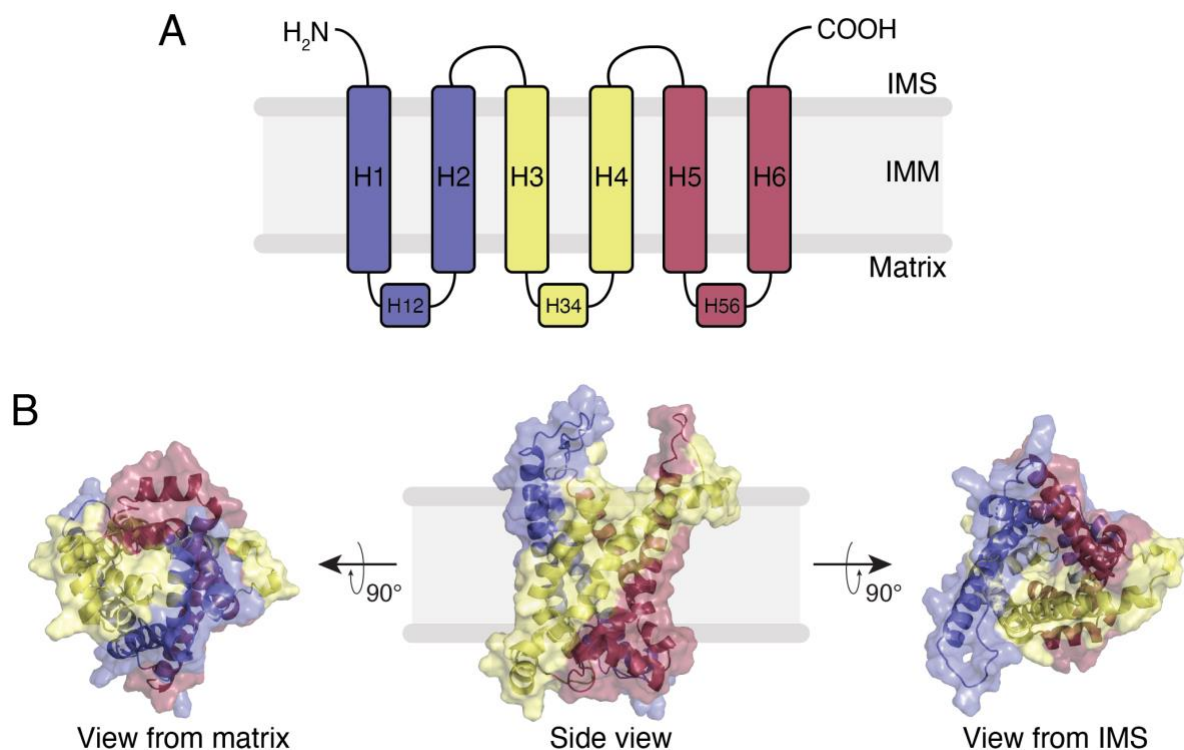
**Figure 6. General topology and structure of mitochondrial carriers.** (**A**) Topology of carriers in the inner membrane. The six transmembrane helices are organized into three homologous domains (repeats) colored blue, yellow, and red. Each repeat contains an odd-numbered helix, a short matrix helix, and an even-numbered helix. The N- and C-termini are in the cytosol (intermembrane space). (**B**) Structure of a mitochondrial carrier open to the intermembrane space, or cytosol (c-state). Views from the matrix, side, and intermembrane space are shown. The three repeats organize around a central translocation pathway, forming a tripartite pseudosymmetry. The common substrate binding site, located at the midpoint in the membrane, is open to the intermembrane space but closed to the matrix.

Uptake assays in isolated mitochondria and reconstituted proteoliposomes showed that carriers act as exchangers[94]. It was thought that this occurred though an alternating-access

mechanism, where the substrate binding site is exposed to either the intermembrane space or the matrix[112]. This would allow substrate transport while preserving the membrane potential–a key aspect of Mitchell's chemiosmotic theory. Proving this mechanism required structures of the carrier in both conformations. However, the carriers' small size, monomeric nature, and instability as membrane proteins made solving these structures challenging. Early structures of the ADP/ATP carrier were solved by using the inhibitor carboxyatractyloside (CATR) to stabilize the carrier in the c-state (carrier open to the cytosol or intermembrane space). The m-state (carrier open to the matrix) structure, bound to the inhibitor BKA, was finally solved in 2019[113]. These two structures helped confirm the alternative-access mechanism and provided structural insight into the transport mechanism.

At any point in time, the substrate binding site is only open to the intermembrane space (c-state) or the matrix[110] (m-state). To achieve these conformations, a network of salt-bridges seals off the substrate binding site from the matrix or the intermembrane space in the c- or m-state, respectively. In the c-state, the charged residues of the PX[D/E]XX[K/R]X[K/R] motif form interdomain salt bridges on the matrix side of the carrier (matrix network). The proline residues also contribute by causing kinks in the odd-numbered helices that help close off the substrate binding site from the matrix. In the m-state, the charged residues of another highly conserved motif [Y/F][D/E]xx[R/K], located on the even-numbered helices, form another set of interdomain salt bridges on the cytoplasmic side of the carrier (cytoplasmic network). The m-state is assisted by two additional conserved motifs: $\pi$G$\pi$x$\pi$Gxx$\pi$xxx$\pi$ on odd-numbered helices and $\pi$xxx$\pi$ on even-numbered helices, where $\pi$ represents a small amino acid. The enrichment of small amino acids at these motifs allow the helices to pack closely together, thus allowing the salt bridges to form.

From these solved structures, a structural mechanism of transport was proposed in which binding of the substrate disrupts the existing salt bridge network[110]. The domains then rock outward, using the substrate binding site as a hinge. This opens the previously occluded side and closes the previously open side, which now forms its own salt bridge network. The transported substrate is then released and a new substrate binds, causing the same events to happen in reverse. The need for a counter-substrate depends on the strength of the salt bridge networks in the c- and m- states, and it is the strength of these networks that decides whether a carrier is a strict exchanger, net importer, or net exporter[111]. In carriers that are strict exchangers, both the cytoplasmic and matrix salt bridge networks are intact, with the majority of charged residues forming ionic interactions. Thus, the binding energy of a counter-substrate is needed to disrupt the salt bridges and allow for conformation change. In a net importer or exporter, the cytoplasmic and matrix networks, respectively, are only partially intact. In these cases, the carrier can revert to its previous conformation spontaneously without the need for a counter-substrate. This explains why mitochondrial carriers, despite being annotated as exchangers, can function as importers and exporters. Bioinformatics studies have examined the integrity of these salt bridge networks in numerous yeast and human carriers, resulting in predicted directions of transport for these carriers.

While all carriers have this this tripartite symmetry, some transporters have additional regulatory domains[110]. The human aspartate/glutamate carriers SLC25A12 and SCL25A13 have N-terminal calcium binding EF-hand motifs and a C-terminal amphipathic helix. The yeast ortholog, Agc1p, has the amphipathic helix but no EF-hands. The ATP-Mg/$P_i$ carriers SLC25A24 and Sal1p also contain N-terminal calcium binding EF-hand motifs and an amphipathic helix. These carriers are activated upon calcium binding; however, the structural mechanism of this regulation is poorly understood.

*Non-SLC25 carriers*

Several non-SLC25 carriers have been identified, expanding our list of mitochondrial transporters beyond those of the canonical SLC25 family[114]. These carriers can be broadly organized in to three classes: ABC transporters, mitochondrial pyruvate carrier (MPC) complex, and sideroflexins.

ABC transporters are a large family of translocases that utilize the hydrolysis of ATP to transport substrates[97]. Each ABC transporter contains four domains: two nucleotide binding domains and two transmembrane domains consisting of multiple helices. The yeast Atm1p was the first mitochondrial ABC transporter to be discovered[96]. Since then, additional transporters have been identified in yeast and human mitochondria. Currently, yeast and humans each have at least three mitochondrial ABC transporters. Based on their membrane orientation, they are all predicted to be exporters. Cells lacking ABC transporters have disrupted heme and iron homeostasis, suggesting that they have roles in these processes[97]. Atm1p, which is homologous to the human ABCB7, exports Fe-S clusters into the cytosol[115]. Human ABCB10, homologous to the yeast Mdl1p, forms complexes with heme biosynthetic enzymes and has been shown to export biliverdin[116,117]. Substrates for the remaining ABC transporter have not been identified.

The carriers of the MPC complex make up the SLC54 family. Two proteins from this group, MPC1 and MPC1 (Mpc1 and Mpc2p in yeast), are required to form this complex[118,119]. The MPC transports pyruvate, thus linking cytosolic glycolysis to the mitochondrial TCA cycle. The proteins of the MPC were identified in 2012, although they may have been discovered back in 1981[120]. Transport by MPC is dependent on the proton gradient. The transport mechanism and subunit stoichiometry of the MPC is still poorly understood.

The sideroflexin (SFXN) carriers constitute the SLC56 family. Humans have five members of this family (SFXN1-SFXN5) while yeast have only one member (Fsf1p). These proteins were originally named after the two phenotypes of mice with mutated *Sfxn1*: sideroblastic anemia and a flexed tail[121]. However, a mechanistic link between SFXN1 and the observed phenotype was never established. Studies in the 1990s and early 2000s suggested that SFXNs are mitochondrial tricarboxylate transporters[122,123]. This fell out of favor as SLC25A1 was shown to be the primary transporter of tricarboxylates[124]. In 2018, SFXN1 was identified as a mitochondrial serine transporter[125]. In doing so, SFXN1 supports the generation of 5,10-methylene-tetrahydrofolate and 10-formyl-tetrahydrofolate, which act a one-carbon donors for nucleotide synthesis. Expression of the yeast Fsf1p partially rescued the phenotypes of SFXN1$^{-/-}$ cells, suggesting a conserved function in yeast. While expression of SFXN3 fully compensated for SFXN1 loss, expression of the other three SFXN members (SFXN2, 4, and 5) rescued phenotypes to varying extents. Thus, its likely that the other SFXNs have other cellular functions outside of serine transport and one-carbon metabolism. Another report implicated SFXN1 in respiratory chain function[126]. Imported serine contributes to heme and α-ketoglutarate metabolism, thereby supporting Complex III integrity and activity. The substrates and cellular functions of the other SFXNs are largely unknown.

A few non-SLC25 carriers have been identified that do not belong to the classes listed above. These include the glutamine carrier[127] (a variant of SLC1A5) and the riboflavin carrier[128] (SLC22A14). The exact number of these other carriers is unknown.

*Outstanding questions in mitochondrial transporters*

Transporters are notoriously difficult to study, as nearly every step in their characterization process is highly prone to failure. As such, elucidating their substrates and defining their

physiological roles is a painstakingly slow task. The large number of mitochondrial transporters–
the most of any SLC family–only adds to this challenge. The result is our limited understanding
of mitochondrial transporter function. Below, I summarize a few of the outstanding gaps in
knowledge in the field.

One of the most pressing issues is the lack of a complete annotation of mitochondrial
transporter substrates. The past three decades have greatly advanced our knowledge of
transporters, resulting in the biochemical characterization of many mitochondrial transporters[95].
Nevertheless, an inherent limitation of these studies is their low throughput. The technical
challenges of the EPRA method means that only a limited number of substrates can be practically
tested. Furthermore, these assays rely radiolabeled substrates, which can be unavailable or
expensive to procure. Thus, even if a carrier's substrates have been confirmed by uptake assays, it
is possible that it can still transport other substrates. Additionally, many more carriers are
hypothesized to transport a particular substrate, but lack biochemical evidence. While the proposed
substrates are backed by genetic and phenotypic data, direct uptake is still needed to validate those
claims. Lastly, there are still several orphan mitochondrial transporters without an identified or
proposed substrate. Thus, while there is still a place for biochemical transporter studies, novel
unbiased and high-throughput chemical screening approaches are needed to accelerate these
characterization efforts.

Many metabolites that are known to be transported into mitochondria lack an identified
transporter. The exact number of these metabolites is unknown, but is likely to be higher than the
number of known mitochondrial transporters[129]. Given that most, if not all, SLC25 carriers have
been identified, it suggests that SLC25 carriers can accommodate additional substrates. It also
implies that non-SLC25 carriers play a larger role in mitochondrial metabolite transport. However,

the number and identity of these non-SLC25 carriers are unknown. Finding these transporters is a difficult task without any prior information. The use of genetic screens to generate leads and hypotheses should help us identify new transporters. However, given that mitochondrial carriers often have overlapping substrate specificities as well as multiple mechanisms of redundancy, these genetic screens may need to be tailored for an individual substrate[130]. Knockout, knockdown, or overexpression of transporters, followed by phenotyping, can often provide clues into a transporter's function. However, phenotypes can be masked if multiple physiologically relevant substrates are transported.

Mutations in mitochondrial carriers have been implicated in an increasing number of human diseases[131]. However, our ability to diagnose, counsel, and treat these patients is limited by our incomplete understanding of mitochondrial transporters. Thus, it is imperative that we dissect the physiological roles of these carriers and their related pathways. By gaining insight into how these carriers contribute to normal physiology and how their dysfunction leads to mitochondrial disease, we can develop novel diagnostic (e.g., biomarkers) and therapeutic (e.g., supplementation) approaches.

The issues mentioned above represent only a few of those regarding mitochondrial transporters. Other important aspects include the regulation of carrier expression, the coordination of multiple carriers, the bioenergetics of importing anions, and the structural basis of substrate recognition[110,132]. Thus, it is clear there is much more to learn about these carriers.

**Transport of CoQ precursors**

Mitochondrial carriers are also believed to contribute to CoQ biosynthesis by transporting the cytosolic precursors 4-HB and isoprenoid pyrophosphates into the matrix[2]. Due to their

negative charge, these precursors cannot passively diffuse across the impermeable membrane. Thus, a protein carrier must mediate this process. While transporters for 4-HB and IPP have been described in bacteria[133] and plant chloroplasts[134–136], respectively, none have been identified in mitochondria. The reasons for this are the redundant mechanisms inherent to the mitochondrial carrier system[132]. Overlapping substrates, combined with shifts in metabolic processes, make the cell robust to single carrier disruptions. Furthermore, yeast are capable of growing on non-fermentable carbon sources with decreased CoQ abundance[137]. Thus, large-scale genetic screens based on respiratory growth have missed these transporters. In the remainder of this dissertation, I will describe my efforts to identify and functionally characterize mitochondrial carriers in CoQ biosynthesis.

**References:**

1. Stefely, J. A. & Pagliarini, D. J. Biochemistry of Mitochondrial Coenzyme Q Biosynthesis. *Trends Biochem Sci* 42, 824–843 (2017).

2. Guerra, R. M. & Pagliarini, D. J. Coenzyme Q biochemistry and biosynthesis. *Trends Biochem Sci* (2023) doi:10.1016/j.tibs.2022.12.006.

3. Mitchell, P. The protonmotive Q cycle: A general formulation. *Febs Lett* 59, 137–139 (1975).

4. Jones, M. E. Pyrimidine Nucleotide Biosynthesis in Animals: Genes, Enzymes, and Regulation of UMP Biosynthesis. *Annu Rev Biochem* 49, 253–279 (1980).

5. Martínez-Reyes, I. *et al.* Mitochondrial ubiquinol oxidation is necessary for tumour growth. *Nature* 585, 288–292 (2020).

6. Frerman, F. E. Acyl-CoA dehydrogenases, electron transfer flavoprotein and electron transfer flavoprotein dehydrogenase. *Biochem Soc T* 16, 416–418 (1988).

7. Vettore, L. A., Westbrook, R. L. & Tennant, D. A. Proline metabolism and redox; maintaining a balance in health and disease. *Amino Acids* 53, 1779–1788 (2021).

8. Ziosi, M. *et al.* Coenzyme Q deficiency causes impairment of the sulfide oxidation pathway. *Embo Mol Med* 9, 96–111 (2017).

9. Chang, C.-F. *et al.* CoQ Regulates Brown Adipose Tissue Respiration and Uncoupling Protein 1 Expression. *Antioxidants* 12, 14 (2022).

10. Fontaine, E., Ichas, F. & Bernardi, P. A Ubiquinone-binding Site Regulates the Mitochondrial Permeability Transition Pore*. *J Biol Chem* 273, 25734–25740 (1998).

11. Navas, P., Villalba, J. M. & Cabo, R. de. The importance of plasma membrane coenzyme Q in aging and stress responses. *Mitochondrion* 7, S34–S40 (2007).

12. Do, T. Q., Schultz, J. R. & Clarke, C. F. Enhanced sensitivity of ubiquinone-deficient mutants of Saccharomyces cerevisiae to products of autoxidized polyunsaturated fatty acids. *Proc National Acad Sci* 93, 7534–7539 (1996).

13. Poon, W. W., Do, T. Q., Marbois, B. N. & Clarke, C. F. Sensitivity to treatment with polyunsaturated fatty acids is a general characteristic of the ubiquinone-deficient yeast coq mutants. *Mol Aspects Med* 18, 121–127 (1997).

14. Doll, S. *et al.* FSP1 is a glutathione-independent ferroptosis suppressor. *Nature* 575, 693–698 (2019).

15. Bersuker, K. *et al.* The CoQ oxidoreductase FSP1 acts in parallel to GPX4 to inhibit ferroptosis. *Nature* 575, 688–692 (2019).

16. Sévin, D. C. & Sauer, U. Ubiquinone accumulation improves osmotic-stress tolerance in Escherichia coli. *Nat Chem Biol* 10, 266–272 (2014).

17. Alcázar-Fabra, M., Trevisson, E. & Brea-Calvo, G. Clinical syndromes associated with Coenzyme Q10 deficiency. *Essays Biochem* 62, 377–398 (2018).

18. Nunnari, J. & Suomalainen, A. Mitochondria: in sickness and in health. *Cell* 148, 1145–59 (2012).

19. Emmanuele, V. *et al.* Heterogeneity of Coenzyme Q10 Deficiency: Patient Study and Literature Review. *Arch Neurol-chicago* 69, 978–983 (2012).

20. Navas, P. *et al.* Secondary CoQ10 deficiency, bioenergetics unbalance in disease and aging. *Biofactors* 47, 551–569 (2021).

21. Gempel, K. *et al.* The myopathic form of coenzyme Q10 deficiency is caused by mutations in the electron-transferring-flavoprotein dehydrogenase (ETFDH) gene. *Brain* 130, 2037–44 (2007).

22. Wang, Y. & Hekimi, S. Mitochondrial dysfunction and longevity in animals: Untangling the knot. *Science* 350, 1204–7 (2015).

23. Wang, Y. & Hekimi, S. Understanding Ubiquinone. *Trends Cell Biol* 26, 367–378 (2016).

24. Kalen, A., Appelkvist, EL. & Dallner, G. Age-related changes in the lipid compositions of rat and human tissues. *Lipids* 24, 579–84 (1989).

25. Liu, J. L., Yee, C., Wang, Y. & Hekimi, S. A single biochemical activity underlies the pleiotropy of the aging-related protein CLK-1. *Sci Rep* 7, 859 (2017).

26. Liu, X. *et al.* Evolutionary conservation of the clk-1-dependent mechanism of longevity: loss of mclk1 increases cellular fitness and lifespan in mice. *Genes Dev* 19, 2424–34 (2005).

27. Larsen, P. L. & Clarke, C. F. Extension of life-span in Caenorhabditis elegans by a diet lacking coenzyme Q. *Science* 295, 120–3 (2002).

28. Crane, F. L., Hatefi, Y., Lester, R. L. & Widmer, C. Isolation of a quinone from beef heart mitochondria. *Biochim Biophys Acta* 25, 220–221 (1957).

29. MORTON, R. A. Ubiquinone. *Nature* 182, 1764–1767 (1958).

30. Crane, F. L. Discovery of ubiquinone (coenzyme Q) and an overview of function. *Mitochondrion* 7, S2–S7 (2007).

31. Morton, R. A. Ubiquinones (Coenzymes Q), Ubichromenols, and Related Substances. *Vitamins Hormones* 19, 1–42 (1962).

32. Bentley, R., Ramsey, V. G., Springer, C. M., Dialameh, G. H. & Olson, R. E. The origin of the benzoquinone ring of coenzyme Q9 in the rat. *Biochem Bioph Res Co* 5, 443–446 (1961).

33. OLSON, R. E. *et al.* BENZOATE DERIVATIVES AS INTERMEDIATES IN THE BIOSYNTHESIS OF COENZYME Q IN THE RAT. *J Biological Chem* 238, 3146–8 (1963).

34. RUDNEY, H. & PARSON, W. W. THE CONVERSION OF P-HYDROXYBENZALDEHYDE TO THE BENZOQUINONE RING OF UBIQUINONE IN RHODOSPIRILLUM RUBRUM. *J Biological Chem* 238, 3137–8 (1963).

35. Parson, W. W. & Rudney, H. THE BIOSYNTHESIS OF THE BENZOQUINONE RING OF UBIQUINONE FROM p-HYDROXYBENZALDEHYDE AND p-HYDROXYBENZOIC ACID IN RAT KIDNEY, AZOTOBACTER VINELANDII, AND BAKER'S YEAST*. *Proc National Acad Sci* 51, 444–450 (1964).

36. Gloor, U. & Wiss, O. Zur Biosynthese des Ubichinons. *Experientia* 14, 410–411 (1958).

37. Gloor, U. & Wiss, O. On the biosynthesis of ubiquinone (50). *Arch Biochem Biophys* 83, 216–222 (1959).

38. Friis, P., Daves, G. D. & Folkers, K. Complete Sequence of Biosynthesis from p-Hydroxybenzoic Acid to Ubiquinone 1. *J Am Chem Soc* 88, 4754–4756 (1966).

39. Young, I. G., Leppik, R. A., Hamilton, J. A. & Gibson, F. Biochemical and Genetic Studies on Ubiquinone Biosynthesis in Escherichia coli K-12: 4-Hydroxybenzoate Octaprenyltransferase. *J Bacteriol* 110, 18–25 (1972).

40. Cox, G. B., Young, I. G., McCann, L. M. & Gibson, F. Biosynthesis of Ubiquinone in Escherichia coli K-12: Location of Genes Affecting the Metabolism of 3-Octaprenyl-4-hydroxybenzoic Acid and 2-Octaprenylphenol. *J Bacteriol* 99, 450–458 (1969).

41. Young, I. G., McCann, L. M., Stroobant, P. & Gibson, F. Characterization and Genetic Analysis of Mutant Strains of Escherichia coli K-12 Accumulating the Ubiquinone Precursors 2-Octaprenyl-6-Methoxy-1,4-Benzoquinone and 2-Octaprenyl-3-Methyl-6-Methoxy-1,4-Benzoquinone. *J Bacteriol* 105, 769–778 (1971).

42. Stroobant, P., Young, I. G. & Gibson, F. Mutants of Escherichia coli K-12 Blocked in the Final Reaction of Ubiquinone Biosynthesis: Characterization and Genetic Analysis. *J Bacteriol* 109, 134–139 (1972).

43. Trumpower, B. L., Houser, R. M. & Olson, R. E. Studies on Ubiquinone DEMONSTRATION OF THE TOTAL BIOSYNTHESIS OF UBIQUINONE-9 IN RAT LIVER MITOCHONDRIA. *J Biol Chem* 249, 3041–3048 (1974).

44. Casey, J. & Threlfall, D. R. Synthesis of 5-demethoxyubiquinone-6 and ubiquinone-6 from 3-hexaprenyl-4-hydroxybenzoate in yeast mitochondria. *Febs Lett* 85, 249–253 (1978).

45. Tzagoloff, A., Akai, A. & Needleman, R. B. Assembly of the mitochondrial membrane system. Characterization of nuclear mutants of Saccharomyces cerevisiae with defects in mitochondrial ATPase and respiratory enzymes. *J Biological Chem* 250, 8228–35 (1975).

46. Goewert, R. R., Sippel, C. J. & Olson, R. E. Identification of 3,4-dihydroxy-5-hexaprenylbenzoic acid as an intermediate in the biosynthesis of ubiquinone-6 by Saccharomyces cerevisiae. *Biochemistry-us* 20, 4217–4223 (1981).

47. Ashby, N. M. & Edwards, P. A. Elucidation of the deficiency in two yeast coenzyme Q mutants. Characterization of the structural gene encoding hexaprenyl pyrophosphate synthetase. *J Biol Chem* 265, (1990).

48. Tzagoloff, A. & Dieckmann, C. L. PET genes of Saccharomyces cerevisiae. *Microbiol Rev* 54, 211–225 (1990).

49. Jonassen, T. & Clarke, C. F. Isolation and Functional Expression of Human COQ3, a Gene Encoding a Methyltransferase Required for Ubiquinone Biosynthesis*. *J Biol Chem* 275, 12381–12387 (2000).

50. Belogrudov, G. I. *et al.* Yeast COQ4 Encodes a Mitochondrial Protein Required for Coenzyme Q Synthesis. *Arch Biochem Biophys* 392, 48–58 (2001).

51. Barkovich, R. J. *et al.* Characterization of the COQ5 Gene from Saccharomyces cerevisiae EVIDENCE FOR A C-METHYLTRANSFERASE IN UBIQUINONE BIOSYNTHESIS*. *J Biol Chem* 272, 9182–9188 (1997).

52. Marbois, B. N. & Clarke, C. F. The COQ7 Gene Encodes a Protein in Saccharomyces cerevisiae Necessary for Ubiquinone Biosynthesis (∗). *J Biol Chem* 271, 2995–3004 (1996).

53. Johnson, A. *et al.* COQ9, a New Gene Required for the Biosynthesis of Coenzyme Q in Saccharomyces cerevisiae *. *J Biol Chem* 280, 31397–31404 (2005).

54. Awad, A. M. *et al.* Coenzyme Q10 deficiencies: pathways in yeast and humans. *Essays Biochem* 62, 361–376 (2018).

55. Barros, M. H. *et al.* The Saccharomyces cerevisiae COQ10 Gene Encodes a START Domain Protein Required for Function of Coenzyme Q in Respiration*. *J Biol Chem* 280, 42627–42635 (2005).

56. Allan, C. M. *et al.* Identification of Coq11, a New Coenzyme Q Biosynthetic Protein in the CoQ-Synthome in Saccharomyces cerevisiae *. *J Biol Chem* 290, 7517–7534 (2015).

57. Morgenstern, M. *et al.* Definition of a High-Confidence Mitochondrial Proteome at Quantitative Scale. *Cell Reports* 19, 2836–2852 (2017).

58. Gin, P. & Clarke, C. F. Genetic evidence for a multi-subunit complex in coenzyme Q biosynthesis in yeast and the role of the Coq1 hexaprenyl diphosphate synthase. *J Biol Chem* 280, 2676–81 (2005).

59. Hsieh, E. J. *et al.* Saccharomyces cerevisiae Coq9 polypeptide is a subunit of the mitochondrial coenzyme Q biosynthetic complex. *Arch Biochem Biophys* 463, 19–26 (2007).

60. Floyd, B. J. *et al.* Mitochondrial Protein Interaction Mapping Identifies Regulators of Respiratory Chain Function. *Mol Cell* 63, 621–632 (2016).

61. Stefely, J. A. *et al.* Mitochondrial protein functions elucidated by multi-omic mass spectrometry profiling. *Nat Biotechnol* 34, 1191–1197 (2016).

62. Payet, L. A. *et al.* Mechanistic Details of Early Steps in Coenzyme Q Biosynthesis Pathway in Yeast. *Cell Chem Biol* 23, 1241–1250 (2016).

63. Robinson, K. P. *et al.* Defining intermediates and redundancies in coenzyme Q precursor biosynthesis. *J Biological Chem* 296, 100643 (2021).

64. Banh, R. S. *et al.* The polar oxy-metabolome reveals the 4-hydroxymandelate CoQ10 synthesis pathway. *Nature* 597, 420–425 (2021).

65. Fernández-del-Río, L. & Clarke, C. F. Coenzyme Q Biosynthesis: An Update on the Origins of the Benzenoid Ring and Discovery of New Ring Precursors. *Metabolites* 11, 385 (2021).

66. Buhaescu, I. & Izzedine, H. Mevalonate pathway: a review of clinical and therapeutical implications. *Clin Biochem* 40, 575–84 (2007).

67. Poulter, C. D., Wiggins, P. L. & Le, A. T. Farnesylpyrophosphate synthetase. A stepwise mechanism for the 1'-4 condensation reaction. *J Am Chem Soc* 103, 3926–3927 (1981).

68. Okada, K. *et al.* Polyprenyl diphosphate synthase essentially defines the length of the side chain of ubiquinone. *Biochimica Et Biophysica Acta Bba - Lipids Lipid Metabolism* 1302, 217–223 (1996).

69. Ashby, M. N., Kutsunai, S. Y., Ackerman, S., Tzagoloff, A. & Edwards, P. A. COQ2 is a candidate for the structural gene encoding para-hydroxybenzoate:polyprenyltransferase. *J Biological Chem* 267, 4128–36 (1992).

70. Pierrel, F. *et al.* Involvement of mitochondrial ferredoxin and para-aminobenzoic acid in yeast coenzyme Q biosynthesis. *Chem Biol* 17, 449–59 (2010).

71. Ozeir, M. *et al.* Coenzyme Q biosynthesis: Coq6 is required for the C5-hydroxylation reaction and substrate analogs rescue Coq6 deficiency. *Chem Biol* 18, 1134–42 (2011).

72. Subramanian, K. *et al.* Coenzyme Q biosynthetic proteins assemble in a substrate-dependent manner into domains at ER-mitochondria contacts. *J Cell Biol* 218, 1353–1369 (2019).

73. Eisenberg-Bord, M. *et al.* The Endoplasmic Reticulum-Mitochondria Encounter Structure Complex Coordinates Coenzyme Q Biosynthesis. *Contact* 2, 2515256418825409 (2019).

74. Nakahigashi, K., Miyamoto, K., Nishimura, K. & Inokuchi, H. Isolation and characterization of a light-sensitive mutant of Escherichia coli K-12 with a mutation in a gene that is required for the biosynthesis of ubiquinone. *J Bacteriol* 174, 7352–7359 (1992).

75. Gulmezian, M., Hyman, K. R., Marbois, B. N., Clarke, C. F. & Javor, G. T. The role of UbiX in Escherichia coli coenzyme Q biosynthesis. *Arch Biochem Biophys* 467, 144–153 (2007).

76. Manicki, M. *et al.* Structure and functionality of a multimeric human COQ7:COQ9 complex. *Mol Cell* 82, 4307-4323.e10 (2022).

77. KENNEDY, E. P. & LEHNINGER, A. L. Oxidation of fatty acids and tricarboxylic acid cycle intermediates by isolated rat liver mitochondria. *J Biological Chem* 179, 957–72 (1949).

78. Ernster, L. & Schatz, G. Mitochondria: a historical review. *J Cell Biology* 91, 227s–255s (1981).

79. MITCHELL, P. Coupling of Phosphorylation to Electron and Hydrogen Transfer by a Chemi-Osmotic type of Mechanism. *Nature* 191, 144–148 (1961).

80. Mitchell, P. Chemiosmotic coupling in oxidative and photosynthetic phosphorylation. *Biochimica Et Biophysica Acta Bba - Bioenergetics* 1807, 1507–1538 (2011).

81. Maloney, P. C., Kashket, E. R. & Wilson, T. H. A Protonmotive Force Drives ATP Synthesis in Bacteria. *Proc National Acad Sci* 71, 3896–3900 (1974).

82. Jagendorf, A. T. & Uribe, E. ATP formation caused by acid-base transition of spinach chloroplasts. *Proc National Acad Sci* 55, 170–177 (1966).

83. Kagawa, Y. & Racker, E. Partial resolution of the enzymes catalyzing oxidative phosphorylation. IX. Reconstruction of oligomycin-sensitive adenosine triphosphatase. *J Biological Chem* 241, 2467–74 (1966).

84. Sluse, F. Mitochondrial metabolite carrier family, topology, structure and functional properties: an overview. *Acta biochimica Polonica* 43, 349—360 (1996).

85. CHAPPELL, J. B. SYSTEMS USED FOR THE TRANSPORT OF SUBSTRATES INTO MITOCHONDRIA. *Brit Med Bull* 24, 150–157 (1968).

86. Henderson, P. J. F. & Lardy, H. A. Bongkrekic Acid AN INHIBITOR OF THE ADENINE NUCLEOTIDE TRANSLOCASE OF MITOCHONDRIA. *J Biol Chem* 245, 1319–1326 (1970).

87. Winkler, H. H., Bygrave, F. L. & Lehninger, A. L. Characterization of the Atractyloside-sensitive Adenine Nucleotide Transport System in Rat Liver Mitochondria. *J Biol Chem* 243, 20–28 (1968).

88. Nicholls, D. G. & Ferguson, S. J. Bioenergetics (Fourth Edition). *Introd Part 1* 13–25 (2013) doi:10.1016/b978-0-12-388425-1.00002-6.

89. Palmieri, F. & Klingenberg, M. [26] Direct methods for measuring metabolite transport and distribution in mitochondria. *Methods Enzymol* 56, 279–301 (1979).

90. Riccio, P., Aquila, H. & Klingenberg, M. Purification of the carboxy-atractylate binding protein from mitochondria. *Febs Lett* 56, 133–138 (1975).

91. Kraemer, R., Aquila, H. & Klingenberg, M. Isolation of the unliganded adenosine 5'-diphosphate,adenosine 5'-triphosphate carrier-linked binding protein and incorporation into the membranes of liposomes. *Biochemistry-us* 16, 4949–4953 (1977).

92. Kraemer, R. & Klingenberg, M. Reconstitution of inhibitor binding properties of the isolated adenosine 5'-diphosphate,adenosine 5'-triphosphate carrier-linked binding protein. *Biochemistry-us* 16, 4954–4961 (1977).

93. Krämer, R. & Klingenberg, M. Reconstitution of adenine nucleotide transport with purified ADP, ATP-carrier protein. *Febs Lett* 82, 363–367 (1977).

94. Palmieri, F., Indiveri, C., Bisaccia, F. & Iacobazzi, V. [25] Mitochondrial metabolite carrier proteins: Purification, reconstitution, and transport studies. *Methods Enzymol* 260, 349–369 (1995).

95. Palmieri, F. & Monne, M. Discoveries, metabolic roles and diseases of mitochondrial carriers: A review. *Biochimica Et Biophysica Acta Bba - Mol Cell Res* 1863, 2362–78 (2016).

96. Leighton, J. & Schatz, G. An ABC transporter in the mitochondrial inner membrane is required for normal growth of yeast. *Embo J* 14, 188–195 (1995).

97. Schaedler, T. A. *et al.* Structures and functions of mitochondrial ABC transporters. *Biochem Soc T* 43, 943–951 (2015).

98. Fiermonte, G., Walker, J. E. & Palmieri, F. Abundant bacterial expression and reconstitution of an intrinsic membrane-transport protein from bovine mitochondria. *Biochem J* 294, 293–299 (1993).

99. Palmieri, F. The mitochondrial transporter family (SLC25): physiological and pathological implications. *Pflügers Archiv* 447, 689–709 (2004).

100. Monné, M., Chan, K. W., Slotboom, D. & Kunji, E. R. S. Functional expression of eukaryotic membrane proteins in Lactococcus lactis. *Protein Sci* 14, 3048–3056 (2005).

101. Ravaud, S. *et al.* Impaired Transport of Nucleotides in a Mitochondrial Carrier Explains Severe Human Genetic Diseases. *Acs Chem Biol* 7, 1164–1169 (2012).

102. Hediger, M. A., Clémençon, B., Burrier, R. E. & Bruford, E. A. The ABCs of membrane transporters in health and disease (SLC series): Introduction. *Mol Aspects Med* 34, 95–107 (2013).

103. Robinson, A. J. & Kunji, E. R. S. Mitochondrial carriers in the cytoplasmic state have a common substrate binding site. *Proc National Acad Sci* 103, 2617–2622 (2006).

104. Kunji, E. R. S. & Robinson, A. J. The conserved substrate binding site of mitochondrial carriers. *Biochimica Et Biophysica Acta Bba - Bioenergetics* 1757, 1237–1248 (2006).

105. Agrimi, G., Russo, A., Scarcia, P. & Palmieri, F. The human gene SLC25A17 encodes a peroxisomal transporter of coenzyme A, FAD and NAD+. *Biochem J* 443, 241–247 (2012).

106. Abrams, A. J. *et al.* Mutations in SLC25A46, encoding a UGO1-like protein, cause an optic atrophy spectrum disorder. *Nat Genet* 47, 926–932 (2015).

107. Guna, A. *et al.* MTCH2 is a mitochondrial outer membrane protein insertase. *Science* 378, 317–322 (2022).

108. Kunji, E. R. S. & Harding, M. Projection Structure of the Atractyloside-inhibited Mitochondrial ADP/ATP Carrier of Saccharomyces cerevisiae *. *J Biol Chem* 278, 36985–36988 (2003).

109. Pebay-Peyroula, E. *et al.* Structure of mitochondrial ADP/ATP carrier in complex with carboxyatractyloside. *Nature* 426, 39–44 (2003).

110. Ruprecht, J. J. & Kunji, E. R. S. Structural Mechanism of Transport of Mitochondrial Carriers. *Annu Rev Biochem* 90, 535–558 (2021).

111. Robinson, A. J., Overy, C. & Kunji, E. R. The mechanism of transport by mitochondrial carriers based on analysis of symmetry. *Proc National Acad Sci* 105, 17766–71 (2008).

112. Ruprecht, J. J. *et al.* Structures of yeast mitochondrial ADP/ATP carriers support a domain-based alternating-access transport mechanism. *Proc Natl Acad Sci U S A* 111, E426-34 (2014).

113. Ruprecht, J. J. *et al.* The Molecular Mechanism of Transport by the Mitochondrial ADP/ATP Carrier. *Cell* 176, 435-447.e15 (2019).

114. Cunningham, C. N. & Rutter, J. 20,000 picometers under the OMM: diving into the vastness of mitochondrial metabolite transport. *Embo Rep* 21, e50071 (2020).

115. Kispal, G., Csere, P., Prohl, C. & Lill, R. The mitochondrial proteins Atm1p and Nfs1p are essential for biogenesis of cytosolic Fe/S proteins. *Embo J* 18, 3981–3989 (1999).

116. Shintre, C. A. *et al.* Structures of ABCB10, a human ATP-binding cassette transporter in apo- and nucleotide-bound states. *Proc National Acad Sci* 110, 9710–9715 (2013).

117. Shum, M. *et al.* ABCB10 exports mitochondrial biliverdin, driving metabolic maladaptation in obesity. *Sci Transl Med* 13, (2021).

118. Bricker, D. K. *et al.* A mitochondrial pyruvate carrier required for pyruvate uptake in yeast, Drosophila, and humans. *Science* 337, 96–100 (2012).

119. Herzig, S. *et al.* Identification and functional expression of the mitochondrial pyruvate carrier. *Science* 337, 93–6 (2012).

120. Thomas, A. P. & Halestrap, A. P. Identification of the protein responsible for pyruvate transport into rat liver and heart mitochondria by specific labelling with [3H] N - phenylmaleimide. *Biochem J* 196, 471–479 (1981).

121. Fleming, M. D., Campagna, D. R., Haslett, J. N., Trenor, C. C. & Andrews, N. C. A mutation in a mitochondrial transmembrane protein is responsible for the pleiotropic hematological and skeletal phenotype of flexed-tail (f/f) mice. *Gene Dev* 15, 652–657 (2001).

122. Azzi, A., Glerum, M., Koller, R., Mertens, W. & Spycher, S. The mitochondrial tricarboxylate carrier. *J Bioenerg Biomembr* 25, 515–524 (1993).

123. Miyake, S. *et al.* Identification and characterization of a novel mitochondrial tricarboxylate carrier. *Biochem Bioph Res Co* 295, 463–468 (2002).

124. Mosaoa, R., Kasprzyk-Pawelec, A., Fernandez, H. R. & Avantaggiati, M. L. The Mitochondrial Citrate Carrier SLC25A1/CIC and the Fundamental Role of Citrate in Cancer, Inflammation and Beyond. *Biomol* 11, 141 (2021).

125. Kory, N. *et al.* SFXN1 is a mitochondrial serine transporter required for one-carbon metabolism. *Science* 362, (2018).

126. Acoba, M. G. *et al.* The mitochondrial carrier SFXN1 is critical for complex III integrity and cellular metabolism. *Cell Reports* 34, 108869 (2021).

127. Yoo, H. C. *et al.* A Variant of SLC1A5 Is a Mitochondrial Glutamine Transporter for Metabolic Reprogramming in Cancer Cells. *Cell Metab* 31, 267-283.e12 (2020).

128. Kuang, W. *et al.* SLC22A14 is a mitochondrial riboflavin transporter required for sperm oxidative phosphorylation and male fertility. *Cell Reports* 35, 109025 (2021).

129. Chen, W. W., Freinkman, E., Wang, T., Birsoy, K. & Sabatini, D. M. Absolute Quantification of Matrix Metabolites Reveals the Dynamics of Mitochondrial Metabolism. *Cell* 166, 1324-1337 e11 (2016).

130. Shi, X. *et al.* Combinatorial GxGxE CRISPR screen identifies SLC25A39 in mitochondrial glutathione transport linking iron homeostasis to OXPHOS. *Nat Commun* 13, 2483 (2022).

131. Palmieri, F. The mitochondrial transporter family SLC25: Identification, properties and physiopathology. *Mol Aspects Med* 34, 465–484 (2013).

132. Taylor, E. B. Functional Properties of the Mitochondrial Carrier System. *Trends Cell Biol* 27, 633–644 (2017).

133. Nichols, N. N. & Harwood, C. S. PcaK, a high-affinity permease for the aromatic compounds 4-hydroxybenzoate and protocatechuate from Pseudomonas putida. *J Bacteriol* 179, 5056–5061 (1997).

134. Soler, E., Clastre, M., Bantignies, B., Marigo, G. & Ambid, C. Uptake of isopentenyl diphosphate by plastids isolated from Vitis vinifera L. cell suspensions. *Planta* 191, 324–329 (1993).

135. Flugge, U. I. & Gao, W. Transport of isoprenoid intermediates across chloroplast envelope membranes. *Plant Biology* 7, 91–7 (2005).

136. Bick, J. A. & Lange, B. M. Metabolic cross talk between cytosolic and plastidial pathways of isoprenoid biosynthesis: unidirectional transport of intermediates across the chloroplast envelope membrane. *Arch Biochem Biophys* 415, 146–154 (2003).

137. Desbats, M. A. *et al.* The COQ2 genotype predicts the severity of coenzyme Q 10 deficiency. *Hum Mol Genet* 25, 4256–4265 (2016).

## Chapter 2: Hem25p is a mitochondrial IPP transporter

Jonathan Tai, Rachel M. Guerra, Sean W. Rogers, Zixiang Fang, Laura K. Muehlbauer, Evgenia Shishkova, Katherine A. Overmyer, Joshua J. Coon, David J. Pagliarini

**Author contributions:**

Conceptualization: JT, DJP

Methodology: JT, RMG, SWR, ZF, KAO, DJP

Formal analysis: JT, RMG, SWR, ZF, LKM, ES, KAO

Investigation: JT, RMG, SWR, ZF, LKM, ES, KAO

Funding acquisition: DJP

Supervision: JJC, DJP

Writing – original draft: JT, DJP

Writing – review & editing: JT, RMG, SWR, ZF, LKM, ES, KAO, JJC, DJP

This chapter, in full, was submitted as a manuscript to a peer-reviewed journal.

**Abstract**

Coenzyme Q (CoQ, ubiquinone) is an essential cellular cofactor comprised of a redox-active quinone head group and a long hydrophobic polyisoprene tail. How mitochondria access cytosolic isoprenoids for CoQ biosynthesis is a longstanding mystery. Here, via a combination of genetic screening, metabolic tracing, and targeted uptake assays, we reveal that Hem25p—a mitochondrial glycine transporter required for heme biosynthesis—doubles as an isopentenyl pyrophosphate (IPP) transporter in *Saccharomyces cerevisiae.* Mitochondria lacking Hem25p fail to efficiently incorporate IPP into early CoQ precursors, leading to loss of CoQ and turnover of CoQ biosynthetic proteins. Expression of Hem25p in *Escherichia coli* enables robust IPP uptake demonstrating that Hem25p is sufficient for IPP transport. Collectively, our work reveals that Hem25p drives the bulk of mitochondrial isoprenoid transport for CoQ biosynthesis in yeast.

**Introduction**

Coenzyme Q (CoQ, ubiquinone) is a redox-active lipid that functions as an essential cofactor for multiple cellular processes, including oxidative phosphorylation, pyrimidine biosynthesis, fatty acid oxidation, and ferroptotic defense[1-4]. Deficiencies in CoQ underlie multiple human pathologies, all of which have limited therapeutic options[5,6]. Despite being discovered 65 years ago, significant gaps in knowledge persist for how CoQ is synthesized and distributed throughout the cell, thereby limiting the development of interventional strategies[7-9].

CoQ is comprised of a fully-substituted quinone ring and a long hydrophobic tail consisting of repeating isoprene units (Fig. 1A). CoQ is synthesized on the matrix side of the inner mitochondrial membrane beginning with the precursors 4-hydroxybenzoate (4-HB) and isoprenoid pyrophosphates[10,11]. These precursors are each formed in the cytosol: 4-HB is derived from tyrosine or the shikimate pathway, and the isoprenoid pyrophosphates are produced by the mevalonate pathway[8]. Prior work has shown that mitochondria are able to import 4-HB and the isoprenoid isopentenyl pyrophosphate (IPP) for CoQ biosynthesis *in vitro*[12,13]; however, the protein(s) that enable this transport have remained elusive for decades. Previous efforts to identify proteins necessary for CoQ production — largely by leveraging the inability of yeast lacking CoQ to grow in respiratory conditions — have failed to identify candidate transporters[8,14,15], suggesting that there is either redundancy in the system or that the requisite transporter is essential for growth under common conditions[16].

**A targeted genetic screen for transporters in CoQ biosynthesis identifies Hem25p**

To identify mitochondrial transporters important for CoQ production, we created a custom panel of *S. cerevisiae* gene knockout (*geneΔ*) strains each lacking an established or potential mitochondrial transporter. This panel comprised *geneΔ* strains for all 35 members of the SLC25 family of mitochondrial transporters, which are responsible for nearly all known metabolite transport into mitochondria[17], and seven poorly characterized mitochondrial inner membrane proteins that might possess transporter function[18,19]. We grew strains in triplicate under fermentative conditions and monitored their ability to produce CoQ via targeted electrochemical detection coupled to HPLC (HPLC-ECD). Using this strategy, we identified four strains with significantly decreased CoQ levels (Fig. 1B). Of these strains, two lacked transporters (Flx1p and Sam5p) known to carry substrates required for the later, head-group modifying steps of CoQ biosynthesis[20-23] (the cofactors FAD and S-adenosylmethionine, respectively). The third lacked Mtm1p, an uncharacterized mitochondrial transporter. Cells lacking Mtm1p demonstrate elevated mitochondrial manganese levels and disrupted iron-sulfur cluster biogenesis, both of which can compromise late CoQ biosynthesis[7,24-26]. The final strain lacked Hem25p, a glycine carrier with no established connection to CoQ[27,28].

To further prioritize these candidates, we then measured the levels of polyprenyl-hydroxybenzoate (PPHB). PPHB and, to a lesser extent polyprenyl-aminobenzoate (PPAB), are the first intermediates of CoQ produced within mitochondria and are known to accumulate when the downstream pathway is disrupted. We reasoned that loss of cofactor transporters important for enzymes in the later stages of CoQ biosynthesis would likewise cause an accumulation of PPHB, whereas loss of a 4-HB or IPP transporter would prevent PPHB formation[29]. Of the four candidates, only the *hem25Δ* strain had decreased levels of PPHB (Fig. 1C). This finding is consistent with data from our recent systematic analyses of mitochondrial protein functions, in which the *hem25Δ*

strain exhibited decreased levels of CoQ and the prenylated CoQ precursors PPHB and PPAB (Fig.
1D)[30]. In reanalyzing data from all 176 strains in that study (which included few transporter KO
strains), *hem25Δ* exhibited PPHB depletion comparable to strains lacking the established early-
stage CoQ proteins Hfd1p (which produces 4-HB) and Coq1p and Coq2p (which collectively
produce PPHB and PPAB) (Fig. 1E). Intriguingly, large-scale chemical genomic screens have also
linked *HEM25* to the mevalonate pathway and statin sensitivity (Fig. S1A and Fig. S1B),
suggesting unexplored connections to isoprenoid biology[31]. Thus, we proceeded to investigate
Hem25p in biochemical depth.
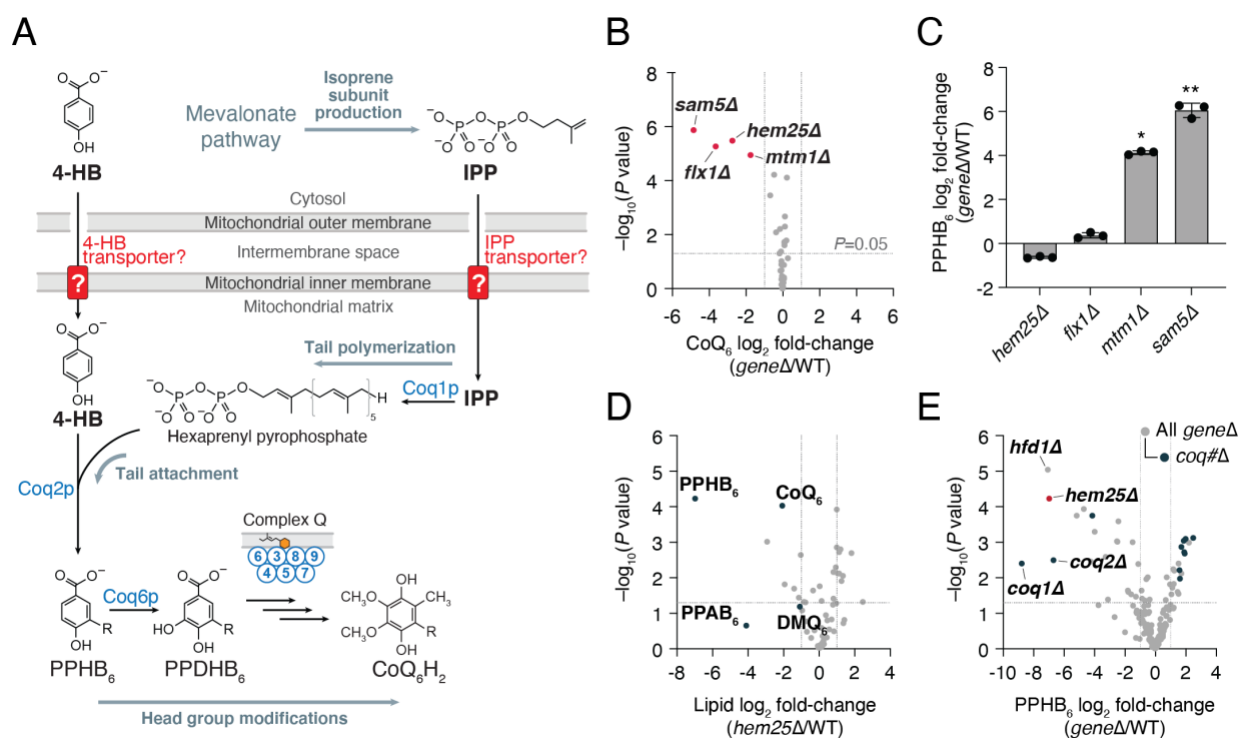


**Fig. 1. A targeted genetic screen identifies Hem25p as a potential transporter of CoQ
precursors.** (**A**) Schematic of CoQ biosynthesis in *S. cerevisiae*. 4-HB, 4-hydroxybenzoate; IPP,
isopentenyl pyrophosphate; $PPHB_6$, polyprenyl-hydroxybenzoate; $PPDHB_6$, polyprenyl-
dihydroxybenzoate. (**B**) Relative CoQ abundance in all *geneΔ* strains compared to WT verses
statistical significance. Hits with significantly decreased levels of CoQ are highlighted (mean, *n*=3

independent samples, two-sides Student's $t$-test). (**C**) Relative PPHB levels in each of the hits from (**B**) (\*$p$=1.02×10$^{-5}$ WT vs $mtm1\Delta$, \*\*$p$=0.0012 WT vs $sam5\Delta$; mean ± SD, $n$=3 independent samples). (**D**) Relative lipid abundances in $hem25\Delta$ yeast compared to WT verses statistical significance with CoQ and CoQ biosynthetic intermediates highlighted. PPAB$_6$, polyprenyl-aminobenzoate; DMQ$_6$, demethoxy-coenzyme Q. (**E**) Relative PPHB abundances verses statistical significance across all Y3K $gene\Delta$ strains with $hem25\Delta$, $hfd1\Delta$, and coq#$\Delta$ strains highlighted. For panels (D) and (E), raw data from the Y3K dataset[30] (respiration-RDR condition) is displayed as the mean from 3 independent samples with two-sided Student's $t$-test used for both panels.

## Hem25p has distinct roles in heme and CoQ production

Hem25p was previously established as a mitochondrial glycine transporter necessary for heme biosynthesis[27,28] (Fig. 2A). Imported glycine condenses with succinyl-CoA to form the heme precursor aminolevulinate (ALA). ALA is then exported out of the mitochondrial matrix to the cytosol where it proceeds along the heme biosynthetic pathway. Yeast lacking Hem25p can still produce low levels of heme[28], suggesting that mitochondria contain a secondary glycine carrier. However, its identity remains unknown.

To determine if the effect of Hem25p on CoQ levels is related to its role in heme production, we supplemented the $hem25\Delta$ strain with either ALA or high levels of glycine, both of which have been shown to bypass the requirement of Hem25p for heme production[27,28]. Without supplementation, $hem25\Delta$ cells had markedly reduced levels of heme and CoQ (Fig. 2B). Consistent with prior work, both glycine and ALA supplementation fully rescued heme in the $hem25\Delta$ strain to wild-type (WT) levels. However, supplementation had minimal effect on CoQ levels, demonstrating distinct roles for this transporter. Notably, the residual levels of CoQ in

*hem25Δ* suggests that other transporters may enable limited isoprenoid uptake. This may explain why Hem25p has been difficult to identify by screens for respiratory incompetency, as very little CoQ is required for yeast to survive on non-fermentable carbon sources[32].

To further probe Hem25p's distinct roles in heme and CoQ biosynthesis, we performed whole-cell proteomic analyses on the *hem25Δ* strain. Unsurprisingly, disruption of Hem25p resulted in widespread protein changes, with 185 proteins showing greater than two-fold decrease in abundance versus WT cells. Of these significantly decreased proteins, 121 were mitochondrial, including select CoQ biosynthetic proteins (Fig. 2C). A similar proteomic response was seen in our previous large-scale proteomics analyses[30] (Fig. S2A). Remarkably, *hem25Δ* cells supplemented with ALA exhibited a decrease in only four proteins, all of which are enzymes in the later stages of the CoQ biosynthesis pathway (Fig. 2C). Furthermore, this reduction in CoQ biosynthetic proteins was independent of transcript levels (Fig. S2B). Previous studies have demonstrated that CoQ or a late CoQ intermediate is essential for stabilizing the CoQ biosynthetic complex (complex Q, CoQ synthome) responsible for the later, head-group modifying reactions and that multiple subunits of this complex are degraded in its absence[33,34]. These results suggest that Hem25p supports the production of CoQ or a stabilizing intermediate, consistent with a role in transporting IPP or 4-HB. Importantly, our proteomic analyses showed an overall decrease in respiratory chain complexes in *hem25Δ* cells that is completely restored to WT levels upon ALA supplementation (Fig. S2C). This is consistent with previous reports of Hem25p's effect on respiratory chain stability, and further demonstrates Hem25p's distinct roles in heme and CoQ biosynthesis[27,35].

To assess Hem25p's contribution to CoQ production, we monitored the incorporation of heavy isotope-labeled 4-HB ([*phenyl*-^{13}C]-4-HB) into the CoQ pathway in *hem25Δ* cells

supplemented with ALA using a custom mass spectrometry (MS) analysis. Incorporation of labeled 4-HB into PPHB and CoQ was markedly decreased in the *hem25Δ* strain when compared to the WT strain, again suggesting that Hem25p enables PPHB production (Fig. 2D). To minimize any potentially confounding results from decreased complex Q levels in *hem25Δ*, we also compared these results to those from a *coq6Δ* background strain. Coq6p, a hydroxylase, is the first enzyme to act upon PPHB once formed. Yeast lacking Coq6p are unable to hydroxylate PPHB, leading to decreased levels of complex Q proteins, disrupted CoQ biosynthesis, and an accumulation of labeled PPHB[20,34]. This strain thus enables us to isolate a potential role for Hem25p upstream of Coq6p. Indeed, the *coq6Δ* PPHB accumulation was greatly decreased in the *coq6Δhem25Δ* strain, providing additional evidence that Hem25p enables PPHB production, likely by providing one or both precursors required for its formation (Fig. 2D).

To directly measure Hem25p's contribution to CoQ biosynthesis *in vitro*, we cultured the *coq6Δ* and *coq6Δhem25Δ* strains with ALA, isolated their mitochondria, and monitored their ability to form PPHB in the presence of 4-HB, $MgCl_2$, and $[1,2-^{13}C]$-IPP. Consistent with our whole cell results, disruption of Hem25p greatly reduced the ability of mitochondria to generate $^{13}C_{12}$-PPHB (Fig. 2E). Thus, even with ALA supplementation, cells and mitochondria lacking Hem25p exhibit a major deficiency in generating CoQ and CoQ intermediates. Collectively, these results show that Hem25p directly contributes to CoQ biosynthesis and that this role is independent of its established function in glycine transport and heme biosynthesis.
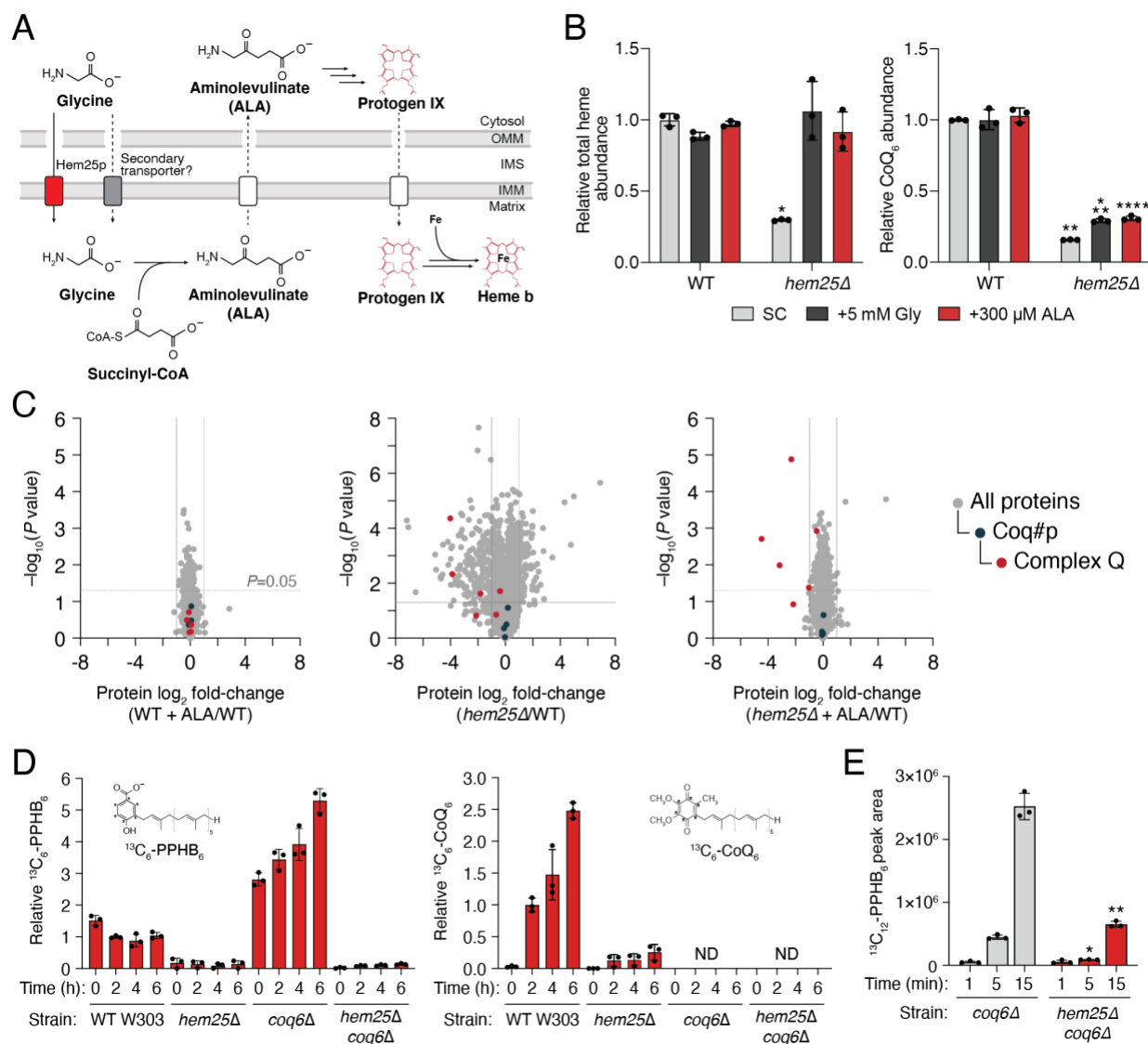
**Fig. 2. Hem25p drives CoQ production independently of its role in heme biosynthesis.** (**A**) Overview of heme biosynthesis and the role of Hem25p. (**B**) Relative total heme and CoQ abundances in WT and *hem25Δ* yeast grown in synthetic complete (SC) media with and without glycine and aminolevulinate (ALA) supplementation (\*$p$=1.01×10$^{-5}$ WT SC heme vs *hem25Δ* SC heme, \*\*$p$=7.56×10$^{-10}$ WT SC CoQ vs *hem25Δ* SC CoQ, \*\*\*$p$=8.47×10$^{-8}$ WT SC CoQ vs *hem25Δ* +Gly CoQ, \*\*\*\*$p$=2.22×10$^{-7}$ WT SC CoQ vs *hem25Δ* +ALA CoQ; mean ± SD, $n$=3 independent samples). (**C**) Relative protein abundances of WT cells with ALA, *hem25Δ* cells without ALA, and

*hem25Δ* cells with ALA supplementation compared to WT cells without ALA supplementation verses statistical significance. CoQ biosynthetic proteins and complex Q proteins are highlighted (mean, $n$=3 independent samples, two-sides Student's $t$-test). (**D**) Relative abundance of *de novo* synthesized $^{13}C_6$-PPHB and $^{13}C_6$-CoQ in WT, *hem25Δ*, *coq6Δ*, and *coq6Δhem25Δ* cells grown in -*p*ABA SD, 3% (w/v) glycerol, and 50 μM $^{13}C_6$-4-HB (mean ± SD, $n$=3 independent samples); ND, not detected. (**E**) Normalized abundance of *de novo* synthesized $^{13}C_{12}$-PPHB in isolated *coq6Δ* and *coq6Δhem25Δ* mitochondria (\**p*=5.73×10$^{-5}$ WT vs *hem25Δ* at 5 min, \*\**p*=0.0001 WT vs *hem25Δ* at 15 min; mean ± SD, $n$=3 independent samples).

**Hem25p transports isoprenes in bacteria**

Our results above suggest a model whereby Hem25p transports a precursor—either 4-HB or IPP—into the mitochondrial matrix for CoQ biosynthesis. To test this directly, we generated a construct encoding an in-frame fusion of the periplasmic maltose-binding protein (MBP) gene with *HEM25,* enabling expression at the *E. coli* plasma membrane[36,37]. Control (empty vector) *E. coli* cells, or those expressing MBP-Yhm2p, the mitochondrial citrate and oxoglutarate carrier[38], exhibited little to no ability to take up [1-$^{14}$C]-IPP (Figs. 3A, S3 B and C). However, cells expressing MBP-Hem25p demonstrated a clear, time-dependent [1-$^{14}$C]-IPP uptake that was inhibited by excess unlabeled IPP (Fig. 3A). This IPP import was saturatable with a Michaelis constant ($K_M$) of ~11 μM (Fig. 3C and Fig. S3A). In contrast, no 4-HB import was detected in cells expressing MBP-Hem25p (Fig. 3B). Uptake of 4-HB was only seen when the known bacterial 4-HB transporter PcaK was expressed[39] (Fig. S3B).

To ensure that IPP uptake was the result of Hem25p function, we generated three Hem25p point mutants: G124, R128, and R181. All three residues are highly conserved in *HEM25*

orthologs, with R128 and R181 located in the common substrate binding site of mitochondrial carriers[40] (Fig. 3D). When expressed from the endogenous *HEM25* promoter, none of the three mutants was able to rescue CoQ levels (Fig. 3E and Fig. S3, D and E). Constitutive overexpression of the mutants resulted in only a partial rescue in the R128H and R181P mutants (Fig. S3, F and G), suggesting that these residues are important for Hem25p's IPP transport function. Consistent with our CoQ rescue observations, none of the mutants demonstrated IPP transport when expressed in bacteria (Fig. 3F and Fig. S3, H and I). Taken together, our results show that Hem25p is sufficient to transport IPP into the mitochondrial matrix for CoQ biosynthesis.
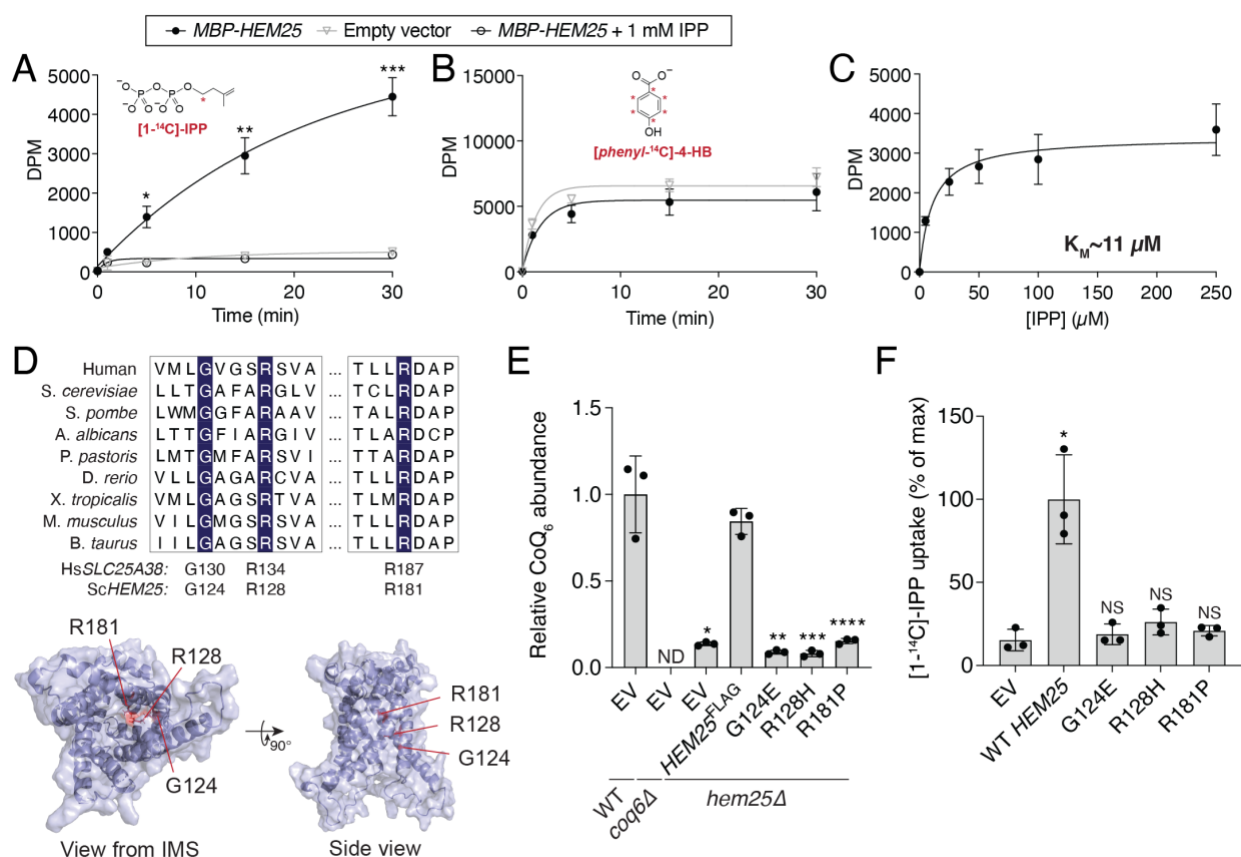


**Fig 3. Bacteria expressing Hem25p import IPP. (A)** Time course of 50 µM $[1\text{-}^{14}C]$-IPP uptake by *E. coli* cells expressing MBP-Hem25p. Cells carrying the empty expression vector and competition by excess unlabeled IPP were used as controls (**p=0.0022, ***p=0.0006,

***p=0.0001 empty vector vs *MBP-HEM25*, mean ± SD from 3 independent samples); DPM, disintegrations per minute. (**B**) Time course of 50 µM [*phenyl*-^{14}C]-4-HB uptake by *E. coli* cells expressing MBP-Hem25p. Cells carrying the empty expression were used as controls. Data reflect the mean ± SD from 3 independent samples. (**C**) Steady-state kinetics of [1-^{14}C]-IPP uptake. For each time point, the corresponding empty vector control was subtracted. Data reflect the mean ± SD from 3 independent samples. (**D**) Top, multiple sequence alignment of *HEM25* orthologs with residues mutated in congenital sideroblastic anemia highlighted. Bottom, predicted structure of Hem25p showing the location of the disease-related residues; IMS, intermembrane space. (**E**) Relative CoQ abundances in *hem25Δ* yeast carrying WT and mutant *HEM25*[FLAG] constructs. Levels are relative to WT yeast carrying the empty expression vector (*$p=8.58\times10^{-5}$, **$p=6.67\times10^{-5}$, ***$p=6.78\times10^{-5}$, ****$p=9.73\times10^{-5}$ *HEM25*[FLAG] vs mutants or empty vector, mean ± SD from 3 independent samples); ND, not detected. (**F**) Relative [1-^{14}C]-IPP uptake by *E. coli* cells expressing WT and mutant MBP-Hem25p. Uptake levels reflect 30 minutes of incubation time and are relative to that of WT MBP-Hem25p (*p=0.006 empty vector vs WT *HEM25*, mean ± SD, 3 independent samples); NS, not significant.

## Hem25p's role in CoQ biosynthesis is restricted to fungi

Hem25p exhibits high overall sequence conservation with human SLC25A38, an established glycine transporter whose disruption results in congenital sideroblastic anemia[41,42]. Given Hem25p's function in yeast CoQ biosynthesis, we next tested whether the human SLC25A38 also doubles as an IPP transporter. Expression of the human SLC25A38 in the *hem25Δ* strain restored total heme levels, but had no effect on CoQ (Fig. 4A and Fig. S4A). Consistently, when expressed in bacteria, MBP-SLC25A38 failed to transport IPP (Fig. 4B). Thus, despite

sharing many of the same substrate binding residues as Hem25p, only the glycine transport function is conserved in human SLC25A38. This is further supported by our recent MITOMICS dataset, whereby the human HAP1 cells lacking *SLC25A38* had normal levels of CoQ and complex Q members[43] (Fig. S4B and Fig. S4C).

We next sought to better understand the evolutionary divergence of Hem25p and SLC25A38 function. *HEM25* is highly conserved among opisthokonts. Thus, we used the PANTHER database to compile a list of *HEM25* orthologs from a number of model organisms across this group[44]. We expressed each ortholog in *hem25Δ* yeast and measured their ability to rescue CoQ levels. Full rescue was largely limited to fungal orthologs, with little to no rescue with metazoan orthologs (Fig. 4D). Phylogenic analysis supports this functional split, showing an early evolutionary event resulting in separate fungal and metazoan branches[44] (Fig. 4D). To validate Hem25p's role in fungi, we expressed the *Schizosaccharomyces pombe* ortholog in bacteria and measured IPP uptake. Consistent with our rescue experiment, Hem25p from *S. pombe* and *S. cerevisiae*—two highly evolutionarily diverse yeast species—demonstrated similar levels of IPP uptake (Fig. 4E). Collectively, our results show that the mitochondrial glycine carrier Hem25p doubles as an IPP transport in fungi, and will empower subsequent studies to identify IPP transporters in metazoans.
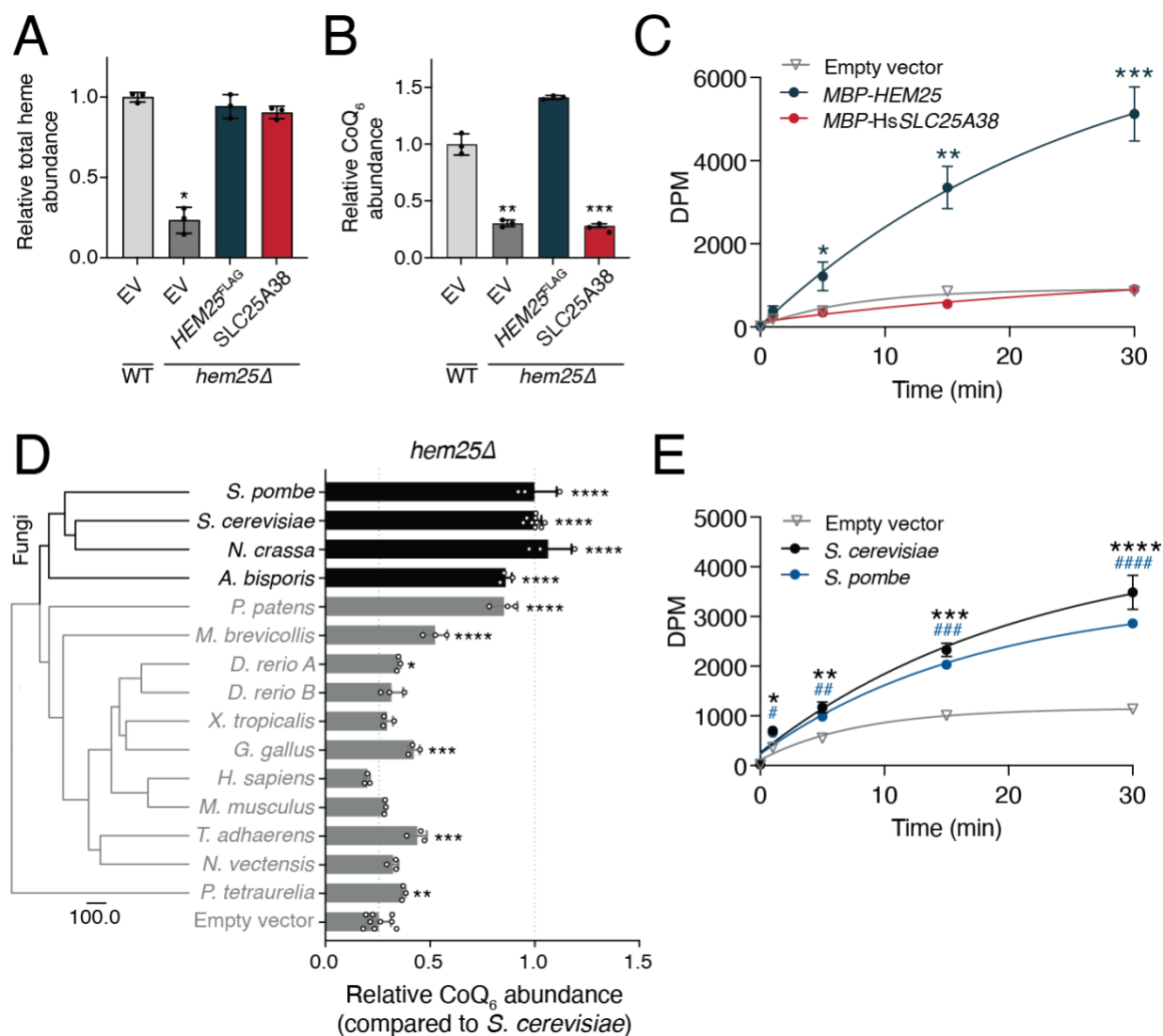
**Fig. 4. Hem25p's role in CoQ biosynthesis is conserved in fungi. (A)** Heme and **(B)** CoQ rescue by SLC25A38 in *hem25Δ* yeast. Levels are relative to the WT strain carrying the empty expression vector (*$p$=0.0001 **$p$=0.0002, ***$p$=0.0001, mean ± SD, 3 independent samples). **(C)** Time course of 50 μM [1-$^{14}$C]-IPP uptake by *E. coli* cells expressing MBP-SLC25A38 and MBP-Hem25p. Uptake by cells carrying the empty expression vector is included as a control (*$p$=0.0147, **$p$=0.0011, ***$p$=0.0003 empty vector vs *MBP-HEM25*, mean ± SD, *n*=3 independent samples). **(D)** Phylogenetic analysis of Hem25p orthologs, and relative CoQ abundance in *hem25Δ* cells expressing different Hem25p orthologs. Levels are relative to that of

the *S. cerevisiae* Hem25p (****$p<0.0001$, ***$p<0.001$, **$p<0.01$, *$p<0.05$ vs empty vector; mean $\pm$ SD, at least 3 independent samples). (**E**) Time course of [1-$^{14}$C]-IPP uptake by *E. coli* cells expressing *S. cerevisiae* Hem25p, *S. pombe* Hem25p, or the empty vector. (*$p=0.0012$, **$p=0.0007$, ***$p=7.7\times10^{-5}$, ****$p=0.0003$ empty vector vs *S. cerevisiae* Hem25p, [#]$p=0.0053$, [##]$p=0.0112$, [###]$p=0.0004$, [####]$p=7.0\times10^{-5}$ empty vector vs *S. pombe* Hem25p, mean $\pm$ SD, $n=3$ independent samples).


## Discussion

In this work, we identify Hem25p as a mitochondrial IPP transporter. Our results reveal a novel function for this established glycine transporter and propose a model whereby a single carrier, Hem25p, enables the bulk of mitochondrial heme and CoQ biosynthesis. However, even in the absence of Hem25p, heme and CoQ are still produced at low levels (Fig. 2B). This suggests that functional redundancy is inherent among mitochondrial transporters, and may explain why previous large-scale screens for CoQ biosynthetic proteins have missed Hem25p[16,17]. In our targeted screen, we did not find any strong candidates for secondary transporters, despite having screened every known yeast mitochondrial transporter. It is possible that multiple SLC25 transporters each have low level IPP transport capability or that a non-SLC25 protein not included in our screen is the secondary transporter. Compensatory mechanisms may also mask subtle changes when a secondary transporter is disrupted. CoQ biosynthetic proteins have been shown to organize into domains at ER-mitochondria contact sites[45,46]. Given that the mevalonate pathway, which supplies IPP, is partially associated with the ER, one possible function for this co-localization is the transport of substrates and biosynthetic precursors. Thus, it is possible that these

domains provide an additional layer of redundancy. Further efforts are needed to dissect the complete mechanisms of isoprenoid pyrophosphate transport.

Hem25p's ability to support two separate biosynthetic pathways raises the possibility that other mitochondrial transporters carry multiple substrates. Indeed, the yeast Pic2p and its mammalian homolog SLC25A3 were recently shown to transport copper in addition to phosphate—two highly distinct substrates, much like glycine and IPP[47,48]. Thus, in that case, a single carrier enables oxidative phosphorylation by supporting both ATP synthesis and cytochrome *c* oxidase activity. Many metabolites still lack a defined transporter, despite evidence of mitochondrial uptake. The fact that yeast and humans have only 35 and 53 SLC25 carriers, respectively, suggests that functional redundancy is widespread[17]. However, potential contribution from non-SLC25 carriers, many of which remain unidentified, must also be considered. Thus, a complete and accurate definition of mitochondrial transporters and their substrate specificities is still needed. The development of new experimental technologies and screening approaches will accelerate these characterization efforts.

A previous study identified six SLC25 members that genetically interact with *HEM25,* including *FLX1*, *MTM1*, and *SAM5*[35]. Interestingly, disruption of these three genes resulted in decreased CoQ levels in our screen (Fig. 1B). *FLX1* and *SAM5* encode transporters for FAD and SAM, respectively, both of which are necessary cofactors for CoQ biosynthesis[20-23]. Mtm1p is an uncharacterized mitochondrial transporter that was originally proposed to assist with mitochondrial manganese trafficking. However, it was later suggested that it participates in iron-sulfur cluster biogenesis[24,26]. Cells lacking Mtm1p exhibit elevated mitochondrial manganese levels, which can result in the mismetallation and degradation of Coq7p, the diiron hydroxylase responsible for the penultimate step of CoQ biosynthesis[24,25]. Additionally, *mtm1Δ* cells

phenocopy disruptions in the biosynthesis of iron-sulfur clusters—cofactors necessary for electron transfer reactions that enable Coq6p function[7]. Thus, it is possible that the observed decrease of CoQ in *mtm1Δ* is a result of Coq7p mismetallation and degradation, dysfunctional Coq6p, or both. These roles are supported by our CoQ and PPHB measurements and may underlie the observed genetic interactions with *HEM25*. Additional work is needed to confirm the molecular basis of these interactions.

Our results corroborate previous *in vitro* experiments showing that imported IPP is sufficient to generate CoQ's polyprenyl tail[12,13] (Fig. 2E). We did not assess whether other isoprenoid pyrophosphates, such as dimethylallyl pyrophosphate (DMAPP), geranyl pyrophosphate (GPP), or farnesyl pyrophosphate (FPP), can be imported. Coq1p, a mitochondrial prenyltransferase, has shown an ability to use GPP and FPP in isolated membrane preparations[49], but whether these isoprenoids can be transported into mitochondria remains unknown. Moreover, it has been argued that a common cytosolic FPP pool supplies precursors for CoQ and other isoprenoids, however this remains unresolved[50-52]. While our investigation shows that yeast mitochondria can bypass this cytosolic FPP pool by importing and incorporating IPP alone, we cannot exclude the contribution of other isoprenoid pyrophosphate species to CoQ biosynthesis.

Despite being the closest ortholog to Hem25p, SLC25A38 did not transport IPP nor did it functionally rescue CoQ levels in *hem25Δ* (Fig. 4B and Fig. 4C). We also did not identify any reports of CoQ deficiency in patients with SLC25A38 mutations. At first glance, this seems surprising given that both carriers share many of the same key binding site residues[40] (Fig. 3D). Moreover, we found these conserved residues to be important for Hem25p stability or substrate binding (Fig. 3E and Fig. 3F). However, our experimental and phylogenetic analyses show a clear divergence between fungal and metazoan orthologs, with IPP import limited to fungal orthologs

(Fig. 4D). It is likely that the emergence of multicellular and multiorgan animals necessitated a higher level of regulation of heme and CoQ biosynthesis, such that a common carrier was no longer sufficient. Consistent with this model, human *SLC25A38* demonstrates preferential expression in early erythroid cells and both zebrafish orthologs are strongly associated with hematopoiesis and hematopoietic tissues[28,41]. Given that CoQ is produced in nearly every mammalian cell type, we would expect ubiquitous expression from a mammalian isoprenoid transporter. Additional differences in both the heme and CoQ biosynthetic pathways have been identified between yeasts and metazoans[53-55], and more work is needed to dissect the physiological underpinnings of these differences.

The divergence in Hem25p and SLC25A38 functions implies the existence of a separate metazoan IPP transporter. Such an occurrence would not be unique to IPP, with NAD being the most recent example of a substrate having distantly related fungal and metazoan transporters[56-59]. Our identification of the primary fungal IPP transporter here lays the foundation for future efforts to identify the functional metazoan ortholog.

**Materials and Methods**

Yeast strains and cultures

The S. *cerevisiae* haploid strain W303 (MATa leu2 trp1 can1 ura3 ade2 his3) was used. Single (*gene*Δ) and double (*gene*Δ*gene*Δ) deletion strains were generated using standard homologous recombination[60]. Open reading frames were replaced with the kanMX6, His3MX6, or Trp1 cassettes and confirmed by PCR assay[61,62].

For the targeted screen, cells were grown in YPD media consisting of 1% (w/v) yeast extract (Research Products International, RPI), 2% (w/v) peptone (RPI), and 2% (w/v) dextrose

(Fisher). YP media without dextrose were sterilized by automatic autoclave. Glucose was sterile filtered (0.22 μm pore size, VWR) and added to sterile YP prior to use. For all other cultures, synthetic complete (SC) or synthetic dropout (SD) media was used, containing yeast nitrogen base (YNB) with ammonium sulfate and without amino acids (US Biological), the corresponding drop-out mix (US Biological), and the indicated carbon source. pABA⁻ media contained YNB without amino acids and without pABA (Formedium), Complete Supplement Mixture (Formedium), and the indicated carbon source. All synthetic yeast media were sterile filtered (0.22 μm pore size, VWR) prior to use. Where indicated, ALA or glycine were added to the media prior to sterile filtration.

For measurements in respiration[30], starter cultures (3 mL, SC or SD, 2%D) were inoculated with individual colonies and incubated (30 ºC, 230 rpm, 14-16 h). Cell density was measured at $OD_{600}$ and converted to cells/mL (1 OD = 1 x $10^7$ cells/mL). Respiratory media (100 mL, SC or SD, 0.1%D, 3%G) in a sterile 250 mL Erlenmeyer flask were inoculated with 2.5 x $10^6$ yeast cells. Samples were incubated (30 ºC, 230 rpm) for 25 h, a time point that corresponds to early respiratory growth.

Lipid extraction

Lipid extractions were performed essentially as described previously[63]. 1x$10^8$ cells were harvested by centrifugation (4,000 x *g*, 5 min, RT). The supernatant was removed and the cells washed with water (600 μL). Cells were pelleted again (15,000 x *g*, 30 s, RT) and the supernatant removed. Cell pellets were either used immediately for lipid extraction or snap-frozen in $LN_2$ and stored at -80 ºC until analysis. Frozen pellets were thawed on ice prior to extraction. To extract lipids from whole cells, 150 mM KCl (50 μL) was added to each sample, followed by ice-cold

methanol (600 µL; with 1 µM CoQ$_8$ as an internal standard). Glass beads (100 µL; 0.5 mm; BioSpec) were then added and the samples were vortexed (10 min, 4 ºC) to lyse the cells. Ice-cold petroleum ether (400 µL; Sigma) was added to extract lipids, and the samples were vortexed again (3 min, 4 ºC). Samples were centrifuged (1000 x $g$, 3 min, RT) and the top petroleum ether layer was collected in a new tube. The petroleum ether extraction was repeated a second time, with the petroleum ether layer from the second extraction combined with that from the first. The extracted lipids were dried under argon before being resuspended in 2-propanol (50 µL) and transferred to an amber glass vial (Sigma; QSertVial, 12 x 32 mm, 0.3 mL).

Targeted yeast genetic screen

Yeast from a -80 ºC glycerol stock were struck on to YPD plates and incubated (30 ºC, 230 rpm, 48 h). Starter cultures of YPD (3 mL) were inoculated with individual colonies and grown overnight (30 ºC, 14-16 h). Overnight cultures were diluted to an OD$_{600}$ = 0.2 (3 mL) and incubated until OD$_{600}$~1 (30 ºC, 230 rpm, 4-5 h), corresponding to mid-log phase. Cultures were harvested by centrifugation (4,000 x $g$, 5 min, RT), washed once with water, and transferred to a 1.5 mL microcentrifuge tube. Cells were centrifuged again (15,000 x $g$, 30 s, RT), snap frozen in LN$_2$, and stored at -80 ºC until analysis. Lipids were extracted from cell pellets as described above and CoQ measurements were then performed by HPLC-ECD.

Targeted HPLC-ECD for CoQ

Extracted lipids were resuspended in 2-propanol (50 µL) and transferred to an amber vial. Sodium borohydride (2 µL of 10 mM in 2-propanol) was added to each vial, followed by brief vortexing and incubation (10 min, RT) to reduce CoQ. Methanol (50 µL) was then added to each

sample to remove excess sodium borohydride and the vials were flushed with argon gas. CoQ measurements were performed using reverse-phase high-pressure liquid chromatography with electrochemical detection[63] (HPLC-ECD). Separation was performed using C18 column (Thermo Scientific, Betasil C18, 100 x 2.1 mm, particle size 3 μm) at a flow rate of 0.3 mL/min with a mobile phase of 78% methanol, 10% 2-propanol, 10% acetonitrile, and 2% ammonium acetate (1 M, pH 4.4). Electrochemical detection was performed using an ECD detector (Thermo Scientific ECD3000-RS) containing a 6020RS omni Coulometric Guarding Cell (E1) set to -200 mV and two 6011RS ultra Analytical Cells (E2 and E3) set to 600 mV. CoQ measurements were made on the analytical E2 electrode. For each experiment, $CoQ_6$ and $CoQ_8$ standards (Avanti) were prepared in the same manner as the experimental samples and injected to generate a standard curve. Peak areas were quantified using Chromeleon 7.2.10 software (Thermo), normalized to the $CoQ_8$ internal standard, and converted to absolute values using the standard curve. $CoQ_6$ levels were further normalized per mg of wet pellet weight.

Heme measurements

Yeast total heme measurements were performed using previously described methods with slight modifications[64,65]. Cells were grown under respiratory conditions as described previously and supplemented with glycine or ALA as indicated. $1 \times 10^8$ cells were harvested by centrifugation (4,000 x $g$, 5 min, RT), washed with water, and centrifuged again (15,000 x $g$, 30 s, RT). Pellets were snap frozen in $LN_2$ and stored at -80 ℃. Frozen pellets were thawed on ice before being resuspended in 500 μL oxalic acid (20 mM) and incubated in a closed box (16-24 h, 4 ℃). 500 μL oxalic acid (2 M, preheated to 50 ℃) were added to each sample, and each sample was divided in half into two 1.5 mL amber microcentrifuge tubes. One half of each sample was heated (95-100

ºC, 30 min) while the other was incubated at RT. Each tube was then centrifuged (16,000 x $g$, 2 min) and 200 µL of the supernatant were loaded into a 96-well black-bottom plate (Greiner). Heme fluorescence was measured on a Cytation 3 plate reader (BioTek) with excitation at 400 nm and emission at 620 nm. The fluorescence from the unheated sample was subtracted from the corresponding heated sample.

Quantitative PCR for *COQ* gene expression

Respiring yeast were cultured and harvested as described in "*Yeast strains and cultures*" for heme measurements. Total RNA was extracted using the MasterPure Yeast RNA Purification Kit (Lucigen). First strand cDNA synthesis was performed using the EasyScript Plus cDNA Synthesis Kit (Lamda Biotech) using Oligo(dT) primers and 1 µg of RNA. qPCR was performed using the following reaction: 10 µL *Power* SYBR Green PCR Master Mix (Thermo), 2.5 µL cDNA (diluted 1:20), and 250 nM forward and reverse primers. Primers amplifying the yeast *COQ2*, *COQ3*, *COQ4*, *COQ5*, *COQ6*, *COQ7*, *COQ8*, *COQ9*, and *ACT1* (reference) genes were used. For the qPCR cycle, an initial 2 min incubation at 50 ºC was followed by 10 min denaturing at 95 ºC. Then 40 cycles of 95 ºC for 15 s and 60 ºC for 1 min were performed. RNA abundance was calculated using the $\Delta\Delta Ct$ method. The following primer sequences were used for qPCR:

| Gene | Primer | Sequence |
|---|---|---|
| *COQ2* | FWD | cgcacaccaggataaaaagtt |
| *COQ2* | REV | ccaagccaaagcggtagac |
| *COQ3* | FWD | gccagaagtgagcgtcttg |
| *COQ3* | REV | gcgagcgattcactcaaaa |
| *COQ4* | FWD | gctgaagagcgtaccgagtt |
| *COQ4* | REV | aggttccattggccgagtat |
| *COQ5* | FWD | ttacgcaagctcacagagca |
| *COQ5* | REV | gctgcggatgataaaggact |
| *COQ6* | FWD | ccagaagattttcccagatcc |
| *COQ6* | REV | gccacaacaccataggcatt |
| *COQ7* | FWD | ccttattaacgcctttgtgga |
| *COQ7* | REV | tctggagaaatcaatgcggta |
| *COQ8* | FWD | gggcaactattgtcttttcagg |
| *COQ8* | REV | cccttgataaaatttcgtataattcc |
| *COQ9* | FWD | ccattgttgaatctttaaatgagc |
| *COQ9* | REV | gagttgggagcacctattgaa |
| *ACT1* | FWD | tccgtctggattggtggt |
| *ACT1* | REV | tgagatccacatttgttggaag |

## LC-MS/MS proteomics

*Yeast growth.* Yeast cultures were grown as described previously for respiration. 1 x $10^8$ cells were harvested, snap frozen in $LN_2$, and stored at -80 ºC.

*Lysis and Digestion.* Yeast pellets were removed from -80 °C conditions and resuspended in lysis buffer (6 M guanidine hydrochloride, 100 mM Tris). The samples were then boiled at 100°C for 5 minutes and sonicated in a bath sonicator (Qsonica) with a 5-minute-long program of 20 seconds on, 10 seconds off. Methanol was added to each sample to 90% concentration, and the samples were centrifuged at 10,000 x g for 5 minutes to precipitate proteins. After precipitation, the supernatant was discarded from each sample, and the protein pellets were allowed to air dry for 7 minutes. The dried pellets were resuspended in digestion solution (8 M urea, 10 mM TCEP,

40 mM CAA, 100 mM Tris), and the samples were sonicated in the bath sonicator with the same program as above to facilitate resolubilization. LysC (Wako Chemicals) was added to each resolubilized sample in an estimated 50:1 protein/enzyme ratio. The samples were incubated on a rocker at room temperature for 4 hours before being diluted fourfold with 100 mM Tris. Trypsin (Promega) was added to each sample in an estimated 50:1 protein/enzyme ratio before they were incubated on a rocker at room temperature for 14 hours. Each sample was finally acidified with TFA to pH of 2, desalted by solid phase extraction cartridges (Phenomenex), and dried under vacuum (Thermo Scientific).

*LC-MS/MS Proteomics Data Acquisition.* Peptides were resuspended in 0.2% formic acid, and the concentration of each sample was determined from a NanoDrop One spectrophotometer (Thermo Scientific). The samples were then prepared in autosampler vials and loaded onto a 75 μm i.d. x 360 μm o.d. capillary column (New Objective) that was packed in-house[66] with 1.7 μm BEH C18 particles and held at 50 °C throughout the analysis. Separations were performed with a Dionex UltiMate 3000 nano HPLC system (Thermo Scientific). The mobile phases were 0.2% formic acid in water (A) and 0.2% formic acid in 80% ACN (B). The peptides were analyzed by an Orbitrap Eclipse (Thermo Scientific) with the following parameters: Orbitrap MS1 resolution of 240,000; MS1 automatic gain control target of $1 \times 10^6$; MS1 maximum injection time of 50 ms; MS1 scan range of 300-1500 *m/z*; dynamic exclusion of 20 ms; advanced peak determination[67] toggled on; MS2 isolation window of 0.7 *m/z*; MS2 collision energy of 25%; ion trap MS2 resolution setting of turbo; MS2 automatic gain control target of $3 \times 10^4$; MS2 maximum injection time of 14 ms; and MS2 scan range of 150-1200 *m/z*.

*Data Analysis.* MaxQuant[68] (version 1.5.2.8) was used to process proteomics raw files against a database of reviewed yeast proteins plus isoforms from UniProt (downloaded 11/20/2019). Label-free quantification[69] was used for relative quantification. Match-between-runs was enabled. Data were visualized and analyzed using the Argonaut[70] platform.

*Data Availability.* Proteomics raw files have been deposited to the MassIVE repository, with accession number MSV000089127. Reviewers may access the raw files through the following link with the password "proteomics": [ftp://MSV000089127@massive.ucsd.edu](ftp://MSV000089127@massive.ucsd.edu).

Targeted LC-MS/MS for PPHB and CoQ

*Yeast growth.* For measurements in respiration, yeast cells were grown and harvested as described previously. Yeast pellets were snap frozen in $LN_2$ and stored at -80 ºC.

For *de novo* PPHB and CoQ experiments, starter cultures (3 mL, SC, 2%D, 300 µM ALA) were inoculated with individual colonies and incubated (30 ºC, 230 rpm, 18 h). $OD_{600}$ was measured, and $2.5 \times 10^7$ cells were diluted into 50 mL of pABA⁻ media (2%D, 300 µM ALA) in a sterile 250 mL Erlenmeyer flask. Cells were incubated (30 ºC, 230 rpm) until $OD_{600} \sim 1.5\text{-}2$ to deplete pABA in the cells. $7.5 \times 10^8$ cells were centrifuged (3,000 x *g*, 5 min, RT) and resuspended in 50 mL labeled pABA⁻ media (3%G, 300 µM ALA, 50 µM $^{13}C_6$-4-HB). Immediately after the media swap, and at 2, 4, and 6 h after, $1 \times 10^8$ cells were harvested by centrifugation (3,000 x *g*, 5 min, 4ºC) and washed with water. Cells were pelleted again (15,000 x *g*, 30 s, 4 ºC), snap frozen in $LN_2$, and stored at -80 ºC.

*LC-MS/MS Lipidomics Data Acquisition.* Frozen pellets were thawed on ice and lipid extraction was performed as described previously. A Vanquish Horizon UHPLC system (Thermo Scientific) connected to an Exploris 240 Orbitrap mass spectrometer (Thermo Scientific) was used for targeted LC-MS analysis. A Waters Acquity CSH C18 column (100 mm × 2.1 mm, 1.7 μm) was held at 35°C with the flow rate of 0.3 mL/min for lipid separation. A Vanquish binary pump system was employed to deliver mobile phase A consisted of 5 mM ammonium acetate in ACN/$H_2O$ (70/30, v/v) containing 125 μL/L acetic acid, and mobile phase B consisted of 5 mM ammonium acetate in IPA/ACN (90/10, v/v) containing 125 μL/L acetic acid. The gradient was set as follows: B was at 2% for 2 min and increased to 30% over the next 3 min, then further ramped up to 50% within 1 min and to 85% over the next 14 min, and then raised to 99% over 1 min and held for 4 min, before re-equilibrated for 5 min at 2% B. Samples were ionized by a heated ESI source with a vaporizer temperature of 350°C. Sheath gas was set to 50 units, auxiliary gas was set to 8 units, sweep gas was set to 1 unit. The ion transfer tube temperature was kept at 325°C with 70% RF lens. Spray voltage was set to 3,500 V for positive mode and 2,500 V for negative mode. The targeted acquisition was performed with both $tMS_2$ (targeted $MS_2$) mode and tSIM (targeted selected ion monitoring) mode in the same injection: tMS2 mode was for measuring $CoQ_6$ (*m/z* 591.4408), [13]$C6$-$CoQ_6$ (*m/z* 597.4609) and $CoQ_8$ (*m/z* 727.5660, internal standard) in positive polarity at the resolution of 15,000, isolation window of 2 *m/z*, normalized HCD collision energy of either 40% or stepped HCD energies of 30% and 50%, standard AGC target and auto maximum ion injection time; tSIM mode was for measuring $PPHB_6$ (*m/z* 545.4000), [13]$C6$-$PPHB_6$ (*m/z* 551.4201), and [13]$C12$-$PPHB_6$ (*m/z* 557.4403) in negative polarity at the resolution of 60,000, isolation window of 2 *m/z*, standard AGC target and auto maximum ion injection time.

*Data Analysis.* Targeted quantitative analysis of all acquired compounds was processed using TraceFinder 5.1 (Thermo Scientific) with the mass accuracy of 5 ppm. The result of peak integration was manually examined.

Mitochondrial isolation

Starter cultures (3 mL, SC or SD, 2%D) were inoculated with individual colonies and incubated (30 ºC, 230 rpm, 14-16 h). $2 \times 10^8$ cells were diluted into 1 L SC 2%D in a 5 L Erlenmeyer flask and incubated (30 ºC, 230 rpm) for 14-18 to a final OD ~ 6. Mitochondria were isolated as previously described[71]. Cells were harvested by centrifugation (3000 x *g,* 5 min, RT), washed with water, and centrifuged again (3,000 x *g,* 5 min, RT). The wet pellet weight of the cells was determined. Cells were resuspended in 2 ml/g DTT buffer (100 mM Tris-$H_2SO_4$, 10 mM DTT, pH 9.4) and shaken slowly (30 ºC, 80 rpm, 20 min). Cells were pelleted, washed once with 7 ml/g Zymolyase buffer (1.2 M sorbitol, 20 mM potassium phosphate, pH 7.4), and resuspended in 7 mL/g Zymolyase buffer with 3 mg/g Zymolyase 20T (Fisher) to generate spheroplasts. Yeast were shaken slowly (30 ºC, 80 rpm) for 30 min before being pelleted and washed with 7 mL/g Zymolyase buffer. Pellets were resuspended in 6.5 mL/g ice-cold homogenization buffer (0.6 M sorbitol, 10 mM Tris-HCl, 1 mM PMSF, 0.2% (w/v) fatty acid-free BSA, pH 7.4). Spheroplasts were homogenized using 15 strokes of a tight-fitting glass-Teflon homogenizer and diluted twofold with homogenization buffer. The homogenate was centrifuged (1500 x *g*, 5 min, 4 ºC) to pellet cell debris and nuclei. The supernatant was centrifuged (4,000 x *g,* 5 min, 4 ºC) to pellet additional debris, and the supernatant centrifuged again (4,000 x *g,* 5 min, 4 ºC). Mitochondria were isolated by centrifuging the supernatant (12,000 x g, 15 min, 4 ºC) and resuspended in SEM

(250 mM sucrose, 1 mM EDTA, 10 mM MOPS-KOH, pH 7.2) or SEP (0.6 M sorbitol, 1 mM EGTA, 50 mM potassium phosphate, pH 7.4), where indicated. Mitochondrial protein content was quantified by BCA protein assay (Thermo).

Mitochondrial PPHB synthesis

Isolated mitochondria were resuspended in SEP at a concentration of 8 mg/mL, kept on ice, and used within 4 h of isolation without freezing. PPHB synthesis was carried out using a modified protocol[12]. To begin the assay, 250 µL mitochondria (2 mg per assay) were added to 750 µL of 1.3X substrate buffer (0.6 M sorbitol, 50 mM potassium phosphate, 1 mM EGTA, 9.1 mM $MgCl_2$, 1.3 µM 4-HB, 13.3 µM [1,2-$^{13}$C]-IPP (Cambridge Isotope Laboratories), pH 7.4). The final concentrations in the reaction were the following: 0.6 M sorbitol, 50 mM potassium phosphate, 1 mM EGTA, 7 mM $MgCl_2$, 1 µM 4-HB, 10 µM [1,2-$^{13}$C]-IPP, and 2 mg mitochondria, pH 7.4. Reactions were carried out at 30 ºC in a 5 mL tube (Eppendorf) with constant shaking (500 rpm). At the indicated time points, 300 µL of the reaction were removed and immediately extracted for lipids. 300 µL ice-cold methanol containing 1 µM $CoQ_8$ as an internal standard were added to each sample, followed by 400 µL ice-cold petroleum ether. Samples were vortexed (10 min, 4 ºC) and centrifuged (3,000 x $g$, 3 min, 4 ºC). The top petroleum ether layer was collected, and the extraction repeated again with another 400 µL petroleum ether. The petroleum ether layers were pooled for each sample, dried under argon, and stored at -80 ºC. Lipids were resuspended in 2-propanol (50 µL) and transferred to amber glass vials for targeted LC-MS/MS. Following the third time point, 50 µL of the remaining reaction was diluted with 2X SDS sample buffer for immunoblot analysis.

Bacterial uptake assays

Bacterial expression of mitochondrial carriers and whole-cell uptake assays were performed as described previously with slight modifications[36,37]. MBP-tagged fusion proteins were generated by combining the bacterial maltose binding protein (MBP) containing the MalE signal peptide, a short linker containing a thrombin cleavage site, and the mitochondrial carrier gene. Fusion constructs were synthesized as gBlock gene fragments (IDT) and cloned into the pET-21b expression vector using the restriction enzymes NdeI and XhoI. Inserts were confirmed by sequencing. Mutants were generated by site-directed mutagenesis (NEB).

Expression of MBP-tagged carriers was carried out in E. *coli* C43(DE3) cells[72] (Biosearch Technologies). Single colonies of transformed cells were used to inoculate 4 mL of LB media containing 100 mg/L ampicillin. Cultures were incubated overnight (37 ºC, 230 rpm) before being diluted 1:100 in 50 mL LB media containing 100 mg/L ampicillin. Refreshed cultures were incubated (37 ºC, 230 rpm) until the $OD_{600}$=0.5-0.6, at which point protein expression was induced with 0.1 mM IPTG. Cells were induced overnight (20 ºC, 230 rpm, 14-16 h).

Induced cells were collected by centrifugation (4,000 x *g,* 10 min, 4 ºC), washed once with ice-cold KPi (50 mM potassium phosphate, pH 7.4), and centrifuged again (4,000 x *g,* 10 min, 4 ºC). Cells were resuspended in ice-cold KPi to a cell density of $OD_{600}$=10 and placed on ice until the start of the assay.

To start the assay, 200 µL of cells were added to 200 µL of 2X substrate buffer (2 mM $MgCl_2$ and radiolabeled substrate at double the final concentration in KPi). Assays were carried out at room temperature. [1-$^{14}$C]-IPP and [*phenyl*-$^{14}$C]-4-HB were purchased from American Radiolabeled Chemicals. At each time point, 100 µL of the assay mixture were removed and filtered under vacuum to separate the cells from the incubation media. To reduce non-specific binding of the substrate to the filter, filtration was carried out using 0.22 µm mixed cellulose ester

(MCE) filters (Millipore) for IPP uptake assays and 0.2 µm Whatman Nuclepore track-etched hydrophilic membrane filters (Cytiva) for 4-HB uptake assays[39]. Following filtration, filters were washed with 5 mL of ice-cold KPi before being placed in a 7 mL scintillation vial (Fisher). 5 mL of Ultima Gold MV liquid scintillation cocktail (PerkinElmer) were added to each vial before being analyzed by liquid scintillation counting. Counts per minute were converted to disintegrations per minute (DPM) using the counting efficiency of the counter.

CoQ rescue experiments

The yeast expression vector p416 GPD was modified to contain the endogenous *HEM25* promoter. PCR was used to amplify a 744 bp segment directly upstream of the *HEM25* gene from yeast genomic DNA. This segment, containing the endogenous promoter, was then cloned into the SacI-BamHI sites of the p416 GPD vector, yielding a p416 vector containing the <u>*HEM25* endogenous promoter</u> (p416 HEP). The *HEM25* gene was amplified from yeast genomic DNA and cloned into the BamHI-XhoI sites of the p416 GPD or the p416 HEP vectors. The PCR primers were designed so that a short linker and a FLAG tag was added to the end of the open reading frame. *HEM25*-FLAG mutants were synthesized as gBlocks (IDT) and cloned into the BamHI-XhoI sites of the p416 GPD or the p416 HEP vectors. We were not able to PCR amplify p416, thus SDM could not be performed. The sequences of the cloned *HEM25* promoter and the inserts were confirmed by sequencing. Verified constructs were transformed into *hem25Δ* yeast using the LiAc/SS carrier DNA/PEG method[73]. For controls, empty vectors were also transformed into WT W303, *coq6Δ, hem25Δ* yeast. Respiratory growth and targeted lipidomics were performed as described above.

*HEM25* orthologs were synthesized as codon-optimized gBlocks (IDT) and cloned into the BamHI-XhoI sites of the p416 ADH vector. Constructs were sequenced and transformed into *hem25Δ* yeast. Fermentative growth and targeted lipidomics were performed as described above.

Sequence alignments and bioinformatics analysis

Hem25p orthologs were curated from the PANTHER database[44]. Sequences were aligned using Clustal Omega in Jalview[74,75]. The phylogenetic tree was generated using Jalview and FigTree. The structure of Hem25p was predicted using AlphaFold and visualized using PyMol 2.0[76,77].

Immunoblotting

*Antibodies.* Primary antibodies for this study include anti-FLAG (Sigma F1804, 1:2500-1:5000), anti-Act1 (Abcam ab8224, 1:5000), anti-Coq1 (custom made at Genscript, 1:2000), anti-Vdac1 (Abcam ab110326, 1:4000), and Anti-MBP (NEB E8032S, 1:10000). Secondary antibodies include IRDye 680RD goat anti-rabbit (LI-COR 926-68071, 1:15000), IRDye 680RD goat anti-mouse (LI-COR 926-68070, 1:15000), IRDye 800CW (LI-COR 926-32210, 1:15000), and anti-mouse IgG HRP-linked (Cell Signaling Technology #7076, 1:2000-1:100000).

*Whole yeast cell lysates.* Protein lysates from whole yeast cells were prepared as described[78]. Yeast pellets were lysed using 150 µL of lysis buffer (2 M NaOH, 1 M β-mercaptoethanol) for 10 min on ice with periodic vortexing. 150 µL of 50% TCA was added, and the samples were incubated on ice for 10 min with periodic vortexing to precipitate proteins. The samples were centrifuged (14,000 x *g*, 2 min, RT) and the supernatant discarded. The remaining

pellet was washed with 1 mL acetone before being pelleted again (14,000 x *g*, 2 min, RT). The pellet was left to air dry before being resuspended in 120 µL of 0.1 M NaOH. Protein concentrations were determined by BCA protein assay (Thermo) and diluted twofold with 2X SDS sample buffer.

30 µg of protein were loaded onto NuPAGE 4-12% Bis-Tris Gels (Thermo) and separated (200 V, 35 min). Proteins were transferred to a PVDF membrane (Sigma) and blocked with 5% non-fat dry milk in TBST (1 h, RT). Membranes were then probed with primary anti-FLAG (Sigma F1804, 1:2500) antibodies diluted in 5% (NFDM) in TBST (overnight, 4 ºC). Membranes were washed three times with TBST and then probed with secondary antibodies diluted in 5% NFDM in TBST (1 h, RT). Membranes were washed three timed with TBST and developed by enhanced chemiluminescence (ECL). For the blotting of cells harboring constructs containing the endogenous *HEM25* promoter, the SuperSignal West Atto substrate (Thermo, A38554) was used. Blotting for cells harboring constructs containing the constitutive GPD promoter used the SuperSignal West Dura substrate (Thermo, 34075). Developed membranes were imaged on a ChemiDoc system (Bio-Rad) before being stripped (Thermo, 46430). Stripped membranes were blocked in 5% NFDM in TBST (1 h, RT) before being probed with anti-Act1 (Abcam ab8224, 1:5000) loading control antibody (1 h, RT). Membranes were washed three times with TBST before being probed with the secondary antibody diluted in 5% NFDM (1 h, RT). Membranes were washed three times before being developed using the SuperSignal West Dura substrate. Membranes then were imaged using the ChemiDoc.

*Isolated mitochondria.* Samples were collected and prepared as described in "Mitochondrial PPHB synthesis." 15 µg of protein were loaded onto a NuPAGE 4-12% Bis-Tris

Gel (Thermo) and separated (200 V, 35 min). Proteins were transferred to a PVDF membrane (Sigma), cut between the expected sizes of Coq1p and VDAC, and blocked with 4% non-fat dry milk in TBST (1 h, RT). The membranes were then probed with primary antibodies diluted in 4% NFDM (overnight, 4 ºC). Membranes were washed three times with TBST before being probed with secondary antibodies (1 h, RT). Membranes were washed three times with TBST before being imaged on a LI-COR Odyssey CLx Imaging System and analyzed with LI-COR Image Studio Software (version 5.2.5).

*E. coli membranes.* Approximately 40 mL*OD of induced cells were collected (4000 x *g,* 15 min, 4 ºC), the supernatant removed, snap frozen in $LN_2$, and stored at -80 ºC until blotting. Frozen pellets were thawed on ice and resuspended in 2 mL ice-cold lysis buffer (10 mM Tris pH 7 containing protease inhibitors). Cells were sonicated until clear (Branson Ultrasonics, 45% amplitude, 5 s pulse, 50% duty cycle, microtip). Lysed cells were diluted with ice-cold lysis buffer to a final volume of 9 mL. Unlysed cells and insoluble material were pelleted by centrifugation (27,000 x *g,* 15 min, 4 ºC). The supernatant was transferred to a 14 mL tube (Beckman 344060) and ultracentrifuged to pellet membranes (150,000 x *g,* 1 h, 4 ºC). The supernatant was removed, and the membrane pellet was resuspended in 75 µL ice-cold lysis buffer. Protein concentrations were determined by BCA protein assay (Thermo) and the sample diluted twofold in 2X SDS sample buffer.

5 µg of protein were loaded onto a NuPAGE 4-12% Bis-Tris Gel (Thermo) and separated (150 V, 1 h). Proteins were transferred to a PVDF membrane (Sigma) and blocked with 5 % NFDM in TBST. The membrane was then probed with the primary anti-MBP antibody (NEB E8032S, 1:10000) diluted in 5% NFDM (overnight, 4 ºC). The membrane was washed three times with

TBST and probed with secondary antibodies (1 h, RT) diluted in 5% NFDM in TBST. The membrane was washed three times with TBST before being imaged on a LI-COR Odyssey CLx Imaging System.

Statistical analysis

All experiments were performed in at least biological triplicate, unless otherwise stated. All results are presented as the arithmetic mean ± standard deviation (SD). Statistical analysis were performed in Prism 9.0 (GraphPad Software) or in Microsoft Excel. *P* values were calculated using unpaired, two-sided Student's *t*-test with values less than 0.05 considered significant. For fold changes, the average of the control or wild-type replicates was set to 1, with the other samples normalized accordingly.

**Competing interests**

J.J.C. is a consultant for Thermo Fisher Scientific, 908 Devices, and Seer. The remaining authors

declare no competing interests.
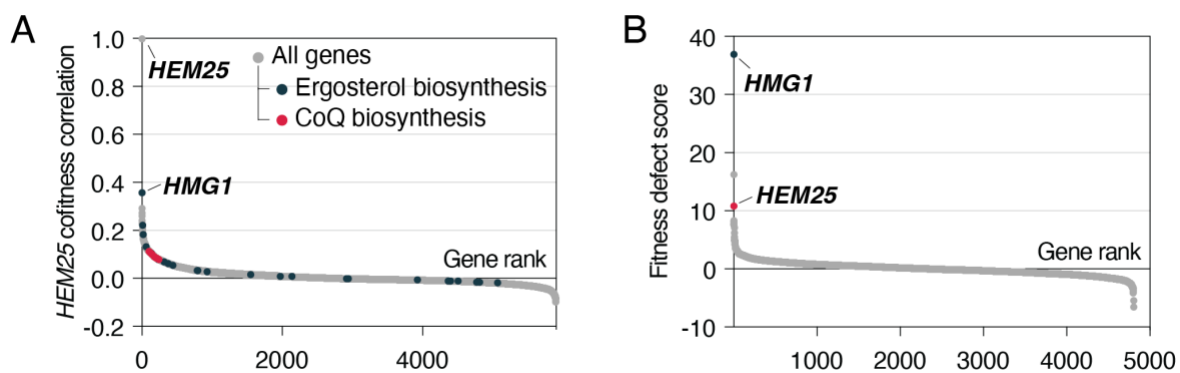
**Fig. S1.** (**A**) Gene fitness correlations with *HEM25*. Genes involved with ergosterol and CoQ biosynthesis are highlighted. (**B**) Fitness ranking of *gene*Δ strains in the presence of 78.68 µM atorvastatin. Raw data for (A) and (B) are from the HIPHOP chemogenomics database (*31*). Fitness defect scores reflect the homozygous deletion profiles for atorvastatin (compound SGTC_2648)
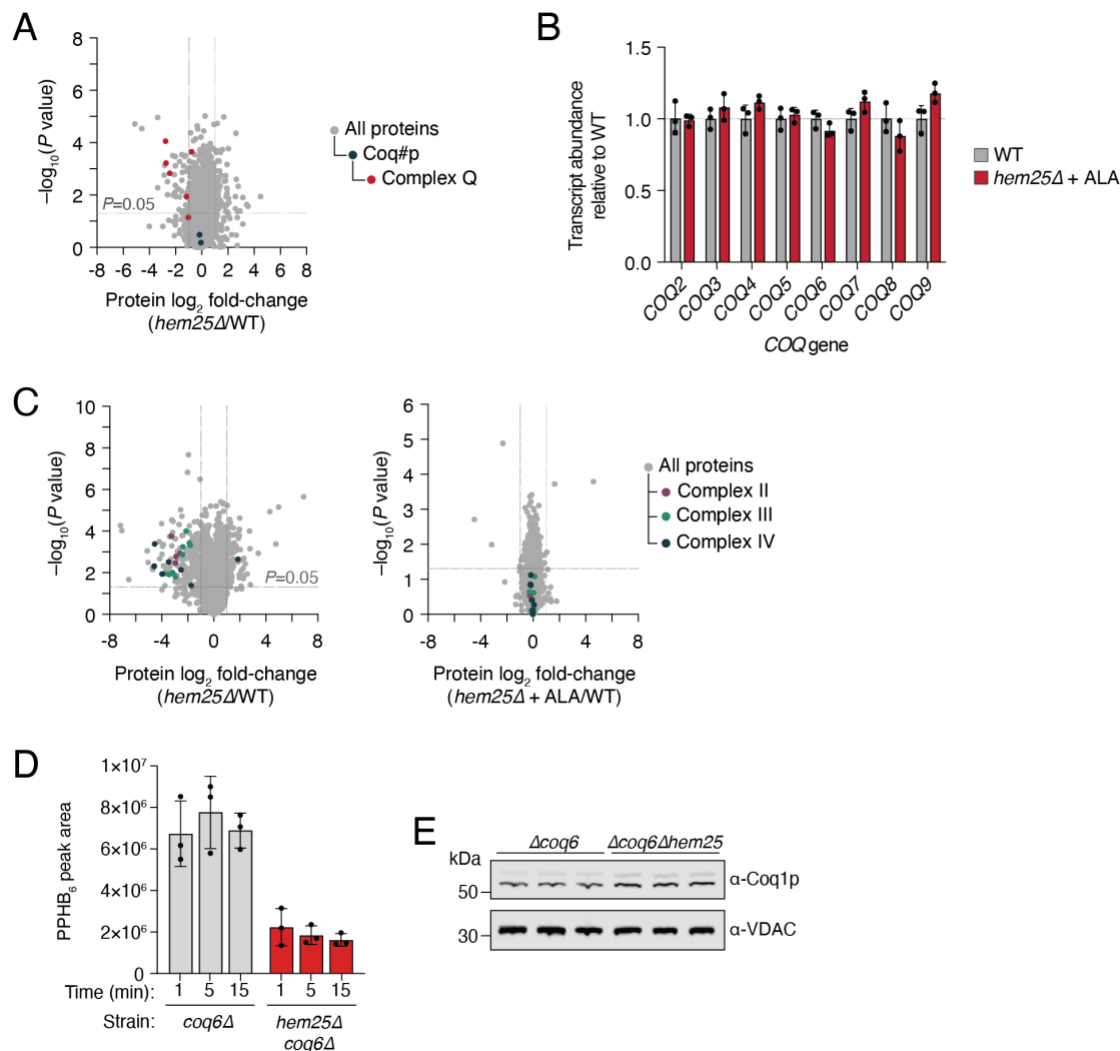
**Fig. S2.** (**A**) Relative protein abundances of *hem25Δ* cells compared to WT cells verses statistical significance. CoQ biosynthetic proteins and Complex Q proteins are highlighted. Raw data from the Y3K dataset[30] (respiration-RDR condition) are displayed as the mean from 3 independent samples with two-sided Student's *t*-test used. (**B**) Relative protein abundances of *hem25Δ* cells ± ALA supplementation compared to WT cells without ALA supplementation verses statistical significance. Components of the electron transport chain are highlighted (mean, *n*=3 independent samples, two-sides Student's *t*-test). (**C**) Relative transcript abundances of CoQ biosynthetic genes from *hem25Δ* with ALA supplementation compared to WT cells without ALA supplementation (mean, *n*=3 independent samples). (**D**) Normalized abundance of unlabeled PPHB levels in

isolated *coq6Δ* and *coq6Δhem25Δ* mitochondria (mean ± SD, *n*=3 independent samples). (**E**) Coq1p levels in isolated mitochondria from each replicate, assessed by immunoblotting.
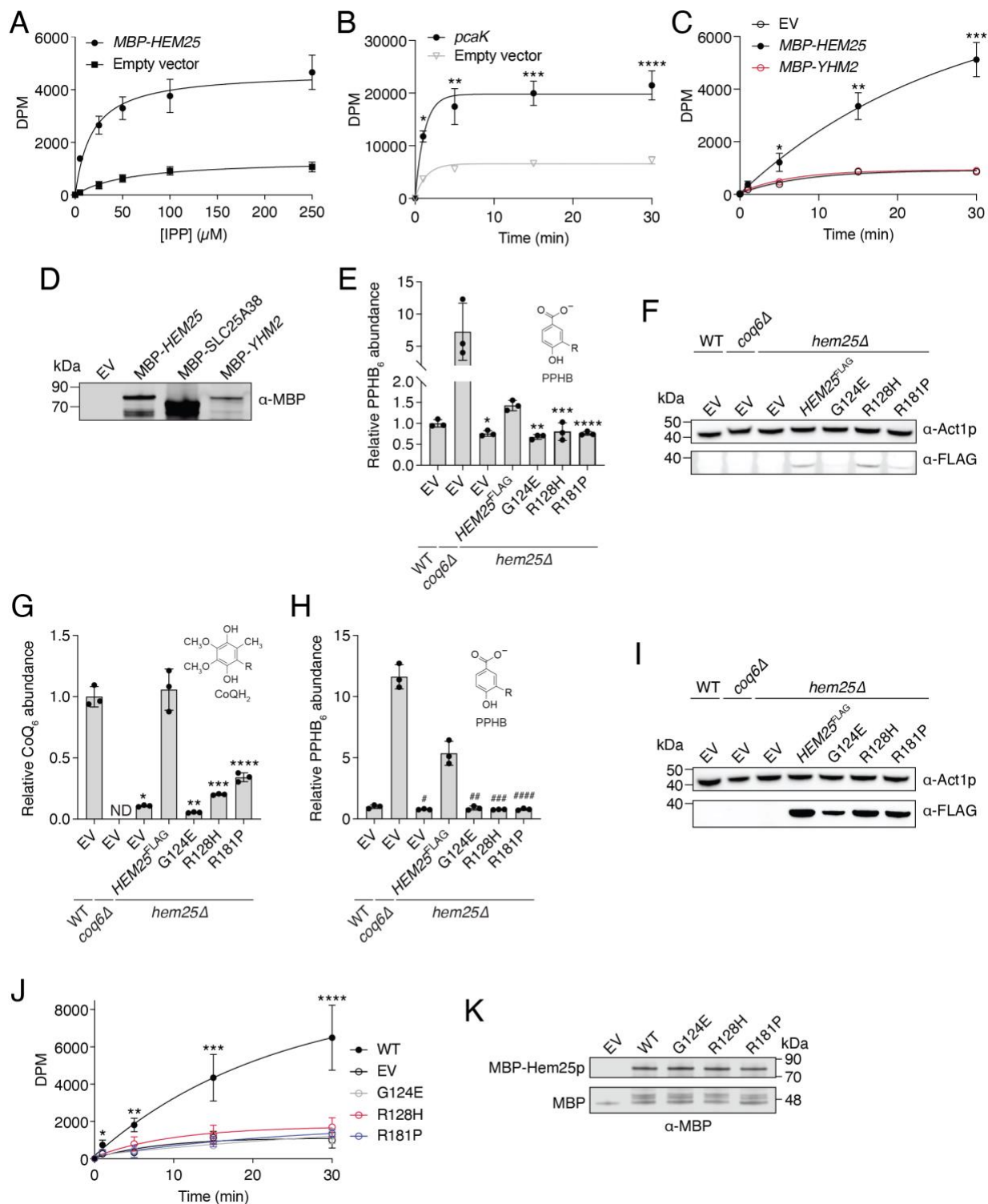
**Fig. S3. (A)** Steady-state kinetics of [1-$^{14}$C]-IPP uptake in cells expressing MBP-Hem25p or the empty vector. Raw DPM values represent the mean ± SD of 3 independent samples. **(B)** Time course of 50 µM [*phenyl*-$^{14}$C]-4-HB uptake by *E. coli* cells expressing the *Pseudomonas putida*

PcaK or the empty vector (*$p$=0.0002, **$p$=0.0038, ***$p$=0.0006, ****$p$=0.0009 empty vector vs *pcaK,* mean ± SD from 3 independent samples) (**C**) Time course of 50 μM [1-$^{14}$C]-IPP uptake by *E. coli* cells expressing MBP-Hem25p, MBP-Yhm2p, or the empty vector (*$p$=0.0147, **$p$=0.0011, ***$p$=0.0003 empty vector vs *MBP-HEM25*, mean ± SD, $n$=3 independent samples). (**D**) Immunoblot for MBP-Hem25p, MBP-SLC25A38, and MBP-Yhm2p in *E. coli* membranes preparations. (**E**) Relative PPHB abundances in *hem25Δ* yeast carrying WT and mutant *HEM25*$^{FLAG}$ constructs under the control of the endogenous *HEM25* promoter. Levels are relative to WT yeast carrying the empty expression vector (*$p$=0.0011, **$p$=0.0006, ***$p$=0.0116, ****$p$=0.0009 *HEM25*$^{FLAG}$ vs mutants or empty vector, mean ± SD from 3 independent samples). (**F**) Immunoblot of *hem25Δ* cells expressing WT and mutant Hem25p-FLAG under the control of the endogenous *HEM25* promoter. (**G**), (**H**) Relative (G) CoQ and (H) PPHB abundances in *hem25Δ* yeast carrying WT and mutant *HEM25*$^{FLAG}$ constructs under the control of the constitutive GPD promoter. Levels are relative to WT yeast carrying the empty expression vector (*$p$=0.0006, **$p$=0.0005, ***$p$=0.0009, ****$p$=0.0019, $^{#}p$=0.0012, $^{##}p$=0.0014, $^{###}p$=0.0012, $^{####}p$=0.0012 *HEM25*$^{FLAG}$ vs mutants or empty vector, mean ± SD from 3 independent samples); (**I**) Immunoblot of *hem25Δ* cells expressing WT and mutant Hem25p-FLAG under the control of the constitutive *GPD* promoter. (**J**) Time course of 50 μM [1-$^{14}$C]-IPP uptake by *E. coli* cells expressing WT MBP-Hem25p, mutant MBP-Hem25p, or the empty vector (*$p$=0.0429, **$p$=0.0021, ***$p$=0.0124, ****$p$=0.006 empty vector vs WT, mean ± SD, $n$=3 independent samples). (**K**) Immunoblot for WT and mutant MBP-Hem25p in *E. coli* membranes preparations.
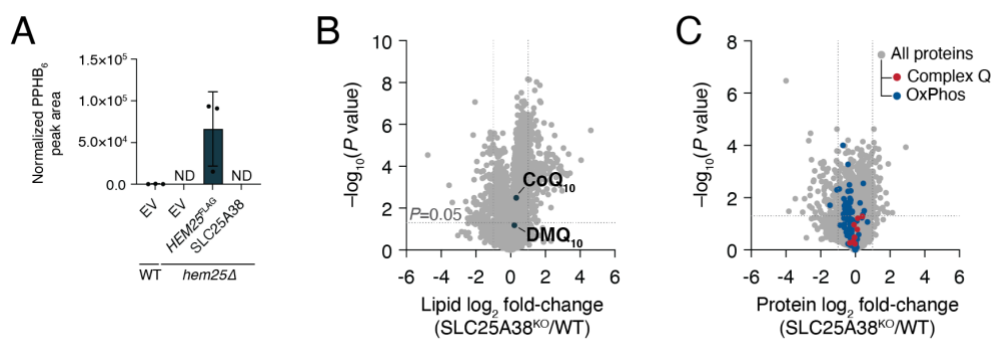
**Fig. S4.** (**A**) Normalized PPHB abundance in *hem25Δ* cells expressing Hem25p-FLAG or SLC25A38. (mean ± SD from 3 independent samples) (**B**) Relative lipid abundances in *hem25Δ* yeast compared to WT verses statistical significance with $CoQ_{10}$ and the $CoQ_{10}$ biosynthetic intermediate demethoxy-coenzyme Q ($DMQ_{10}$,) highlighted. (**C**) Relative protein abundance $SLC25A38^{KO}$ cells compared to WT cells verses statistical significance with CoQ-related (COQ3-COQ9) and OXPHOS-related proteins highlighted. For panels (B) and (C), raw lipidomic and proteomic data, respectively, from the MITOMICS resource[43] are displayed as the mean from 3 independent samples with two-sided Welch's *t*-test used.

**Table S1. Primers used in this study for amplification.**

| Amplicon | Primer | Sequence |
|---|---|---|
| HEM25 | HEM25-FWD | CAAGCggatccATGACTGAGCAAGCAACTAA |
| HEM25-FLAG | HEM25-FLAG-REV | TAACTCTCGAGTCACTTGTCGTCATCGTCTTTGTAGTCtccggatgaaccCATGAATCTTTTGACCAACTCCTCATATAT |
| HEM25 Promoter | HEM25 Promoter-FWD | agctggagctcACAGCAGTAGATCA |
| HEM25 Promoter | HEM25 Promoter-REV | ATCGTggatccGTATGCTGCTTCAC |

**Table S2. Primers used in this study for site directed mutagenesis.**

| Primer | Sequence |
|---|---|
| HEM25 G124E-FWD | GAGCGAAAGCttCGGTCAGCAG |
| HEM25 G124E-REV | GTGGTCTGGTTGGTTACATC |
| HEM25 R128H-FWD | AACCAGACCAtGAGCGAAAGC |
| HEM25 R128H-REV | GGTTACATCACCATGCCG |
| HEM25 R181P-FWD | ACGGAGCGTCcgGCAGGCAGGT |
| HEM25 R181P-REV | ACGCTGGTCTGTACGTTC |

# References

1. R. L. Lester, F. L. Crane, The Natural Occurrence of Coenzyme Q and Related Compounds. *J Biol Chem*. **234**, 2169–2175 (1959).

2. M. E. Jones, Pyrimidine Nucleotide Biosynthesis in Animals: Genes, Enzymes, and Regulation of UMP Biosynthesis. *Annu Rev Biochem*. **49**, 253–279 (1980).

3. F. E. Frerman, Acyl-CoA dehydrogenases, electron transfer flavoprotein and electron transfer flavoprotein dehydrogenase. *Biochem Soc T*. **16**, 416–418 (1988).

4. R. M. Guerra, D. J. Pagliarini, Coenzyme Q biochemistry and biosynthesis. *Trends Biochem Sci* (2023), doi:10.1016/j.tibs.2022.12.006.

5. V. Emmanuele, L. C. López, L. López, A. Berardo, A. Naini, S. Tadesse, B. Wen, E. D'Agostino, M. Solomon, S. DiMauro, C. Quinzii, M. Hirano, Heterogeneity of Coenzyme Q10 Deficiency: Patient Study and Literature Review. *Arch Neurol-chicago*. **69**, 978–983 (2012).

6. Y. Wang, S. Hekimi, The efficacy of coenzyme Q10 treatment in alleviating the symptoms of primary coenzyme Q10 deficiency: A systematic review. *J Cell Mol Med*. **26**, 4635–4644 (2022).

7. J. A. Stefely, D. J. Pagliarini, Biochemistry of Mitochondrial Coenzyme Q Biosynthesis. *Trends Biochem Sci*. **42**, 824–843 (2017).

8. A. M. Awad, M. C. Bradley, L. Fernández-del-Río, A. Nag, H. S. Tsui, C. F. Clarke, Coenzyme Q10 deficiencies: pathways in yeast and humans. *Essays Biochem*. **62**, 361–376 (2018).

9. Y. Wang, S. Hekimi, Understanding Ubiquinone. *Trends Cell Biol*. **26**, 367–378 (2016).

10. P. H. Gold, R. E. Olson, Studies on Coenzyme Q. The biosynthesis of coenzyme Q9 in rat tissue slices. *J Biol Chem*. **241**, 3507–3516 (1966).

11. L. A. Payet, M. Leroux, J. C. Willison, A. Kihara, L. Pelosi, F. Pierrel, Mechanistic Details of Early Steps in Coenzyme Q Biosynthesis Pathway in Yeast. *Cell Chem Biol*. **23**, 1241–1250 (2016).

12. J. Casey, D. R. Threlfall, Synthesis of 5-demethoxyubiquinone-6 and ubiquinone-6 from 3-hexaprenyl-4-hydroxybenzoate in yeast mitochondria. *Febs Lett*. **85**, 249–253 (1978).

13. K. Momose, H. Rudney, 3-Polyprenyl-4-hydroxybenzoate Synthesis in the Inner Membrane of Mitochondria from p-Hydroxybenzoate and Isopentenylpyrophosphate. A demonstration of isoprenoid synthesis in rat liver mitochondria. *J Biol Chem*. **247**, 3930–3940 (1972).

14. A. Tzagoloff, C. L. Dieckmann, PET genes of Saccharomyces cerevisiae. *Microbiol Rev*. **54**, 211–225 (1990).

15. K. P. Robinson, A. Jochem, S. E. Johnson, T. R. Reddy, J. D. Russell, J. J. Coon, D. J. Pagliarini, Defining intermediates and redundancies in coenzyme Q precursor biosynthesis. *J Biological Chem*. **296**, 100643 (2021).

16. E. B. Taylor, Functional Properties of the Mitochondrial Carrier System. *Trends Cell Biol*. **27**, 633–644 (2017).

17. F. Palmieri, M. Monne, Discoveries, metabolic roles and diseases of mitochondrial carriers: A review. *Biochimica Et Biophysica Acta Bba - Mol Cell Res*. **1863**, 2362–78 (2016).

18. F. N. Vogtle, J. M. Burkhart, H. Gonczarowska-Jorge, C. Kucukkose, A. A. Taskin, D. Kopczynski, R. Ahrends, D. Mossmann, A. Sickmann, R. P. Zahedi, C. Meisinger, Landscape of submitochondrial protein distribution. *Nat Commun*. **8**, 290 (2017).

19. M. Morgenstern, S. B. Stiller, P. Lubbert, C. D. Peikert, S. Dannenmaier, F. Drepper, U. Weill, P. Hoss, R. Feuerstein, M. Gebert, M. Bohnert, M. van der Laan, M. Schuldiner, C. Schutze, S. Oeljeklaus, N. Pfanner, N. Wiedemann, B. Warscheid, Definition of a High-Confidence Mitochondrial Proteome at Quantitative Scale. *Cell Reports*. **19**, 2836–2852 (2017).

20. M. Ozeir, U. Muhlenhoff, H. Webert, R. Lill, M. Fontecave, F. Pierrel, Coenzyme Q biosynthesis: Coq6 is required for the C5-hydroxylation reaction and substrate analogs rescue Coq6 deficiency. *Chem Biol*. **18**, 1134–42 (2011).

21. C. M. T. Marobbio, G. Agrimi, F. M. Lasorsa, F. Palmieri, Identification and functional reconstitution of yeast mitochondrial carrier for S-adenosylmethionine. *Embo J*. **22**, 5975–5982 (2003).

22. R. J. Barkovich, A. Shtanko, J. A. Shepherd, P. T. Lee, D. C. Myles, A. Tzagoloff, C. F. Clarke, Characterization of the COQ5 Gene from Saccharomyces cerevisiae EVIDENCE FOR A C-METHYLTRANSFERASE IN UBIQUINONE BIOSYNTHESIS*. *J Biol Chem*. **272**, 9182–9188 (1997).

23. T. Jonassen, C. F. Clarke, Isolation and Functional Expression of Human COQ3, a Gene Encoding a Methyltransferase Required for Ubiquinone Biosynthesis*. *J Biol Chem*. **275**, 12381–12387 (2000).

24. E. Luk, M. Carroll, M. Baker, V. C. Culotta, Manganese activation of superoxide dismutase 2 in Saccharomyces cerevisiae requires MTM1, a member of the mitochondrial carrier family. *Proc National Acad Sci*. **100**, 10353–10357 (2003).

25. J. Diessl, J. Berndtsson, F. Broeskamp, L. Habernig, V. Kohler, C. Vazquez-Calvo, A. Nandy, C. Peselj, S. Drobysheva, L. Pelosi, F.-N. Vögtle, F. Pierrel, M. Ott, S. Büttner, Manganese-driven CoQ deficiency. *Nat Commun*. **13**, 6061 (2022).

26. A. Naranuntarat, L. T. Jensen, S. Pazicni, J. E. Penner-Hahn, V. C. Culotta, The Interaction of Mitochondrial Iron with Manganese Superoxide Dismutase*. *J Biol Chem*. **284**, 22633–22640 (2009).

27. P. Lunetti, F. Damiano, G. D. Benedetto, L. Siculella, A. Pennetta, L. Muto, E. Paradies, C. M. Marobbio, V. Dolce, L. Capobianco, Characterization of Human and Yeast Mitochondrial Glycine Carriers with Implications for Heme Biosynthesis and Anemia. *J Biol Chem*. **291**, 19746–59 (2016).

28. J. P. Fernandez-Murray, S. V. Prykhozhij, J. N. Dufay, S. L. Steele, D. Gaston, G. K. Nasrallah, A. J. Coombs, R. S. Liwski, C. V. Fernandez, J. N. Berman, C. R. McMaster, Glycine and Folate Ameliorate Models of Congenital Sideroblastic Anemia. *Plos Genet*. **12**, e1005783 (2016).

29. A. Johnson, P. Gin, B. N. Marbois, E. J. Hsieh, M. Wu, M. H. Barros, C. F. Clarke, A. Tzagoloff, COQ9, a New Gene Required for the Biosynthesis of Coenzyme Q in Saccharomyces cerevisiae *. *J Biol Chem*. **280**, 31397–31404 (2005).

30. J. A. Stefely, N. W. Kwiecien, E. C. Freiberger, A. L. Richards, A. Jochem, M. J. P. Rush, A. Ulbrich, K. P. Robinson, P. D. Hutchins, M. T. Veling, X. Guo, Z. A. Kemmerer, K. J. Connors, E. A. Trujillo, J. Sokol, H. Marx, M. S. Westphall, A. S. Hebert, D. J. Pagliarini, J. J. Coon, Mitochondrial protein functions elucidated by multi-omic mass spectrometry profiling. *Nat Biotechnol*. **34**, 1191–1197 (2016).

31. A. Y. Lee, R. P. St.Onge, M. J. Proctor, I. M. Wallace, A. H. Nile, P. A. Spagnuolo, Y. Jitkova, M. Gronda, Y. Wu, M. K. Kim, K. Cheung-Ong, N. P. Torres, E. D. Spear, M. K. L. Han, U. Schlecht, S. Suresh, G. Duby, L. E. Heisler, A. Surendra, E. Fung, M. L. Urbanus, M. Gebbia, E. Lissina, M. Miranda, J. H. Chiang, A. M. Aparicio, M. Zeghouf, R. W. Davis, J. Cherfils, M. Boutry, C. A. Kaiser, C. L. Cummins, W. S. Trimble, G. W. Brown, A. D. Schimmer, V. A. Bankaitis, C. Nislow, G. D. Bader, G. Giaever, Mapping the Cellular Response to Small Molecules Using Chemogenomic Fitness Signatures. *Science*. **344**, 208–211 (2014).

32. M. A. Desbats, V. Morbidoni, M. Silic-Benussi, M. Doimo, V. Ciminale, M. Cassina, S. Sacconi, M. Hirano, G. Basso, F. Pierrel, P. Navas, L. Salviati, E. Trevisson, The COQ2 genotype predicts the severity of coenzyme Q 10 deficiency. *Hum Mol Genet*. **25**, 4256–4265 (2016).

33. C. M. Allan, A. M. Awad, J. S. Johnson, D. I. Shirasaki, C. Wang, C. E. Blaby-Haas, S. S. Merchant, J. A. Loo, C. F. Clarke, Identification of Coq11, a New Coenzyme Q Biosynthetic Protein in the CoQ-Synthome in Saccharomyces cerevisiae *. *J Biol Chem*. **290**, 7517–7534 (2015).

34. E. J. Hsieh, P. Gin, M. Gulmezian, U. C. Tran, R. Saiki, B. N. Marbois, C. F. Clarke, Saccharomyces cerevisiae Coq9 polypeptide is a subunit of the mitochondrial coenzyme Q biosynthetic complex. *Arch Biochem Biophys*. **463**, 19–26 (2007).

35. J. N. Dufay, J. P. Fernández-Murray, C. R. McMaster, SLC25 Family Member Genetic Interactions Identify a Role for HEM25 in Yeast Electron Transport Chain Stability. *G3 Genes Genomes Genetics*. **7**, 1861–1873 (2017).

36. S. Ravaud, A. Bidon-Chanal, I. Blesneac, P. Machillot, C. Juillan-Binard, F. Dehez, C. Chipot, E. Pebay-Peyroula, Impaired Transport of Nucleotides in a Mitochondrial Carrier Explains Severe Human Genetic Diseases. *Acs Chem Biol*. **7**, 1164–1169 (2012).

37. J. Mifsud, S. Ravaud, E.-M. Krammer, C. Chipot, E. R. S. Kunji, E. Pebay-Peyroula, F. Dehez, The substrate specificity of the human ADP/ATP carrier AAC1. *Mol Membr Biol*. **30**, 160–168 (2012).

38. A. Castegna, P. Scarcia, G. Agrimi, L. Palmieri, H. Rottensteiner, I. Spera, L. Germinario, F. Palmieri, Identification and Functional Characterization of a Novel Mitochondrial Carrier for Citrate and Oxoglutarate in Saccharomyces cerevisiae *. *J Biol Chem*. **285**, 17359–17370 (2010).

39. N. N. Nichols, C. S. Harwood, PcaK, a high-affinity permease for the aromatic compounds 4-hydroxybenzoate and protocatechuate from Pseudomonas putida. *J Bacteriol*. **179**, 5056–5061 (1997).

40. A. J. Robinson, C. Overy, E. R. Kunji, The mechanism of transport by mitochondrial carriers based on analysis of symmetry. *Proc National Acad Sci*. **105**, 17766–71 (2008).

41. D. L. Guernsey, H. Jiang, D. R. Campagna, S. C. Evans, M. Ferguson, M. D. Kellogg, M. Lachance, M. Matsuoka, M. Nightingale, A. Rideout, L. Saint-Amant, P. J. Schmidt, A. Orr, S. S. Bottomley, M. D. Fleming, M. Ludman, S. Dyack, C. V. Fernandez, M. E. Samuels, Mutations in mitochondrial carrier family gene SLC25A38 cause nonsyndromic autosomal recessive congenital sideroblastic anemia. *Nat Genet*. **41**, 651–3 (2009).

42. M. M. Heeney, S. Berhe, D. R. Campagna, J. H. Oved, P. Kurre, P. J. Shaw, J. Teo, M. A. Shanap, H. M. Hassab, B. E. Glader, S. Shah, A. Yoshimi, A. Ameri, J. H. Antin, J. Boudreaux, M. Briones, K. E. Dickerson, C. V. Fernandez, R. Farah, H. Hasle, S. B. Keel, T. S. Olson, J. M. Powers, M. J. Rose, A. Shimamura, S. S. Bottomley, M. D. Fleming, SLC25A38 congenital sideroblastic anemia: Phenotypes and genotypes of 31 individuals from 24 families, including 11 novel mutations, and a review of the literature. *Hum. Mutat.* **42**, 1367–1383 (2021).

43. J. W. Rensvold, E. Shishkova, Y. Sverchkov, I. J. Miller, A. Cetinkaya, A. Pyle, M. Manicki, D. R. Brademan, Y. Alanay, J. Raiman, A. Jochem, P. D. Hutchins, S. R. Peters, V. Linke, K. A. Overmyer, A. Z. Salome, A. S. Hebert, C. E. Vincent, N. W. Kwiecien, M. J. P. Rush, M. S. Westphall, M. Craven, N. A. Akarsu, R. W. Taylor, J. J. Coon, D. J. Pagliarini, Defining mitochondrial protein functions through deep multiomic profiling. *Nature*. **606**, 382–388 (2022).

44. P. D. Thomas, D. Ebert, A. Muruganujan, T. Mushayahama, L. Albou, H. Mi, PANTHER: Making genome-scale phylogenetics accessible to all. *Protein Sci*. **31**, 8–22 (2022).

45. K. Subramanian, A. Jochem, M. L. Vasseur, S. Lewis, B. R. Paulson, T. R. Reddy, J. D. Russell, J. J. Coon, D. J. Pagliarini, J. Nunnari, Coenzyme Q biosynthetic proteins assemble in a substrate-dependent manner into domains at ER-mitochondria contacts. *J Cell Biol*. **218**, 1353–1369 (2019).

46. M. Eisenberg-Bord, H. S. Tsui, D. Antunes, L. Fernández-del-Río, M. C. Bradley, C. D. Dunn, T. P. T. Nguyen, D. Rapaport, C. F. Clarke, M. Schuldiner, The Endoplasmic Reticulum-Mitochondria Encounter Structure Complex Coordinates Coenzyme Q Biosynthesis. *Contact*. **2**, 2515256418825409 (2019).

47. K. E. Vest, S. C. Leary, D. R. Winge, P. A. Cobine, Copper Import into the Mitochondrial Matrix in Saccharomyces cerevisiae Is Mediated by Pic2, a Mitochondrial Carrier Family Protein*. *J Biol Chem*. **288**, 23884–23892 (2013).

48. A. Boulet, K. E. Vest, M. K. Maynard, M. G. Gammon, A. C. Russell, A. T. Mathews, S. E. Cole, X. Zhu, C. B. Phillips, J. Q. Kwong, S. C. Dodani, S. C. Leary, P. A. Cobine, The mammalian phosphate carrier SLC25A3 is a mitochondrial copper transporter required for cytochrome c oxidase biogenesis. *J Biol Chem*. **293**, 1887–1896 (2018).

49. J. Casey, D. R. Threlfall, Formation of 3-hexaprenyl-4-hydroxybenzoate by matrix-free mitochondrial membrane-rich preparations of yeast. *Biochim Biophys Acta*. **530**, 487–502 (1978).

50. M. Runquist, J. Ericsson, A. Thelin, T. Chojnacki, G. Dallner, Isoprenoid biosynthesis in rat liver mitochondria. Studies on farnesyl pyrophosphate synthase and trans-prenyltransferase. *J Biol Chem*. **269**, 5804–5809 (1994).

51. J. Grünler, J. Ericsson, G. Dallner, Branch-point reactions in the biosynthesis of cholesterol, dolichol, ubiquinone and prenylated proteins. *Biochimica Et Biophysica Acta Bba - Lipids Lipid Metabolism*. **1212**, 259–277 (1994).

52. R. K. Keller, Squalene synthase inhibition alters metabolism of nonsterols in rat liver. *Biochimica Et Biophysica Acta Bba - Lipids Lipid Metabolism*. **1303**, 169–179 (1996).

53. J. R. Kardon, Y. Y. Yien, N. C. Huston, D. S. Branco, G. J. Hildick-Smith, K. Y. Rhee, B. H. Paw, T. A. Baker, Mitochondrial ClpX Activates a Key Enzyme for Heme Biosynthesis and Erythropoiesis. *Cell*. **161**, 858–867 (2015).

54. C. M. Rondelli, M. Perfetto, A. Danoff, H. Bergonia, S. Gillis, L. O'Neill, L. Jackson, G. Nicolas, H. Puy, R. West, J. D. Phillips, Y. Y. Yien, The ubiquitous mitochondrial protein unfoldase CLPX regulates erythroid heme synthesis by control of iron utilization and heme synthesis enzyme activation and turnover. *J Biol Chem*. **297**, 100972 (2021).

55. J. A. Stefely, F. Licitra, L. Laredj, A. G. Reidenbach, Z. A. Kemmerer, A. Grangeray, T. Jaeg-Ehret, C. E. Minogue, A. Ulbrich, P. D. Hutchins, E. M. Wilkerson, Z. Ruan, D. Aydin, A. S. Hebert, X. Guo, E. C. Freiberger, L. Reutenauer, A. Jochem, M. Chergova, I. E. Johnson, D.

C. Lohman, M. J. P. Rush, N. W. Kwiecien, P. K. Singh, A. I. Schlagowski, B. J. Floyd, U. Forsman, P. J. Sindelar, M. S. Westphall, F. Pierrel, J. Zoll, M. Dal Peraro, N. Kannan, C. A. Bingman, J. J. Coon, P. Isope, H. Puccio, D. J. Pagliarini, Cerebellar Ataxia and Coenzyme Q Deficiency through Loss of Unorthodox Kinase Activity. *Mol Cell*. **63**, 608–620 (2016).

56. M. Ziegler, M. Monné, A. Nikiforov, G. Agrimi, I. Heiland, F. Palmieri, Welcome to the Family: Identification of the NAD+ Transporter of Animal Mitochondria as Member of the Solute Carrier Family SLC25. *Biomol*. **11**, 880 (2021).

57. T. S. Luongo, J. M. Eller, M.-J. Lu, M. Niere, F. Raith, C. Perry, M. R. Bornstein, P. Oliphint, L. Wang, M. R. McReynolds, M. E. Migaud, J. D. Rabinowitz, F. B. Johnson, K. Johnsson, M. Ziegler, X. A. Cambronne, J. A. Baur, SLC25A51 is a mammalian mitochondrial NAD+ transporter. *Nature*. **588**, 174–179 (2020).

58. N. Kory, J. uit de Bos, S. van der Rijt, N. Jankovic, M. Güra, N. Arp, I. A. Pena, G. Prakash, S. H. Chan, T. Kunchok, C. A. Lewis, D. M. Sabatini, MCART1/SLC25A51 is required for mitochondrial NAD transport. *Sci Adv*. **6**, eabe5310 (2020).

59. E. Girardi, G. Agrimi, U. Goldmann, G. Fiume, S. Lindinger, V. Sedlyarov, I. Srndic, B. Gürtl, B. Agerer, F. Kartnig, P. Scarcia, M. A. D. Noia, E. Liñeiro, M. Rebsamen, T. Wiedmer, A. Bergthaler, L. Palmieri, G. Superti-Furga, Epistasis-driven identification of SLC25A51 as a regulator of human mitochondrial NAD import. *Nat Commun*. **11**, 6145 (2020).

60. A. Baudin, O. Ozier-Kalogeropoulos, A. Denouel, F. Lacroute, C. Cullin, A simple and efficient method for direct gene deletion in Saccharomyces cerevisiae. *Nucleic Acids Res*. **21**, 3329–3330 (1993).

61. M. S. Longtine, A. M. III, D. J. Demarini, N. G. Shah, A. Wach, A. Brachat, P. Philippsen, J. R. Pringle, Additional modules for versatile and economical PCR-based gene deletion and modification in Saccharomyces cerevisiae. *Yeast*. **14**, 953–961 (1998).

62. A. Wach, A. Brachat, C. Alberti-Segui, C. Rebischung, P. Philippsen, Heterologous HIS3 Marker and GFP Reporter Modules for PCR-Targeting in Saccharomyces cerevisiae. *Yeast*. **13**, 1065–1075 (1997).

63. A. Ismail, V. Leroux, M. Smadja, L. Gonzalez, M. Lombard, F. Pierrel, C. Mellot-Draznieks, M. Fontecave, Coenzyme Q Biosynthesis: Evidence for a Substrate Access Channel in the FAD-Dependent Monooxygenase Coq6. *Plos Comput Biol*. **12**, e1004690 (2016).

64. S. Sassa, Sequential induction of heme pathway enzymes during erythroid differentiation of mouse Friend leukemia virus-infected cells. *J Exp Medicine*. **143**, 305–315 (1976).

65. P. R. Sinclair, N. Gorman, J. M. Jacobs, *Curr Protoc Toxicol*, in press, doi:10.1002/0471140856.tx0803s00.

66. E. Shishkova, A. S. Hebert, M. S. Westphall, J. J. Coon, Ultra-High Pressure (>30,000 psi) Packing of Capillary Columns Enhancing Depth of Shotgun Proteomic Analyses. *Anal Chem*. **90**, 11503–11508 (2018).

67. A. S. Hebert, C. Thöing, N. M. Riley, N. W. Kwiecien, E. Shiskova, R. Huguet, H. L. Cardasis, A. Kuehn, S. Eliuk, V. Zabrouskov, M. S. Westphall, G. C. McAlister, J. J. Coon, Improved Precursor Characterization for Data-Dependent Mass Spectrometry. A*nal Chem.* 9**0,** 2333–2340 (2018).

68. S. Tyanova, T. Temu, J. Cox, The MaxQuant computational platform for mass spectrometry-based shotgun proteomics. *Nat Protoc*. **11**, 2301–2319 (2016).

69. J. Cox, M. Y. Hein, C. A. Luber, I. Paron, N. Nagaraj, M. Mann, Accurate Proteome-wide Label-free Quantification by Delayed Normalization and Maximal Peptide Ratio Extraction, Termed MaxLFQ*. *Mol Cell Proteomics*. **13**, 2513–2526 (2014).

70. D. R. Brademan, I. J. Miller, N. W. Kwiecien, D. J. Pagliarini, M. S. Westphall, J. J. Coon, E. Shishkova, Argonaut: A Web Platform for Collaborative Multi-omic Data Visualization and Exploration. *Patterns*. **1**, 100122 (2020).

71. C. Meisinger, N. Pfanner, K. N. Truscott, Isolation of yeast mitochondria. *Methods Mol Biol*. **313**, 33–9 (2006).

72. B. Miroux, J. E. Walker, Over-production of Proteins inEscherichia coli: Mutant Hosts that Allow Synthesis of some Membrane Proteins and Globular Proteins at High Levels. *J Mol Biol*. **260**, 289–298 (1996).

73. R. D. Gietz, R. H. Schiestl, High-efficiency yeast transformation using the LiAc/SS carrier DNA/PEG method. *Nat Protoc*. 2, 31–34 (2007).

74. A. M. Waterhouse, J. B. Procter, D. M. A. Martin, M. Clamp, G. J. Barton, Jalview Version 2—a multiple sequence alignment editor and analysis workbench. *Bioinformatics*. **25**, 1189–1191 (2009).

75. F. Sievers, A. Wilm, D. Dineen, T. J. Gibson, K. Karplus, W. Li, R. Lopez, H. McWilliam, M. Remmert, J. Söding, J. D. Thompson, D. G. Higgins, Fast, scalable generation of high-quality protein multiple sequence alignments using Clustal Omega. *Mol Syst Biol*. **7**, 539–539 (2011).

76. M. Varadi, S. Anyango, M. Deshpande, S. Nair, C. Natassia, G. Yordanova, D. Yuan, O. Stroe, G. Wood, A. Laydon, A. Žídek, T. Green, K. Tunyasuvunakool, S. Petersen, J. Jumper, E. Clancy, R. Green, A. Vora, M. Lutfi, M. Figurnov, A. Cowie, N. Hobbs, P. Kohli, G. Kleywegt, E. Birney, D. Hassabis, S. Velankar, AlphaFold Protein Structure Database: massively expanding the structural coverage of protein-sequence space with high-accuracy models. *Nucleic Acids Res*. **50**, D439–D444 (2021).

77. J. Jumper, R. Evans, A. Pritzel, T. Green, M. Figurnov, O. Ronneberger, K. Tunyasuvunakool, R. Bates, A. Žídek, A. Potapenko, A. Bridgland, C. Meyer, S. A. A. Kohl, A. J. Ballard, A. Cowie, B. Romera-Paredes, S. Nikolov, R. Jain, J. Adler, T. Back, S. Petersen, D. Reiman, E. Clancy, M. Zielinski, M. Steinegger, M. Pacholska, T. Berghammer, S. Bodenstein, D. Silver, O. Vinyals, A. W. Senior, K. Kavukcuoglu, P. Kohli, D. Hassabis, Highly accurate protein structure prediction with AlphaFold. *Nature*. **596**, 583–589 (2021).

78. M. T. Veling, A. G. Reidenbach, E. C. Freiberger, N. W. Kwiecien, P. D. Hutchins, M. J. Drahnak, A. Jochem, A. Ulbrich, M. J. P. Rush, J. D. Russell, J. J. Coon, D. J. Pagliarini, Multi-omic Mitoprotease Profiling Defines a Role for Oct1p in Coenzyme Q Production. *Mol Cell*. **68**, 970-977.e11 (2017).

## Chapter 3: Defining the mechanisms of 4-HB transport

Sean W. Rogers, Jonathan Tai, Rachel M. Guerra, David J. Pagliarini

**Author contributions:**

Conceptualization: JT, RMG, SWR, DJP

Methodology: JT, RMG, SWR, DJP

Formal analysis: JT, RMG, SWR

Investigation: JT, RMG, SWR

Funding acquisition: DJP

Supervision: DJP

Writing – original draft: JT

This chapter contains unpublished work.

**Abstract**

4-hydroxybenzoate (4-HB) is the universal head group precursor for coenzyme Q (ubiquinone, CoQ). 4-HB is synthesized from tyrosine in the cytosol before being imported into the mitochondrial matrix for CoQ biosynthesis. However, the mechanism by which 4-HB reaches the matrix is unknown. In the previous chapter, I carried out a targeted yeast genetic screen for CoQ precursor transporters that resulted in the characterization of Hem25p as an isopentenyl pyrophosphate (IPP) transporter. This screen did not yield any leads for a 4-HB transporter, suggesting that it may be mediated by a non-SLC25 transporter. A previous study identified a tunnel within the human integral membrane protein COQ2 that may interact with 4-HB and mediate its transport into COQ2's active site. In this chapter, I will use a combination of *in silico* modeling and uptake assays to investigate 4-HB transport by Coq2p/COQ2.

**Introduction**

In the previous chapter, I performed a targeted yeast genetic screen for mitochondrial transporters involved in CoQ biosynthesis. That screen included all 35 members of the yeast SLC25 carrier family as well as seven non-SLC25 proteins. These non-SLC25 proteins were uncharacterized proteins with properties of mitochondrial transporters–inner membrane localization, multiple transmembrane domains, and metazoan homology. From that screen, four proteins were identified whose *gene*Δ strains had decreased CoQ abundance. One of these hits, Hem25p, was characterized by our group as an IPP transporter. This left 4-HB as the remaining precursor without an identified transporter. The remaining hits from that screen–Flx1p, Sam5p, and Mtm1p–had direct or hypothesized links to specific steps of CoQ biosynthesis[1–7], making them unlikely candidates for a 4-HB transporter. Furthermore, the respective *gene*Δ strains all had elevated PPHB levels, suggesting a defect in late CoQ biosynthesis[8]. Thus, it is unlikely that a 4-HB transporter was identified in our screen.

The results of our screen suggest that 4-HB transport is mediated by a non-SLC25 carrier. A recent report hypothesized that COQ2, a mitochondrial prenyltransferase that attaches the polyisoprenoid tail to 4-HB, doubles as the 4-HB transporter[9]. In patient-derived fibroblasts harboring COQ2 mutations, supplementation with 4-HB, 4-HBz, or 4-HPP was able to rescue CoQ deficiencies. Furthermore, 4-HB supplementation increased the levels of complex Q members COQ7 and COQ4, indicating that supplementation was driving flux through the pathway[10]. As a result, cell proliferation in galactose medium was rescued in COQ2-mutated cells. These effects, which were restricted to COQ2 mutations, suggest 4-HB as a therapeutic target in these patients. However, the mechanism by which this rescue occurs is unknown.
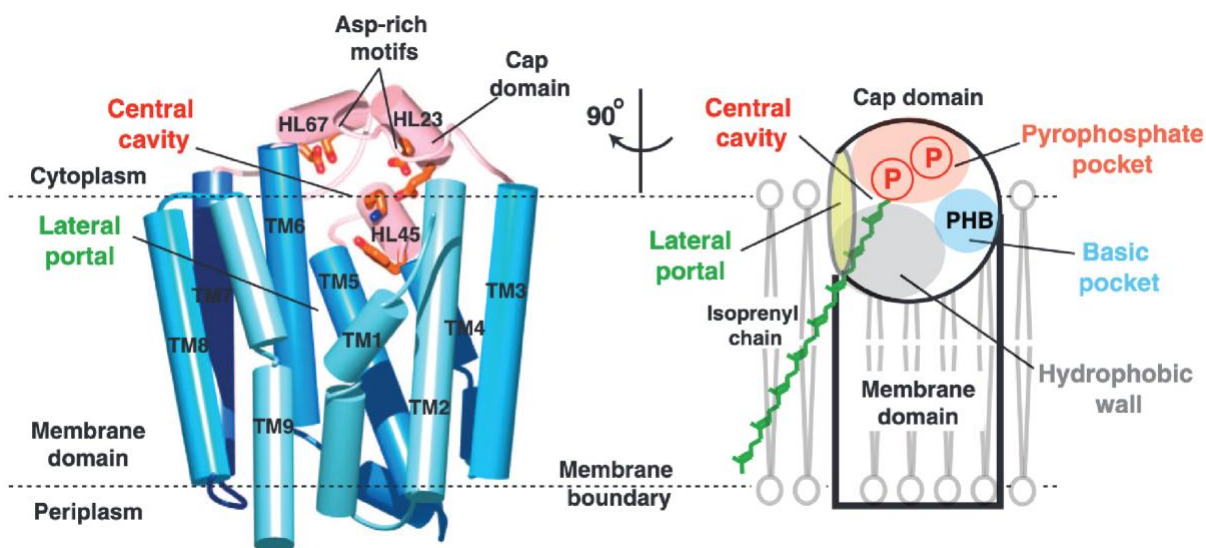
**Figure 1. Overview of UbiA structure.** Members of the UbiA superfamily are integral membrane proteins that catalyze prenyltransferase reactions. The structure of ApUbiA (PDB: 4OD5) is shown. The general structure features a central cavity to carry out the prenyltransferase reaction. There is also lateral portal through which polyprenyl pyrophosphates can enter. Figure from Cheng et al[11].

*In silico* homology modeling of COQ2, an integral membrane protein, showed a central cavity on the matrix side of the protein[9,11] (Figure 1). This central cavity harbors the catalytic prenyltransferase residues and contains a lateral portal into the membrane. This portal is believed to allow the polyprenyl pyrophosphate to enter the central cavity, where the prenyl chain becomes attached to 4-HB. Since the polyprenyl tail remains outside of the protein, this may explain the promiscuity of COQ2 to different tail lengths[12]. The homology models also identified a small tunnel linking the intermembrane space to COQ2's active site (Figure 2). Furthermore, several clinically relevant COQ2 mutations were localized to residues lining this tunnel[9]. Docking simulations also identified several putative 4-HB binding sites along the tunnel path. Importantly,

this rescue of CoQ abundance was only seen upon 4-HB supplementation and did not occur when mevalonate was added. Thus, the authors theorized that COQ2 imports 4-HB through this tunnel, and that the effect of supplementation was due to increased 4-HB flux compensating for decreased transport activity.
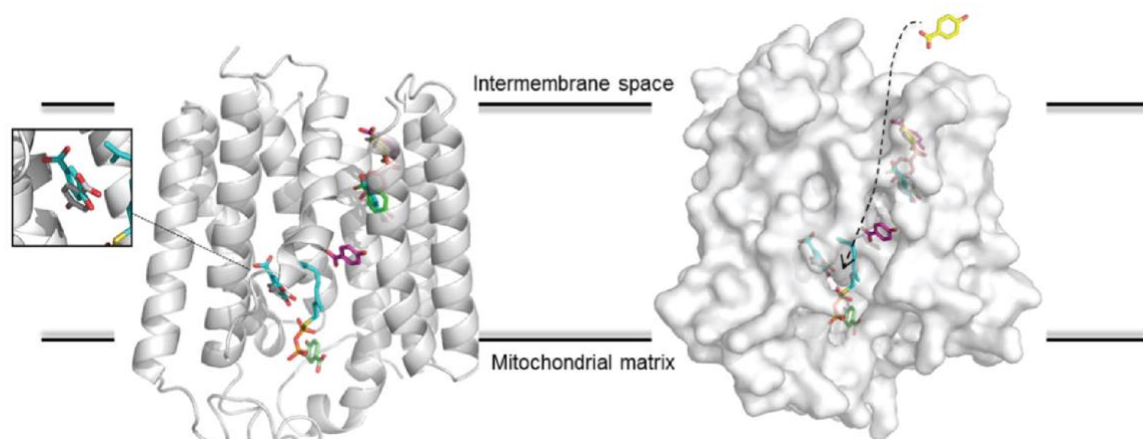


**Figure 2. *In silico* homology model of human COQ2.** Ligand docking of 4-HB to the homology model is shown. A potential path for 4-HB through the tunnel-like strucutre is shown. Figure from Herebian et al[9].

COQ2 is a member of the UbiA prenyltransferase superfamily, whose members catalyze the transfer of prenyl groups to a variety of substrates[13]. In doing so, UbiA superfamily enzymes are involved in the synthesis many key bioactive compounds, including CoQ, vitamins E and K, heme A, chlorophyll, and prenylated flavonoids. As a result, mutations in UbiA superfamily members have been implicated in a number of human diseases, including primary CoQ deficiency[9,14,15]. No secondary functions have been identified for any member of the UbiA superfamily. Thus, if COQ2 is a 4-HB transporter, it would expand our understanding of the UbiA superfamily and open new avenues for studying their functions. In this chapter, I describe our

initial assessment of Coq2p (the yeast homolog of COQ2) as a 4-HB transporter in CoQ biosynthesis. If successful, these efforts will accelerate the development of new therapeutic approaches for patients with *COQ2* mutations.

**The tunnel-like structure is conserved in the yeast Coq2p**

We first assessed the homology between the human COQ2 and the yeast Coq2p. Sequence alignments showed that human COQ2 and yeast Coq2p demonstrate relatively high homology, with approximately 36.5% identity (Figure S1). Nearly all of the clinically relevant COQ2 mutations were in conserved residues (Figure S2). Homology modeling of Coq2p, using the ApUbiA structure[11] (PDB: 4OD5), showed the same tunnel-like structure as the human COQ2 model[9] (Figure 3). All of the mutated residues lining the tunnel were preserved in the Coq2p model. Interestingly, this integral tunnel structure is absent in both of the solved UbiA crystal structures[11,16] (Figures S3A and S3B). When other UbiA superfamily members, Cox10p and the *E. coli* UbiA, are modeled, the tunnels are present, however the paths are more obstructed and less direct than eukaryotic COQ2 homologs (Figure S3C and S3D). Given that heme *b*, the Cox10p substrate[13], is much larger than 4-HB, and that *E. coli* can synthesize 4-HB in the cytoplasm[17] (thereby obviating the need for 4-HB transport), these models suggest that the tunnel's putative function in transport is not conserved among all UbiA superfamily members. Thus, while homology modeling has its limitations, the presence of an integral tunnel containing clinically relevant residues leads us to believe that it is a *bona fide* structural feature of Coq2p and its eukaryotic homologs. We therefore decided to investigate Coq2p-mediated 4-HB transport by uptake assays.
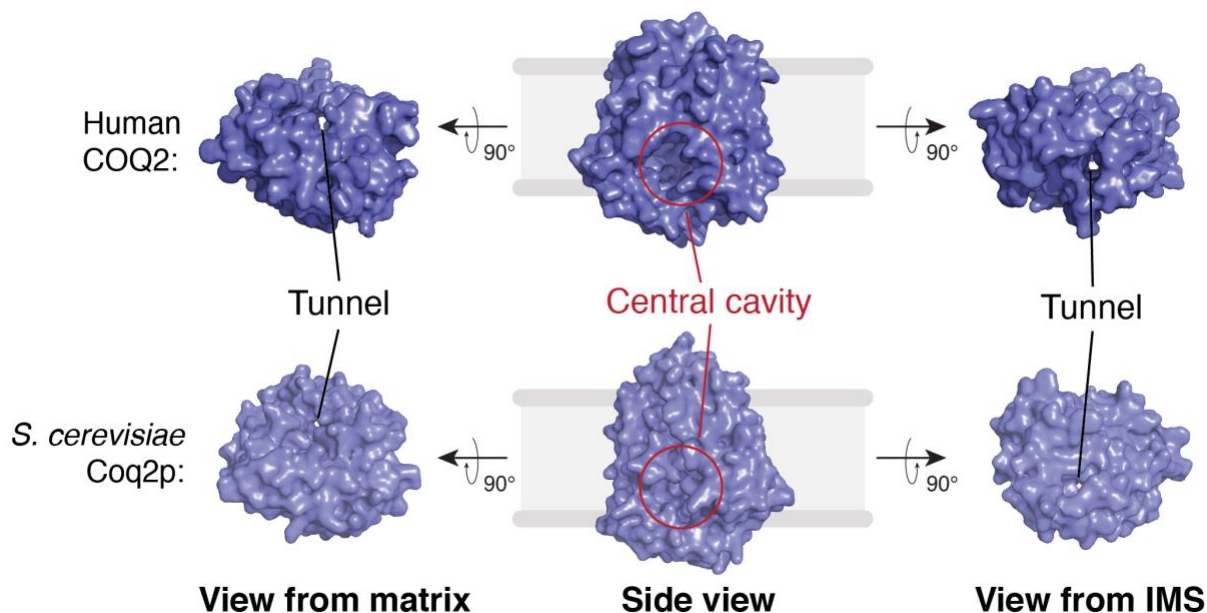
**Figure 3. Conservation between human COQ2 and yeast Coq2p.** Matrix, side, and intermembrane space views are shown. The central cavity containing the active site is marked in red. Views of the tunnel-like structure from the matrix and intermembrane space are shown.

**Bacteria expressing Coq2p import 4-HB**

We expressed the yeast Coq2p in bacterial membranes, allowing us to perform whole-cell uptake assays with radiolabeled 4-HB. As a positive control, we also expressed the known 4-HB transporter pcaK from *Pseudomonas putida*[18]. *E. coli* C43(DE3) cells expressing Coq2p showed increased 4-HB uptake over that of the empty vector (Figure 4). Uptake by pcaK-expressing cells was slightly higher than that from cells expressing Coq2p. In all cases, uptake was rapid, reaching a steady state by the 5-minute timepoint. Though these results are promising, there are some issues that need to be addressed. First, in both the Coq2p and pcaK-expressing cells, uptake leveled off by 5 minutes and remained the same through the end of the assay at 30 minutes. While this could

reflect uptake, it could also be explained by non-specific association with the membrane. Demonstrating time-dependent uptake throughout the assay would increase our confidence that carrier-mediated transport is occurring. Second, the empty vector cells had relatively high levels of uptake. This could represent background from non-specific interactions of 4-HB with the filter and/or the cells. However, the intermediate levels of uptake at the 1-minute timepoint suggest that there is low-level uptake by the empty vector cells. Thus, this background should be minimized in order to accurately study 4-HB transport in isolation.
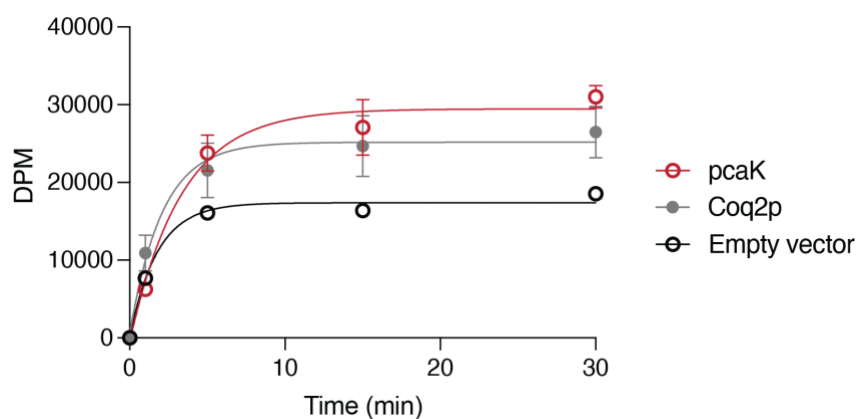


**Figure 4. Radiolabeled 4-HB uptake assay.** Time course of [*phenyl*-^{14}C]-4-HB by C43(DE3) cells expressing pcaK (red), Coq2p (gray), or the empty vector (black). Cells were incubated with 50 µM [*phenyl*-^{14}C]-4-HB.

We therefore modified the uptake assay by adding 10 µM glucose and 10 µM succinate to the reaction[18]. This was added to generate a proton gradient across the bacterial membrane, as pcaK activity is driven by the proton-motive force (PMF). We also changed the cells from C43(DE3) to BL21(DE3). Prior work on 4-HB transport found low background levels in control BL21(DE3) cells[18]. To account for non-specific interactions, a control reaction was run using cells

that had been boiled. The counts from this reaction, representing 4-HB that had associated non-specifically with both the filter and the cells, was subtracted from the experimental values. With these modifications, cells expressing either pcaK or Coq2p demonstrated time-dependent 4-HB uptake, with pcaK cells having higher levels of uptake than the Coq2p cells (Figure 5). Uptake in the empty vector cells leveled off by 5 minutes and remained the same for the rest of the assay. The addition of excess cold 4-HB outcompeted radiolabeled uptake in every condition, including the empty vector control. This confirms the presence of low-level 4-HB import in *E. coli.* Overall, these results show that Coq2p expression leads to 4-HB accumulation in bacteria, consistent with a putative role in 4-HB transport.
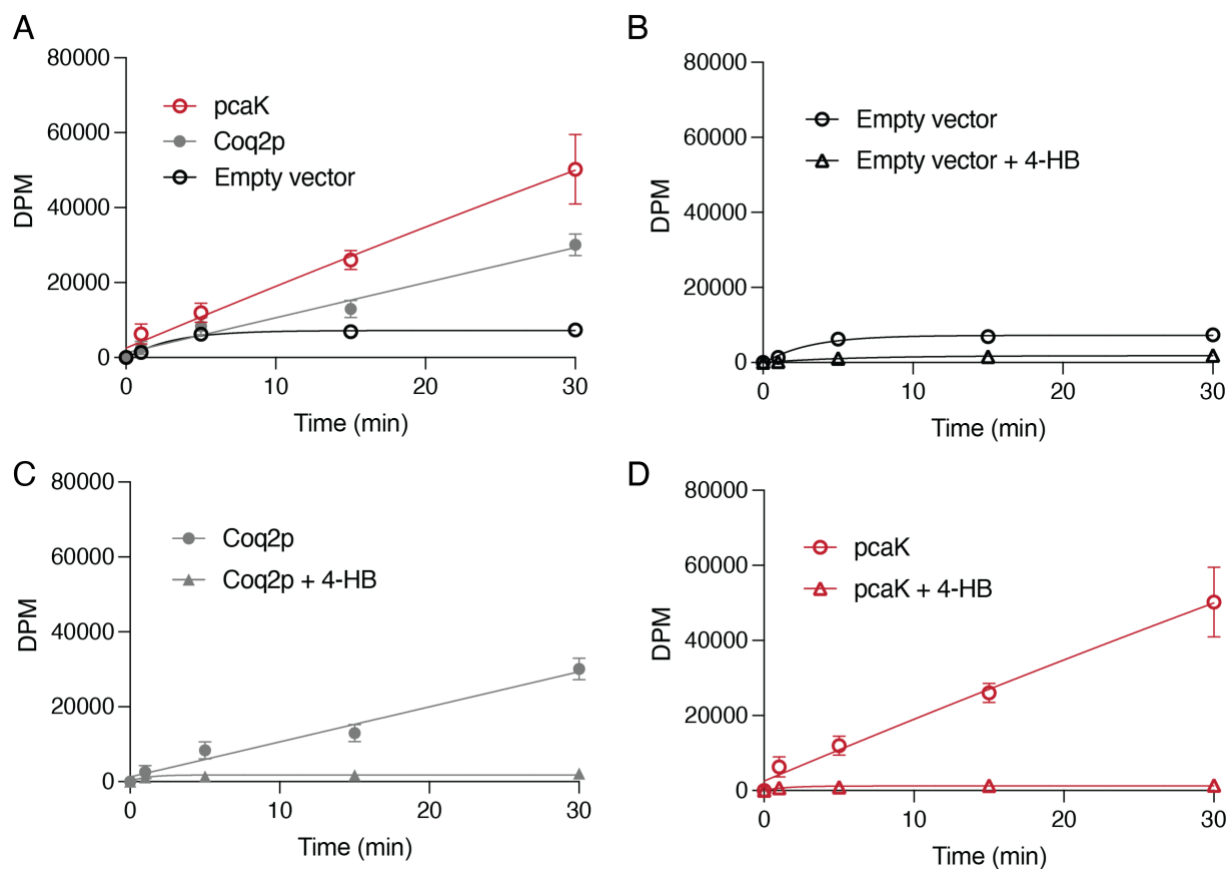
**Figure 5. Time-dependent uptake of 4-HB.** (**A**) Time course of [*phenyl*-^{14}C]-4-HB by BL21(DE3) cells expressing pcaK (red), Coq2p (gray), or the empty vector (black) in the presence of 25 µM [*phenyl*-^{14}C]-4-HB. (**B**), (**C**), (**D**) Individual uptake assays for empty vector, Coq2p, and pcaK conditions, respectively, along with the corresponding competition assays (triangles). For competition experiments, 1 mM unlabeled 4-HB was used.

**Discussion**

In this chapter, I present preliminary evidence of 4-HB transport by Coq2p. We show that cells expressing Coq2p displayed time-dependent accumulation of radiolabeled 4-HB, similar to the known 4-HB transporter pcaK. While promising, these early results do not establish Coq2p as a 4-HB transporter. It is possible that overexpression of Coq2p drives 4-HB import by consuming intracellular 4-HB and sequestering it as PPHB. Thus, additional experiments and controls are needed before any transporter function can be assigned. A key control will be the use of mutants to determine whether the tunnel-like structure is needed for 4-HB uptake. Four clinically relevant COQ2 mutations (S146N, Y297C, G390A, and V393A) have been described in the tunnel region, with varying phenotypes among them[9]. Two of these mutations have been tested in a *coq2Δ* yeast strain, with the S146N mutation having a more severe CoQ defect than the Y297C mutation[19] (Table S1). Thus, measuring 4-HB uptake by these mutant Coq2p variants would provide insight into the function of this tunnel.

It should be noted that in the original 4-HB supplementation paper, the experiments were performed on cells with non-tunnel COQ2 mutations[9]. Thus, its possible that 4-HB supplementation simply compensated for decreased catalytic efficiency, rather than increasing transport though the protein. To validate this tunnel's potential function, these supplementation

experiments should be repeated using the appropriate tunnel mutants. Use of the *coq2Δ* strain would be beneficial here[15], as it can provide a more robust platform for COQ2 function than patient-derived fibroblasts. The results from these experiments can be compared to kinetic measurements from uptake assays, yielding a deeper understanding of this tunnel's function.

Additional experiments should focus on isolating 4-HB transport from prenyltransferase activity. As stated previously, it is possible that Coq2p drives 4-HB import by a mechanism other than direct transport. Mechanisms include disequilibrium from intracellular 4-HB consumption driving its import, or upregulation of a yet to be identified *E. coli* 4-HB transporter. To test these alternative explanations, residues in Coq2p's central cavity can be mutated to generate a prenyltransferase-dead mutant. If 4-HB uptake is preserved, it would strengthen the argument that Coq2p is a *bona fide* transporter, whose transport function is independent of its prenyltransferase activity. However, if 4-HB uptake is decreased, it would suggest that Coq2p is not the transporter, and that 4-HB import is driven by Coq2p's catalytic activity. In this situation, there is also the possibility that Coq2p's transport and prenyltransferase activities are coupled to each other. If so, that would require studies of Coq2p function in a completely isolated system, such as a liposome. Thus, catalytic site mutants will provide valuable insights into the mechanisms of Coq2p function.

Although not conclusive, the work outlined in this chapter provides justification for further investigation into 4-HB transport by Coq2p. These early efforts were bolstered by the development of the *E. coli* uptake assay in the previous chapter. Confirming this dual function in Coq2p will be a challenging task, requiring a rigorous mechanistic biochemistry approach. However, if transport is confirmed, it would answer a longstanding question about CoQ biosynthesis, making us a better equipped to address CoQ deficiencies. It would also further our knowledge of the UbiA superfamily, this serving as a launching pad for future investigations into UbiA functions.

**Materials and Methods**

Sequence alignments and homology modeling

Sequences were aligned using Clustal Omega[20]. Homology models were generated using the Phyre2 web server[21]. The crystal structure of *Aeropyrum pernix* UbiA (PDB: 4OD5) was used as the template[11].

Bacterial uptake assays

Bacterial expression and whole-cell uptake assays were performed as described previously with slight modifications[18,22,23]. Genes encoding the yeast Coq2p and MBP-tagged pcaK (MBP-pcaK) were synthesized as codon-optimized gBlock gene fragments (IDT) and cloned into the pET-21b expression vector using the restriction enzymes NdeI and XhoI. The MBP-pcaK fusion protein was constructed in the same manner as described in the previous chapter. Inserts were confirmed by sequencing.

Expression of was carried out in either *E. coli* C43(DE3)[24] (Biosearch Technologies) or *E. coli* BL21(DE) cells. Single colonies of transformed cells were used to inoculate 4 mL of LB media containing 100 mg/L ampicillin. Cultures were incubated overnight (37 ºC, 230 rpm) before being diluted 1:100 in 50 mL LB media containing 100 mg/L ampicillin. Refreshed cultures were incubated (37 ºC, 230 rpm) until the $OD_{600}$=0.5-0.6, at which point protein expression was induced with 0.1 mM IPTG. Cells were induced overnight (20 ºC, 230 rpm, 14-16 h).

Induced cells were collected by centrifugation (4,000 x *g,* 10 min, 4 ºC), washed once with ice-cold KPi (50 mM potassium phosphate, pH 7.4), and centrifuged again (4,000 x *g,* 10 min, 4

ºC). Cells were resuspended in ice-cold KPi to a cell density of $OD_{600}=10$ and placed on ice until the start of the assay.

A 2X substrate buffer was prepared consisting of 2 mM $MgCl_2$ and [*phenyl*-$^{14}$C]-4-HB (purchased from American Radiolabeled Chemicals) at 2X the indicated assay concentration. To start the assay, 200 µL of cells were added to 200 µL 2X substrate buffer. Assays were carried out at room temperature. At each time point, 100 µL of the assay mixture were removed and filtered under vacuum to separate the cells from the incubation media. Filtration was achieved through either 0.22 µm mixed cellulose ester (MCE) filters (Millipore) or 0.2 µm Whatman Nuclepore track-etched hydrophilic membrane filters[18] (Cytiva). Following filtration, filters were washed with 5 mL of ice-cold KPi before being placed in a 7 mL scintillation vial (Fisher). 5 mL of Ultima Gold MV liquid scintillation cocktail (PerkinElmer) were added to each vial before being analyzed by liquid scintillation counting. Counts per minute were converted to disintegrations per minute (DPM) using the counting efficiency of the counter. In some experiments, background counts were measured by heating cells to 95-100 ºC for 5 min before performing the assay. Counts from this run, representing non-specific binding of 4-HB to the cells and/or filter, were subtracted from the experimental values.

```
sp|Q96H96-4|COQ2_HUMAN    MTPISQVRMRKGSAHTAAQPGRLGLHPAGATAHACRGMTSIRARPGLTSAMLGSRAAGFA      60
sp|P32378|COQ2_YEAST      -----------------------------------MF-IWQR---KSILLGRSILGSG      19
                                                             *  *  *   .* :**    * .

sp|Q96H96-4|COQ2_HUMAN    RGLRAVALAWLPGWRGRSFALA-RAAGAPHGGDLQPPACP---EPRGRQLSLSAAAVVDS     116
sp|P32378|COQ2_YEAST      ----RVTVAGIIGSSRKRYTSSSSSSSSPSSKESAPVFTSKELEVARKERLDGLGPFVSR      75
                              *::* : *     : :: : ::.:* . : *      *    ::   . . .*.

sp|Q96H96-4|COQ2_HUMAN    APRPLQPYLRLMRLDKPIGTWLLYLPCTWSIGLAAEP--GCFPDWYMLSLFGTGAILMR     173
sp|P32378|COQ2_YEAST      LPKKWIPYAELMRLEKPVGTWLLYLPCSWSILMGAMMQGATLSATAGMLGIFGVGALVMR     135
                           *:    ** .****:**:**********:*** :.*          **.:**.**:!**

sp|Q96H96-4|COQ2_HUMAN    GAGCTINDMWDQDYDKKVTRTANRPIAAGDISTFQSFVFLGGQLTLALGVLLCLNYYSIA     233
sp|P32378|COQ2_YEAST      GAGCTINDFLDRKLDQRVIRSVERPIASGRVSPRRALVFLGAQTLVGMGVLSLLPAQCWW     195
                          ********: *:. *::* *:.:****:* :*  :::****.*  :.:*** *   .

sp|Q96H96-4|COQ2_HUMAN    LGAGSLLLVITYPLMKRISYWPQLALGLTFNWGALLGWSAIKGSCDPSVCLPLYFSGVMW     293
sp|P32378|COQ2_YEAST      LGLASLPIVFTYPLFKRFTYYPQAALSACFNWGALLGFPAMGVMS-WPTMIPLYLSSYLW     254
                          ** .** :*:****:**::*:** **.   ********: *:   .     . :***:*. :*

sp|Q96H96-4|COQ2_HUMAN    TLIYDTIYAHQDKRDDVLIGLKSTALRFGENTKPWLSGFSVAMLGALSLVGVNSGQT--A     351
sp|P32378|COQ2_YEAST      CMTYDTIYAHQDKKFDIKAGIKSTALAWGPRTKSIMKAMSASQIALLAVAGLNSGLLWGP     314
                           : **********: *:  *:***** :*  .**  :...:*.: :. *::.*:***

sp|Q96H96-4|COQ2_HUMAN    PYYAALGAVGAHLTHQIYTLDIHRPEDCWNKFISNRTLGLIVFLGIVLGNLWKEKKTDKT     411
sp|P32378|COQ2_YEAST      GFIGGLGVFAYRLFSMIKKVDLDNPKNCWKYFNANINTGLYFTYALAVDYILRLFGFL--     372
                          : ..**... :*   * .:*:..*::**: * :* . ** .   .:.:. : :

sp|Q96H96-4|COQ2_HUMAN    KKGIENKIEN    421
sp|P32378|COQ2_YEAST      ----------    372
```

**Figure S1.** Sequence alignment of human COQ2 and yeast Coq2p. Alignment was performed using Clustal Omega.
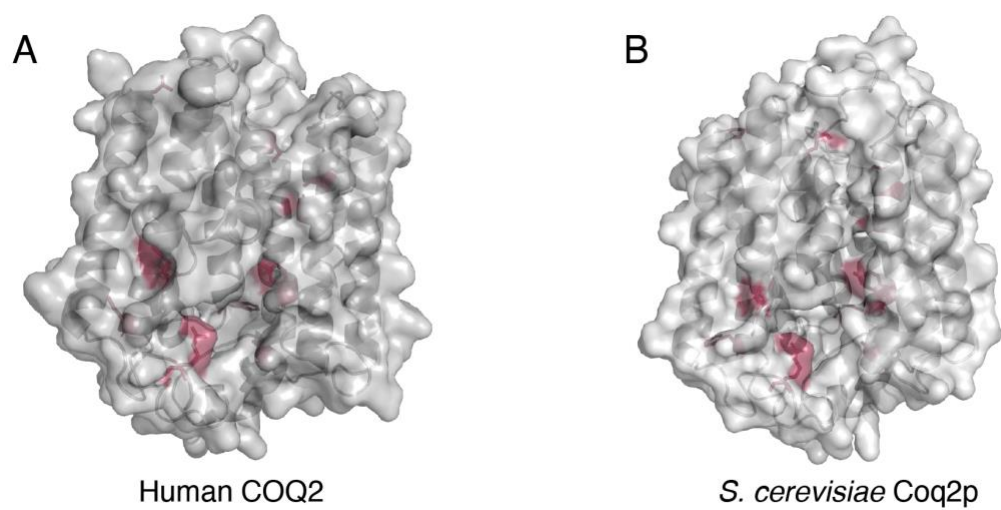
**Figure S2.** Homology models of (**A**) COQ2 and (**B**) Coq2p with patient mutations highlighted in red.
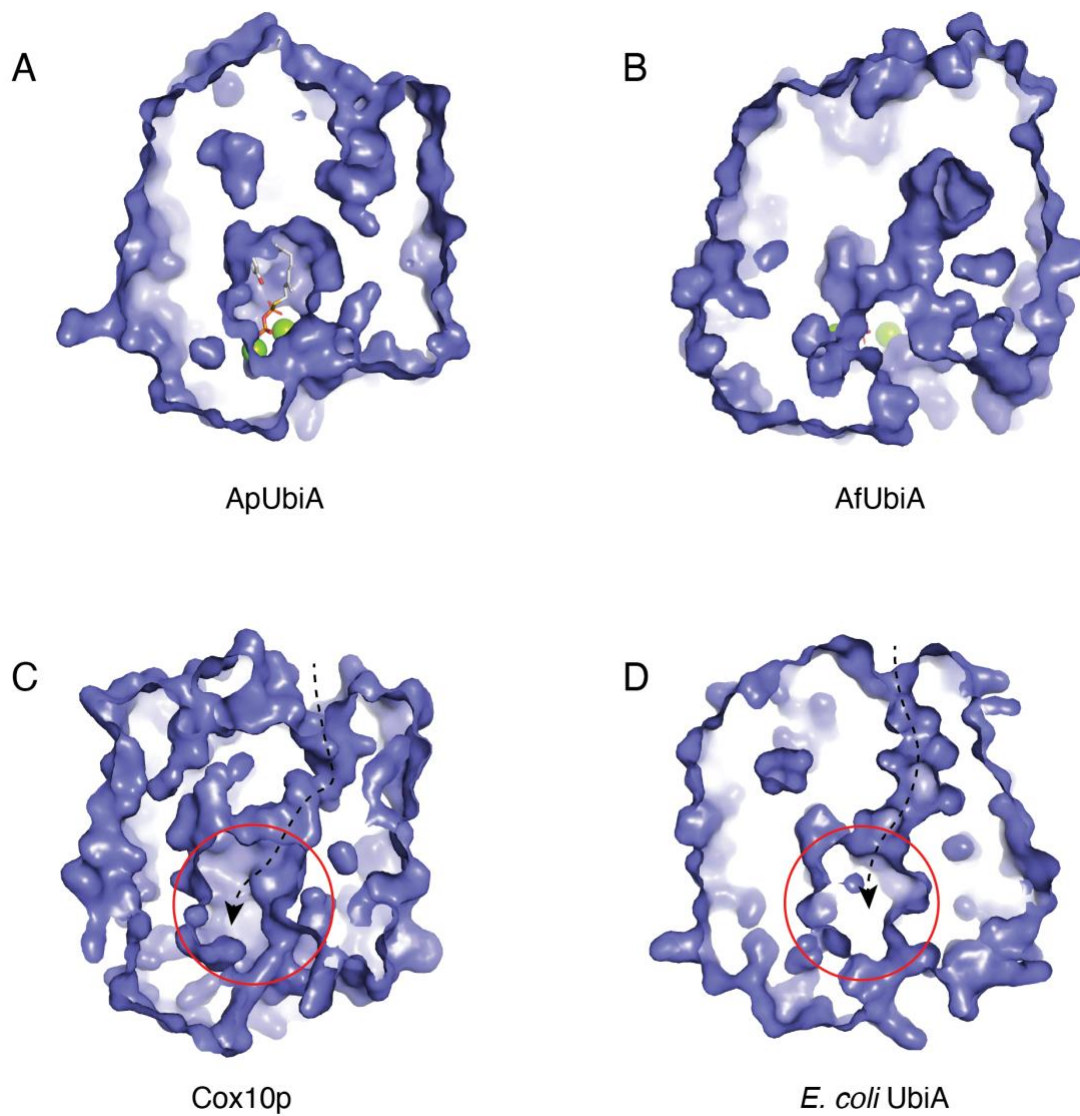
**Figure S3.** Crystal structures of (**A**) ApUbiA (PDB: 4OD5) and (**B**) AfUbiA (PDB: 4TQ3). Homlogy models of (**C**) Cox10p and (**D**) *E. coli* UbiA. Sliced views are shown to highlight the internal tunnel-like structure. In (C) and (D), the central cavity is circled in red and the path through the tunnel is marked with a dotted black line.

| Severity | hCOQ2 Mutation | CoQ levels in yeast (pmol/mg wet weight) | Corresponding yeast residue |
|---|---|---|---|
| Severe | S146N | 2.5 | S105 |
| | M182R | 1.2 | F144 |
| | W254R | N/A | Y216 |
| | A302V | <0.5 | A263 |
| Intermediate | R197H | <0.5* | R159 |
| | N228S | 13.6* | P190 |
| | Y297C | 7.1 | Y258 |
| | G390A | N/A | G353 |
| Late-onset | A32G | N/A | N/A |
| | M128V | 17.6 | M87 |
| | V393A | N/A | F356 |
| | WT | 26.9 | |

* Both mutations present in the same patient

**Table S1.** Clinical COQ2 mutations grouped by disease severity. Some of the mutants were expressed in *coq2Δ* yeast, and the resulting CoQ levels (pmol/mg wet weight) are given. Mutations and CoQ levels are from Herebian et al[9]. and Desbats et al[15].

# References

1. Ozeir, M. *et al.* Coenzyme Q biosynthesis: Coq6 is required for the C5-hydroxylation reaction and substrate analogs rescue Coq6 deficiency. *Chem Biol* 18, 1134–42 (2011).

2. Marobbio, C. M. T., Agrimi, G., Lasorsa, F. M. & Palmieri, F. Identification and functional reconstitution of yeast mitochondrial carrier for S-adenosylmethionine. *Embo J* 22, 5975–5982 (2003).

3. Jonassen, T. & Clarke, C. F. Isolation and Functional Expression of Human COQ3, a Gene Encoding a Methyltransferase Required for Ubiquinone Biosynthesis*. *J Biol Chem* 275, 12381–12387 (2000).

4. Barkovich, R. J. *et al.* Characterization of the COQ5 Gene from Saccharomyces cerevisiae EVIDENCE FOR A C-METHYLTRANSFERASE IN UBIQUINONE BIOSYNTHESIS*. *J Biol Chem* 272, 9182–9188 (1997).

5. Luk, E., Carroll, M., Baker, M. & Culotta, V. C. Manganese activation of superoxide dismutase 2 in Saccharomyces cerevisiae requires MTM1, a member of the mitochondrial carrier family. *Proc National Acad Sci* 100, 10353–10357 (2003).

6. Diessl, J. *et al.* Manganese-driven CoQ deficiency. *Nat Commun* 13, 6061 (2022).

7. Naranuntarat, A., Jensen, L. T., Pazicni, S., Penner-Hahn, J. E. & Culotta, V. C. The Interaction of Mitochondrial Iron with Manganese Superoxide Dismutase*. *J Biol Chem* 284, 22633–22640 (2009).

8. Stefely, J. A. *et al.* Mitochondrial protein functions elucidated by multi-omic mass spectrometry profiling. *Nat Biotechnol* 34, 1191–1197 (2016).

9. Herebian, D. *et al.* 4-Hydroxybenzoic acid restores CoQ10 biosynthesis in human COQ2 deficiency. *Ann Clin Transl Neur* 4, 902–908 (2017).

10. Hsieh, E. J. *et al.* Saccharomyces cerevisiae Coq9 polypeptide is a subunit of the mitochondrial coenzyme Q biosynthetic complex. *Arch Biochem Biophys* 463, 19–26 (2007).

11. Cheng, W. & Li, W. Structural Insights into Ubiquinone Biosynthesis in Membranes. *Science* 343, 878–881 (2014).

12. Okada, K. *et al.* Polyprenyl diphosphate synthase essentially defines the length of the side chain of ubiquinone. *Biochimica Et Biophysica Acta Bba - Lipids Lipid Metabolism* 1302, 217–223 (1996).

13. Li, W. Bringing Bioactive Compounds into Membranes: The UbiA Superfamily of Intramembrane Aromatic Prenyltransferases. *Trends Biochem Sci* 41, 356–370 (2016).

14. Quinzii, C. *et al.* A Mutation in Para-Hydroxybenzoate-Polyprenyl Transferase (COQ2) Causes Primary Coenzyme Q10 Deficiency. *Am J Hum Genetics* 78, 345–349 (2006).

15. Desbats, M. A. *et al.* The COQ2 genotype predicts the severity of coenzyme Q 10 deficiency. *Hum Mol Genet* 25, 4256–4265 (2016).

16. Huang, H. *et al.* Structure of a Membrane-Embedded Prenyltransferase Homologous to UBIAD1. *Plos Biol* 12, e1001911 (2014).

17. Fernández-del-Río, L. & Clarke, C. F. Coenzyme Q Biosynthesis: An Update on the Origins of the Benzenoid Ring and Discovery of New Ring Precursors. *Metabolites* 11, 385 (2021).

18. Nichols, N. N. & Harwood, C. S. PcaK, a high-affinity permease for the aromatic compounds 4-hydroxybenzoate and protocatechuate from Pseudomonas putida. *J Bacteriol* 179, 5056–5061 (1997).

19. Desbats, M. A., Lunardi, G., Doimo, M., Trevisson, E. & Salviati, L. Genetic bases and clinical manifestations of coenzyme Q10 (CoQ10) deficiency. *J Inherit Metab Dis* 38, 145–156 (2015).

20. Sievers, F. *et al.* Fast, scalable generation of high-quality protein multiple sequence alignments using Clustal Omega. *Mol Syst Biol* 7, 539–539 (2011).

21. Kelley, L. A., Mezulis, S., Yates, C. M., Wass, M. N. & Sternberg, M. J. E. The Phyre2 web portal for protein modeling, prediction and analysis. *Nat Protoc* 10, 845–858 (2015).

22. Ravaud, S. *et al.* Impaired Transport of Nucleotides in a Mitochondrial Carrier Explains Severe Human Genetic Diseases. *Acs Chem Biol* 7, 1164–1169 (2012).

23. Mifsud, J. *et al.* The substrate specificity of the human ADP/ATP carrier AAC1. *Mol Membr Biol* 30, 160–168 (2012).

24. Miroux, B. & Walker, J. E. Over-production of Proteins inEscherichia coli: Mutant Hosts that Allow Synthesis of some Membrane Proteins and Globular Proteins at High Levels. *J Mol Biol* 260, 289–298 (1996).

**Chapter 4: Conclusions and future directions**

Jonathan Tai

**Author contributions:**

Conceptualization: JT, RMG, SWR, DJP

Methodology: JT, RMG, SWR, DJP

Formal analysis: JT, RMG, SWR

Investigation: JT, RMG, SWR

Funding acquisition: DJP

Supervision: DJP

Writing – original draft: JT

This chapter contains unpublished work.

**Abstract**

Coenzyme Q (CoQ) is redox active lipid that functions as a crucial component of many cellular processes, including the mitochondrial respiratory chain. The biosynthesis of CoQ requires a set of enzymes that are distributed between the cytosol and the mitochondrial matrix. As such, mitochondrial carriers play a key role in CoQ biosynthesis by facilitating the movement of cofactors and precursors across the inner mitochondrial membrane. While several cofactor transporters have been identified, the molecular identities of the precursor transporters remain elusive. In this dissertation, I have described our efforts to elucidate these steps, providing new insights into the molecular mechanisms of CoQ biosynthesis. In Chapter 2, we combined genetic screening, isotope tracing, and targeted uptake assays to uncover a secondary role for Hem25p, a mitochondrial glycine carrier, as an isopentenyl pyrophosphate (IPP) transporter. In Chapter 3, we used *in silico* homology modeling and targeted uptake assays to investigate the role of Coq2p in 4-hydroxybenzoate (4-HB) transport. Our results suggest that Coq2p enables 4-HB uptake and leads us to hypothesize a novel function for this UbiA superfamily member. Through these efforts, we have partially elucidated the precursor transport steps of CoQ biosynthesis. In this final chapter, I will provide a brief review our findings, followed by a discussion of future directions for studying CoQ biosynthesis and mitochondrial transporters.

**Conclusions**

*Hem25p is a mitochondrial IPP transporter*

We carried out a yeast genetic screen to identify mitochondrial transporters involved in CoQ biosynthesis. Our screen utilized a custom library of *gene*Δ strains, each lacking a member of the SLC25 family of mitochondrial carriers. We also included seven non-SLC25 carriers that had characteristics of a mitochondrial carrier. Our screen identified four genes whose disruption resulted in CoQ deficiency. Three of these genes encoded carriers whose functions could be directly linked to specific steps in CoQ biosynthesis. The remaining gene, *HEM25*, encoded a mitochondrial glycine transporter involved in heme biosynthesis. We then showed that the effect of Hem25p on CoQ abundance was largely independent of its role in glycine transport and heme biosynthesis. This was reinforced by our whole-cell proteomics results, in which *hem25*Δ cells demonstrated decreased levels of complex Q proteins, even after heme levels were restored by ALA supplementation. We then used stable isotope labeled to investigate the exact role of Hem25p on CoQ biosynthesis. Using [*phenyl*-$^{13}$C]-4-HB, we showed that Hem25p drives the formation of PPHB, and thereby early CoQ biosynthesis. We confirmed these results with [1,2-$^{13}$C]-IPP in isolated mitochondria, leading us to hypothesize that Hem25p is a precursor transporter. To test this, we expressed MBP-tagged Hem25p in *E. coli* membranes, allowing us to perform whole-cell uptake assays. Cells expressing MBP-Hem25p showed a time-dependent accumulation of IPP, but not 4-HB. Mutations to the Hem25p substrate binding site abolished transport activity. Thus, we showed that Hem25p transports both glycine and IPP, thereby contributing to mitochondrial heme and CoQ biosynthesis. This dual function is largely conserved in fungi, as the human ortholog SLC25A38 was neither transported IPP in bacteria nor rescued CoQ levels in *hem25*Δ yeast. Thus,

while we have identified the yeast IPP transporter, the identity of the metazoan transporter remains unknown.

*Coq2p enables 4-HB uptake*

*COQ2* mutations were some of the first identified molecular causes of primary CoQ deficiency. The severity of the phenotype, as well as the response to CoQ supplementation, varies by mutation. In a recent report, supplementation with 4-HB restored CoQ biosynthesis in patient-derived fibroblasts harboring *COQ2* mutations. *In silico* homology modeling of the human COQ2 identified a putative substrate tunnel though the center of the protein. It was therefore hypothesized that this tunnel serves as a pathway for 4-HB to reach the matrix. We therefore investigated this using our bacterial uptake assay system. We first repeated the homology modeling, showing that human COQ2 and the yeast Coq2p have the same tunnel-like structure. When Coq2p is expressed in *E. coli,* the cells accumulated radiolabeled 4-HB in a time-dependent manner. This accumulation was lower than that of the known 4-HB transporter pcaK but was higher than the empty vector control cells. Importantly, this accumulation was outcompeted by an excess of unlabeled 4-HB. While additional controls are still necessary, our results are consistent with Coq2p being a 4-HB transporter. Thus, these preliminary results provide a foundation for further investigation into Coq2p function.

*Responsible conduct of research*

The work described in this dissertation represent the scientific training component of the University of Wisconsin Medical Scientist Training Program (MSTP). As such, training in the responsible conduct of research was heavily integrated into my graduate studies to ensure the rigor

and reproducibility of these results. Introductory coursework though the medical school and Integrated Program in Biochemistry curriculums provided a robust foundation in the responsible conduct of research, covering topics such as statistics, research ethics, grant and paper writing, experimental design. An important aspect of this training was that it covered issues specific to basic, translational, and clinical research. Ongoing training was provided through MSTP seminars, in which invited faculty speakers would cover topics such as peer review, broader effects of scientific research, authorship and publication, and data management.

Laboratory-based training was achieved through discussions and meetings with my advisors David Pagliarini and Katherine Henzler-Wildman. These discussions, which occurred at regular intervals, ensured that appropriate methods and analyses were being used. This was supplemented by informal interactions with senior laboratory members to discuss experimental approaches and the use of proper controls. These meetings provided a welcoming space where I could grow and develop as a scientist.

All proteomic data generated in this thesis is freely available on publicly accessible resources. All data are contained within this dissertation, with individual data points for each replicate plotted in the figures when possible. Materials (reagents, cell lines, etc.) and data from published projects will be made available to the scientific community upon reasonable request.

**Future directions**

*Identifying a secondary yeast isoprenoid pyrophosphate transporter*

Despite missing the major mitochondrial glycine and IPP transporter, *hem25Δ* yeast had approximately 15% and 30% of wild-type CoQ and heme levels, respectively. This is consistent with the existence of a secondary transporter(s)[1,2]. Ymc1p was hypothesized to be the secondary glycine transporter, as heme levels in *hem25Δymc1Δ* yeast did not increase in response to glycine supplementation[3]. However, direct evidence of glycine transport by Ymc1p has not been shown.

Our targeted genetic screen did not identify any strong hits for potential secondary IPP transporters. However, it is possible that our cutoffs ($p<0.05$, >two-fold decrease) were too stringent to identify a secondary transporter, as cells lacking this carrier would have only a minor CoQ defect. Thus, the redundant mechanisms that make mitochondrial transporters difficult to identify are amplified when trying to find a secondary transporter[4]. Given these subtle effects, any future attempts to identify the secondary transporter will likely have to use *hem25Δ* as the background strain to increase the sensitivity. It should be noted, however, that this secondary transporter may not limited to IPP. It is possible that other isoprenoid pyrophosphate species such as farnesyl pyrophosphate are transported[5].

One brute-force approach would be to express each transporter in bacteria and test for radiolabeled isoprenoid pyrophosphate uptake. While this would definitively prove import, this approach has many drawbacks. First, it assumes that the secondary transporter is a SLC25 carrier or another known carrier. Furthermore, the use of radiolabeled substrates quickly becomes prohibitively expensive at that scale. An alternative brute-force approach would be to test different *hem25ΔtransporterΔ* strains to see which double-deletion strain has the most pronounced CoQ defect. An analogous strategy involves overexpressing transporters in *hem25Δ* to see which

carriers restore CoQ levels. A key assumption for this approach is that overexpression of a secondary transporter can compensate for Hem25p loss. While these strategies are relatively straightforward, their main limitations are their low-throughput and reliance on known mitochondrial carriers.

Given the limitations of the brute-force strategies, a systems biology approach may be more appropriate. One possibility is to use yeast overexpression libraries along with selective conditions such as statin treatment. Cells lacking Hem25p are sensitive to statin treatment, likely due to the decrease in IPP synthesis[6] (Figure 1). Thus, overexpression of the secondary transporter should buffer the statin sensitivity of *hem25Δ*. The advantages of this approach are that it expands the search beyond known transporters and that it is a positive selection screen. As a result, the specificity of this screen should be higher than those based on negative selection.
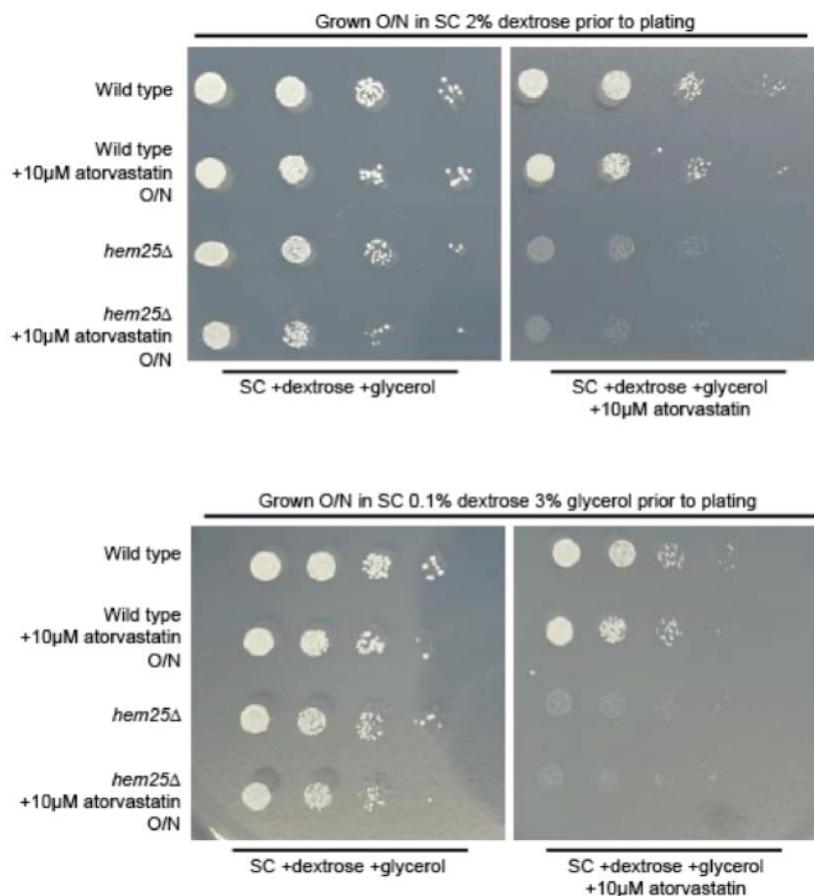
**Figure 1. *hem25Δ* yeast are sensitized to statins.** Drop assay of WT and *hem25Δ* yeast in the presence or absence of 10 μM atorvastatin. Starter cultures were refreshed overnight in either fermentative or respiratory media (± atorvastatin) before being spotted on to respiratory media plates.

In reanalyzing out targeted screen, we identified the mitochondrial phosphate carrier, Mir1p as potential lead. In our screen, *mir1Δ* yeast had ~75% of wild-type CoQ levels. Although this was only a slight defect, it could reflect the smaller contribution of a secondary transporter. Given that phosphate is chemically similar to IPP, Mir1p may be worth further investigation. CoQ measurements in *hem25Δmir1Δ* yeast as well as bacterial uptake assays with MBP-Mir1p represent appropriate first steps.

*Identification of a metazoan ortholog of Hem25p*

We definitively showed that SLC25A38, the human ortholog of Hem25p, does not transport IPP nor does it contribute to CoQ biosynthesis. Furthermore, we demonstrate that IPP transport is absent in metazoan orthologs, being conserved only in fungi. Thus, the identity of the metazoan isoprenoid pyrophosphate carrier remains unknown. A major goal for any future studies is the identification of this transporter. From a biological standpoint, identification of the metazoan homolog would enable further study into the regulation of heme and CoQ biosynthesis, as well as how that regulation evolved with the appearance of multi-cellular and multi-organ species. From a medical perspective, it allows us to identify pathogenic mutations and develop new approaches for treating CoQ deficiencies.

Since Hem25p is a member of the SLC25 family, we hypothesized that the metazoan ortholog would also be SLC25 member. Since humans have 18 more SLC25 members than yeast[1], our assumption was that a separate IPP carrier evolved to enable tighter regulation of heme and CoQ biosynthesis. We therefore cloned each human SLC25 carrier into yeast expression vectors and assessed each carrier's ability to rescue CoQ levels in *hem25Δ* yeast (Figure 2). Unfortunately, this screen resulted in no strong hits, with only a few carriers demonstrating mild rescue. These results suggest that mitochondrial isoprenoid pyrophosphate transporter is not mediated by an SLC25 member. That said, expression levels were not checked for every condition, thus it is possible that our results are due to poor expression and localization. Furthermore, this screen only assessed the primary isoform for each carrier, even though it is known that carriers can have multiple isoforms from alternative splicing[1].
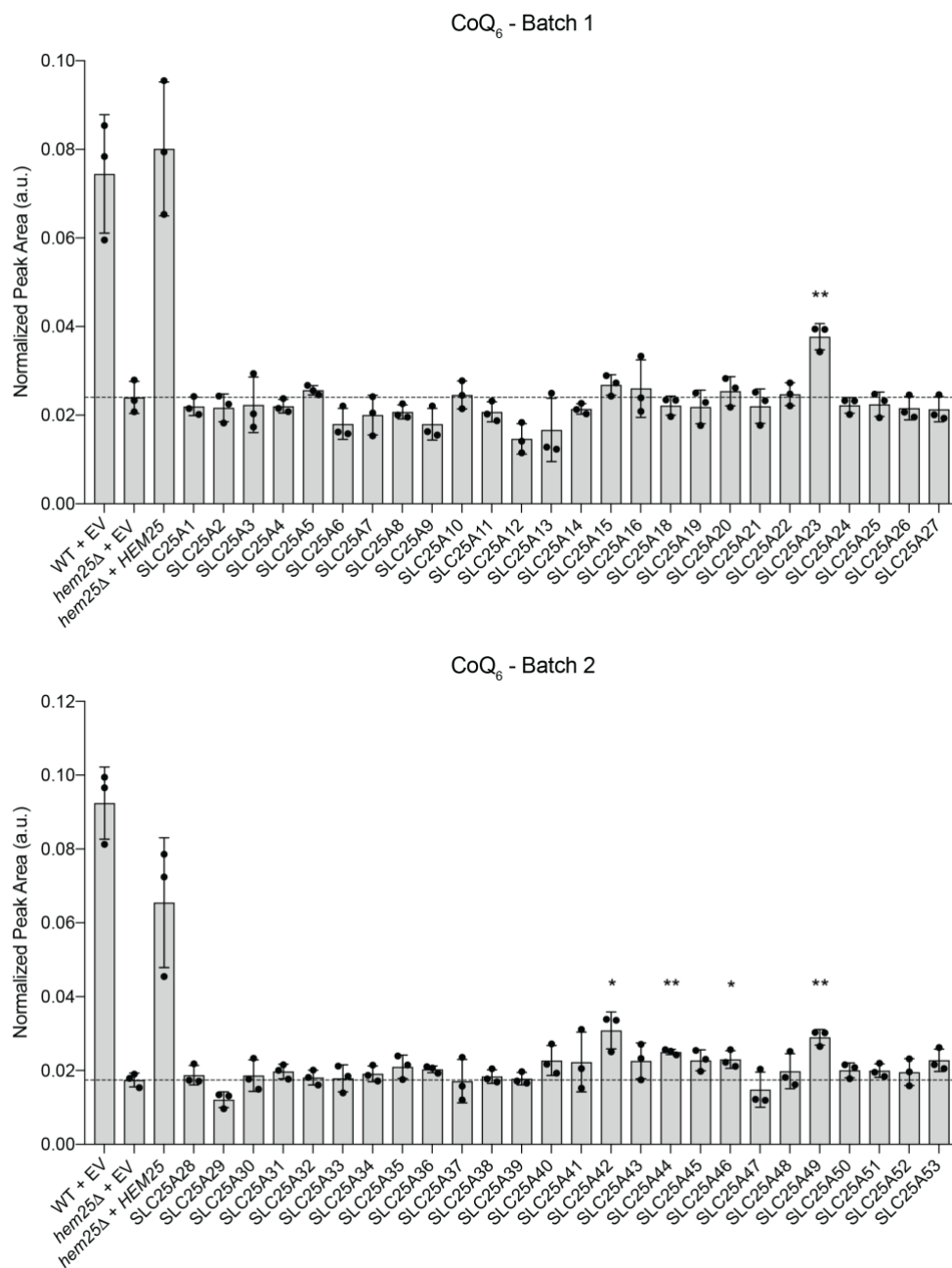
**Figure 2. Rescue of CoQ levels by members of the human SLC25 family.** Human SLC25 carriers were expressed in *hem25Δ* yeast under the control of the GAL promoter. WT and Hem25p conditions were included as positive controls (*$p<0.05$, **$p<0.01$ *hem25Δ+HEM25* vs. SLC25A*##*).

To account for these limitations, genome-wide systems approaches are needed. One strategy is to generate a human expression library which can then be tested in *hem25Δ* yeast under selective conditions (such as a statin). This would ideally cover the entire genome and would account for splice variants. However, generating this library can be challenging as the choice of cell lines can affect coverage. This is also complicated by the low abundance of mitochondrial carriers at baseline[7]. Additionally, despite their convenience, yeast may have difficulty handling the overexpression of human membrane proteins, resulting in decreased sensitivity.

Genome-wide screens in human cell lines can bypass the need for library generation from isolated mRNA. Furthermore, with CRISPR/Cas9-based techniques and reagents readily available, these screens can be easily performed. The biggest challenge of these screens is developing a selection condition to isolate the phenotype. In the case of an isoprenoid pyrophosphate transporter, statins represent the most obvious option, as they limit the production of IPP. Alternatively, a number of ferroptosis inducers can be used to select against cells with lower CoQ levels[8]. These compound treatments can be paired with a CRISPRa library that increases the expression of each gene. Previous CRISPRa screens have shown that upregulation of transporters can compensate for limited substrate availability[9]. Thus, selecting for transporters that compensate for limited intracellular IPP may yield the mammalian mitochondrial IPP transporter.

*Identifying 4-HB transporters*

In Chapter 3, I discussed our investigation into Coq2p as a potential 4-HB transporter. Although our early results are promising, many more experiments need to be performed. Those studies are described in that chapter. Here, I will discuss other potential 4-HB transporters.

When a protein BLAST is performed on *Pseudomonas putida* pcaK, a known 4-HB transporter[10], two yeast hits were identified – Vvs1p (Ybr241fp) and Vps73p (Ygl104cp). Both are members of the sugar porter family of transporters[11]. Vvs1p localized to the vacuole, however, Vps73 is localized to the mitochondria. Little is known about the substrates of these two proteins, however both were identified early in this work as potential non-SLC25 mitochondrial carriers to include in our targeted screen. However, neither ended up being included in the final list. Nevertheless, *vvs1Δ* and *vps73Δ* strains were generated and tested for CoQ levels early in this project. Unfortunately, neither strain had a CoQ defect (Figure 3). Thus, despite being the closest hit to pcaK, it is unlikely that either Vvs1p or Vps73p are 4-HB transporters. Further study is needed to fully rule out this function.
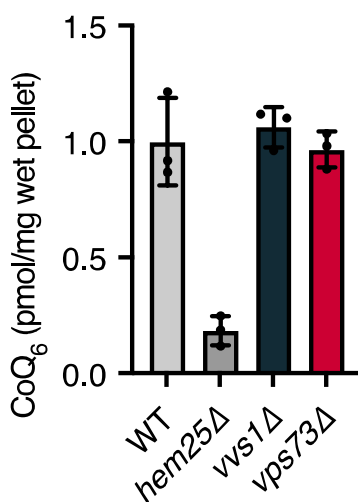


**Figure 3. CoQ levels in *vvs1Δ* and *vps73Δ* yeast.** Values are relative to WT.

Although Vps73p may not be the 4-HB transporter, it is tempting to think that the actual transporter is related to pcaK, albeit distantly. Thus, Vps73p can be used as a starting point for new leads. In one instance, a second protein BLAST was performed using Vps73 to search for human proteins. The highest hit was a protein called GLUT1 (SLC2A1), a plasma membrane glucose

transporter. In 2005, a group found that GLUT1 also localizes to the mitochondrial membrane, where it transports dehydroascorbic acid, the oxidized form of vitamin C, into the matrix[12]. Furthermore, a case of CoQ deficiency was reported in a patient with mutations in *GLUT1*[13]. However, follow up studies later found no link between GLUT1 and CoQ[14]. While the exact role of GLUT1 in CoQ deficiency remains uncertain, the properties of GLUT1 make it, and other SLC2 members, an attractive target for further investigation.

This last protein was identified in another protein BLAST search using pcaK to search for human proteins. The main hit in this search was SLC22A13, a plasma membrane organic anion transporter. Substates for SLC22A13 include nicotinate, *p*-aminohippurate, urate, and orotate[15,16]. Although SLC22A13 has not been localized to the mitochondria, a related protein, SLC22A14, was recently identified as a mitochondrial riboflavin transporter[17]. Thus, it may be worth looking into SLC22A13, as well as other SLC22 members, as potential 4-HB transporters.

*Biochemical methods for studying mitochondrial transporters*

The gold standard for studying transporters remains the proteoliposome. This allows for the study of transporters in isolation without any interference from other transporters or metabolic processes[18]. For mitochondrial transporters, this requires the purification of transporters from either cells or bacterial inclusion bodies. The earliest studies purified carriers from large amounts of animal tissue using hydroxyapatite columns[19]. This worked well for carriers that were abundant in the mitochondria, such as the ADP/ATP carrier, but were inefficient for other carriers that were less abundant. Thus, this approach fell out of favor by the end of the 1980s. As a result, the majority of transporters studies utilize the expression, purification, reconstitution, and assay (EPRA) method[1]. This approach consists of expressing the recombinant protein in *E. coli* inclusion bodies,

purifying the protein, reconstituting it in liposomes, and assaying transport with radiolabeled substrates[20].

We attempted to use this strategy to assay IPP transport by Hem25p[21], however our efforts were largely unsuccessful. When Hem25p was reconstituted into liposomes, we were able to detect time-dependent [$^{14}$C]-glycine uptake (Figure 4A). This uptake was inhibited by high concentrations of pyridoxal 5'-phosphate (PLP) and bathophenathrolinedisulfonic acid (BAT), inhibitors of mitochondrial carriers. However, we were never able outcompete uptake with excess cold glycine. When we looked more into this, we found that liposomes reconstituted with boiled Hem25p, as well as empty liposomes with no protein, also demonstrated glycine uptake (Figures 4B and 4C). Our conclusion was that Hem25p was aggregating during the reconstitution process, resulting in little to no functional protein in the proteoliposome. Any uptake that we saw was likely due to passive diffusion of glycine across the liposome membrane. These results also raised questions about the PLP/BAT inhibitor, as it inhibited glycine uptake even in the absence of functional protein. Our hypothesis is that the high inhibitor concentration resulted in osmotic stress, affecting the accumulation of glycine in the liposome. Given these results, we decided to abandon this approach and moved onto other uptake assay systems.
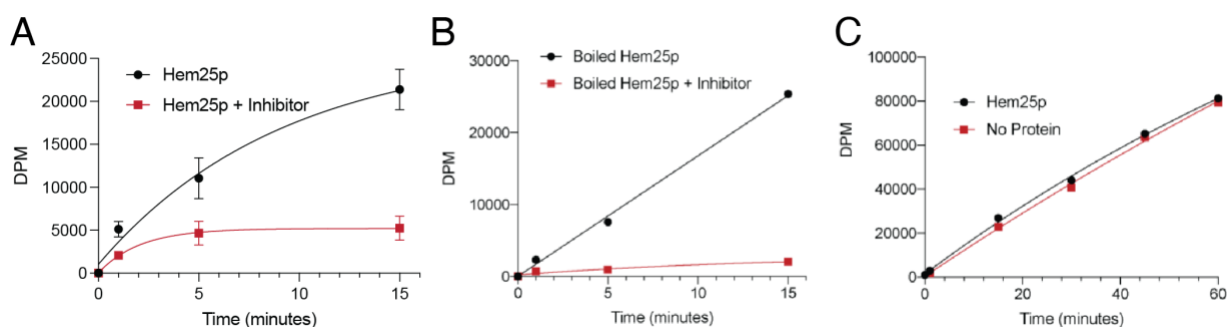


**Figure 4. [$^{14}$C]-glycine uptake in Hem25p proteoliposomes.** (**A**) Glycine uptake by Hem25p proteoliposomes with and without the PLP/BAT inhibitor. (**B**) Uptake by proteolipsomes

reconstituted with boiled Hem25p. (**C**) Uptake by liposomes with and without Hem25p. For each experiment, liposomes were preloaded with 10 mM unlabeled glycine. Assays were carried out using 1 mM [$^{14}$C]-glycine.

Although we were able to develop a bacterial uptake assay, this system relies on bacteria's inability to transport the substrate under investigation. While this worked well for IPP, it may not be the case for other substrates. Thus, there is still a need for isolated assay systems. EPRA is the gold standard, however it is notoriously difficult[22], as evidenced by our attempts. Nevertheless, successful reconstitution may still be possible with additional optimization steps. These include the addition of DTT and lipids to the reconstitution mixture, use of non-frozen protein, and the use of freeze-thaw or extrusion for reconstitution.

The most difficult part of the EPRA method is the refolding of carriers while simultaneously reconstituting them into liposomes[22]. Thus, there has been renewed interest in purifying carriers under native conditions. While early studies used large amounts of animal tissues and hydroxyapatite columns, recent studies have relied on affinity tags for purification. In this approach, fusion proteins consisting of the carrier and an affinity tag (such as GFP or FLAG) are expressed in cultured cells. Cell membranes are then harvested before being solubilized in detergent. The carrier is then purified using commercially available resins that bind the tag. Thus, the carrier is purified under native conditions, with no need to unfold and refold the protein. This approach has been used previously to study transporters such as SFXN1 and MTCH2[23,24]. As such, the development of this approach in our laboratory would be greatly beneficial for future transporter studies.

Another alternative to EPRA is the use of *L. lactis* instead of *E. coli*[22,25]. The advantage of *L. lactis* is that expression of carriers results in their functional insertion into the membrane without the need for signal peptides like MBP. They also contain fewer endogenous membrane transporters and do not form inclusion bodies[22]. Thus, expression in *L. lactis* allows uptake assays to be performed in both whole-cells or reconstituted liposomes[25]. This has been used to study several SLC25 carriers in addition to non-SLC25 carriers such as the mitochondrial pyruvate carrier[26].

*Systematic interrogation of mitochondrial transporters*

We have shown that Hem25p contributes to two different mitochondrial biosynthetic pathways by transporting two chemically distinct molecules. This dual function is not limited to Hem25p, with the mitochondrial phosphate carrier recently shown to transport copper ions[27,28]. Given that mitochondria have many more metabolites than known transporters[29], it is likely that additional carriers have multiple distinct substrates. However, identifying these substrates remains a challenging task[30]. Traditional biochemical methods have low throughput and require labeled substrates that can be unavailable or prohibitively expensive. Systems-level approaches, including many forward-genetic screens, often miss transporters due to redundancies and compensatory mechanisms[4,30]. As a result, we lack a complete inventory of mitochondrial transporters and their substrates. Thus, there is an urgent need to identify all of the mitochondrial transporters and define their substrates.

The unique challenges of studying transporters require the development of novel screening approaches. New technologies such as CRISPR libraries and highly sensitive analytical techniques will greatly accelerate these efforts. Indeed, thermalstability shift assays and thermal proteome profiling are just some of methods currently being developed for transporter studies[31,32]. The

refinement of these techniques will enable future systematic investigations into mitochondrial transporters.

## Materials and Methods

<u>Yeast strains and cultures</u>

All yeast strains and culture conditions are the same as those described in Chapter 2 "*Yeast strains and cultures*" unless otherwise noted.

<u>Human SLC25 rescue</u>

Genes encoding the predominant isoforms of human SLC25 carriers were synthesized as codon-optimized gBlocks (IDT) and cloned into the pYES2 yeast expression vector using the BamHI and XhoI restriction sites. The presence of the insert was confirmed by sequencing. Cloned vectors were transformed into *hem25Δ* yeast using the LiAc/SS method[33] and selected on Ura$^-$ SD 2%D plates.

Singles colonies of transformed cells were used to inoculate starter cultures (Ura$^-$ SD 2%D, 3 mL). Cultures were grown overnight (30 ºC, 14-16 h) before being refreshed to an $OD_{600} = 0.05$ in respiratory media (Ura$^-$ SD 0.1%D, 3%G, 3 mL). Refreshed cells were grown overnight until $OD_{600}$~1 (30 ºC, 230 rpm), at which point the media was switched to galactose media (Ura$^-$ SD 2%Gal, 3 mL) to induce protein expression. Cells were incubated in the galactose media for 5 hours (30 ºC, 230 rpm), after which the $OD_{600}$ was measured and the cultures were harvested by centrifugation (4,000 x *g*, 5 min, RT). Cells were washed once with water before being transferred to a 1.5 mL microcentrifuge tube. Cells were centrifuged again (15,000 x *g*, 30 s, RT), snap frozen

in LN$_2$, and stored at -80 ºC until analysis. Lipid extraction and LC/MS measurements were performed as described in Chapter 2.

<u>EPRA of Hem25p</u>

EPRA of Hem25 was performed essentially as described elsewhere[20,21]. The procedure is briefly described below.

*Expression.* The *HEM25* gene was synthesized as a codon-optimized gBlock (IDT) and cloned into the pET21b expression bector using the NdeI and XhoI restriction enzymes. The resulting construct consisted of the *HEM25* gene, a short linker, and a 6xHis tag (coding for Hem25p-6xHis). Sequence-verified constructs were transformed into BL21 Star (DE3) (Thermo) according to the manufacturer's instructions and selected on LB/Amp plates (37 ºC). Transformed cells were used to inoculate 1 L of 2xYT media in a 4 L flask. Colonies from a single plate were collected using a sterile cell scraper before being suspended in 1 mL of media. Resuspended cells were used to inoculate the culture. Cultures were incubated (~240-250 RPM, 37 ºC) until the OD$_{60}$~0.6-1.0, at which point IPTG was added to a final concentration of 1 mM. Cultures were induced (~240-250 RPM, 37 ºC) for 4 hours. Cells were harvested by centrifugation (4,000 x *g*, 15 min) at stored at -80 ºC until purification.

*Purification*. Cell pellets were thawed on ice before being resuspended in Tris buffer (10 mM Tris/HCl, pH 7.0, 4 ºC). Cells were lysed by probe sonication until clear. Lysate was centrifuged (12,000 x *g*, 20 min, 4 ºC). The supernatant was removed, and the pellet was resuspended in 2 mL of Tris buffer. The resuspended pellet was then layered on top of a

discontinuous sucrose gradient consisting of 4 mL 72% (w/v) sucrose at the bottom, 5 mL 53 % (w/v) sucrose, and 2 mL 40% (w/v) sucrose at the top. This was then ultracentrifuged (131,000 x $g$, 90 min, 4 ºC) using a swinging bucket rotor. Inclusion bodies were isolated as a grey band at the interface of the 53% and 72% sucrose layers. The inclusion bodies were washed with 30 mL Tris buffer, 2 mL HEPES buffer (10 mM HEPES, pH 8.0) containing 3% (w/v) Triton X-114, and 2 mL HEPES buffer without detergent. Between each wash, the inclusion body was isolated by centrifugation (25,000 x $g$, 20 min, 4 ºC). After the final wash, the inclusion body pellet was resuspended in 30 µL HEPES buffer. Inclusion bodies were solubilized in 2.5% Sarkosyl by the addition of 10 µL 10% Sarkosyl (30 min, 0 ºC). The solubilized protein was then diluted 20x with HEPES buffer. Hem25p-6xHis was purified on a Ni-NTA column. Imidazole was removed using a Zeba Spin desalting column. The purified protein was then aliquoted, snap frozen, and stored at -80 ºC until reconstitution.

*Reconstitution*. The reconstitution mixture was assembled in the following order: 100 µL purified protein (0.1-1.0 µg), 90 µL 10% (w/v) Triton X-114, 90 µL 10% (w/v) egg-yolk phospholipids (60% PC) as sonicated liposomes (Avanti), 420 µL HEPES buffer containing preloaded substrate. The reconstitution mixture was mixed by vortexing. The mixture was then loaded through the same Amberlite XAD-2 column 13 times to remove the detergent (RT). External substrate was removed using a Sephadex G-75 column. The result should be ~600 µL proteoliposomes. Keep on ice until assay and use within 4 hours.

*Assay*. For each timepoint, transfer 100 µL of proteoliposomes to a 1.5 mL microcentrifuge tube and preincubate at 25 ºC for 3 min. To start the assay, at 10 µL of 11x radiolabeled substrate

and pipet gently to mix. At the desired timepoint, at 10 µL of 12x inhibitor mixture (360 mM pyridoxal 5'-phosphate, 120 mM bathophenanthrolinedisulfonic acid) and mix by gently pipetting. For inhibitor controls, add the 12x inhibitor mixture at the same time as the substrate. Load the entire reaction on to a Sephadex G-75 column. Elute with HEPES buffer to separate proteoliposomes from external substrate. Collect eluted proteoliposomes in scintillation vials and add scintillation fluid (Ultima Gold MV, PerkinElmer). Measure imported radioactivity by scintillation counting.

# References

1. Palmieri, F. & Monne, M. Discoveries, metabolic roles and diseases of mitochondrial carriers: A review. *Biochimica Et Biophysica Acta Bba - Mol Cell Res* 1863, 2362–78 (2016).

2. Shi, X. *et al.* Combinatorial GxGxE CRISPR screen identifies SLC25A39 in mitochondrial glutathione transport linking iron homeostasis to OXPHOS. *Nat Commun* 13, 2483 (2022).

3. Fernandez-Murray, J. P. *et al.* Glycine and Folate Ameliorate Models of Congenital Sideroblastic Anemia. *Plos Genet* 12, e1005783 (2016).

4. Taylor, E. B. Functional Properties of the Mitochondrial Carrier System. *Trends Cell Biol* 27, 633–644 (2017).

5. Stefely, J. A. & Pagliarini, D. J. Biochemistry of Mitochondrial Coenzyme Q Biosynthesis. *Trends Biochem Sci* 42, 824–843 (2017).

6. Lee, A. Y. *et al.* Mapping the Cellular Response to Small Molecules Using Chemogenomic Fitness Signatures. *Science* 344, 208–211 (2014).

7. Palmieri, F. The mitochondrial transporter family (SLC25): physiological and pathological implications. *Pflügers Archiv* 447, 689–709 (2004).

8. Shimada, K. *et al.* Global survey of cell death mechanisms reveals metabolic regulation of ferroptosis. *Nat Chem Biol* 12, 497–503 (2016).

9. Rebsamen, M. *et al.* Gain-of-function genetic screens in human cells identify SLC transporters overcoming environmental nutrient restrictions. *Life Sci Alliance* 5, e202201404 (2022).

10. Nichols, N. N. & Harwood, C. S. PcaK, a high-affinity permease for the aromatic compounds 4-hydroxybenzoate and protocatechuate from Pseudomonas putida. *J Bacteriol* 179, 5056–5061 (1997).

11. Palma, M., Goffeau, A., Spencer-Martins, I. & Baret, P. V. A Phylogenetic Analysis of the Sugar Porters in Hemiascomycetous Yeasts. *J Mol Microb Biotech* 12, 241–248 (2007).

12. KC, S., Càrcamo, J. M. & Golde, D. W. Vitamin C enters mitochondria via facilitative glucose transporter 1 (Gluti) and confers mitochondrial protection against oxidative injury. *Faseb J* 19, 1657–1667 (2005).

13. Yubero, D. *et al.* Association between coenzyme Q10 and glucose transporter (GLUT1) deficiency. *Bmc Pediatr* 14, 284 (2014).

14. Barca, E. *et al.* JIMD Reports, Volume 29. *Jimd Reports* 29, 47–52 (2015).

15. Shinoda, Y., Yamashiro, T., Hosooka, A., Yasujima, T. & Yuasa, H. Functional characterization of human organic anion transporter 10 (OAT10/SLC22A13) as an orotate transporter. *Drug Metab Pharmacok* 43, 100443 (2022).

16. Bahn, A. *et al.* Identification of a New Urate and High Affinity Nicotinate Transporter, hOAT10 (SLC22A13)*. *J Biol Chem* 283, 16332–16341 (2008).

17. Kuang, W. *et al.* SLC22A14 is a mitochondrial riboflavin transporter required for sperm oxidative phosphorylation and male fertility. *Cell Reports* 35, 109025 (2021).

18. Kraemer, R., Aquila, H. & Klingenberg, M. Isolation of the unliganded adenosine 5'-diphosphate,adenosine 5'-triphosphate carrier-linked binding protein and incorporation into the membranes of liposomes. *Biochemistry-us* 16, 4949–4953 (1977).

19. Palmieri, F., Indiveri, C., Bisaccia, F. & Iacobazzi, V. [25] Mitochondrial metabolite carrier proteins: Purification, reconstitution, and transport studies. *Methods Enzymol* 260, 349–369 (1995).

20. Fiermonte, G., Walker, J. E. & Palmieri, F. Abundant bacterial expression and reconstitution of an intrinsic membrane-transport protein from bovine mitochondria. *Biochem J* 294, 293–299 (1993).

21. Lunetti, P. *et al.* Characterization of Human and Yeast Mitochondrial Glycine Carriers with Implications for Heme Biosynthesis and Anemia. *J Biol Chem* 291, 19746–59 (2016).

22. Monné, M., Chan, K. W., Slotboom, D. & Kunji, E. R. S. Functional expression of eukaryotic membrane proteins in Lactococcus lactis. *Protein Sci* 14, 3048–3056 (2005).

23. Kory, N. *et al.* SFXN1 is a mitochondrial serine transporter required for one-carbon metabolism. *Science* 362, (2018).

24. Guna, A. *et al.* MTCH2 is a mitochondrial outer membrane protein insertase. *Science* 378, 317–322 (2022).

25. King, M. S., Boes, C. & Kunji, E. R. S. Chapter Four Membrane Protein Expression in Lactococcus lactis. *Methods Enzymol* 556, 77–97 (2015).

26. Herzig, S. *et al.* Identification and functional expression of the mitochondrial pyruvate carrier. *Science* 337, 93–6 (2012).

27. Vest, K. E., Leary, S. C., Winge, D. R. & Cobine, P. A. Copper Import into the Mitochondrial Matrix in Saccharomyces cerevisiae Is Mediated by Pic2, a Mitochondrial Carrier Family Protein*. *J Biol Chem* 288, 23884–23892 (2013).

28. Boulet, A. *et al.* The mammalian phosphate carrier SLC25A3 is a mitochondrial copper transporter required for cytochrome c oxidase biogenesis. *J Biol Chem* 293, 1887–1896 (2018).

29. Chen, W. W., Freinkman, E., Wang, T., Birsoy, K. & Sabatini, D. M. Absolute Quantification of Matrix Metabolites Reveals the Dynamics of Mitochondrial Metabolism. *Cell* 166, 1324-1337 e11 (2016).

30. Cesar-Razquin, A. *et al.* A Call for Systematic Research on Solute Carriers. *Cell* 162, 478–87 (2015).

31. Majd, H. *et al.* Screening of candidate substrates and coupling ions of transporters by thermostability shift assays. *Elife* 7, e38821 (2018).

32. Reinhard, F. B. M. *et al.* Thermal proteome profiling monitors ligand interactions with cellular membrane proteins. *Nat Methods* 12, 1129–1131 (2015).

33. Gietz, R. D. & Schiestl, R. H. High-efficiency yeast transformation using the LiAc/SS carrier DNA/PEG method. *Nat Protoc* 2, 31–34 (2007).